Program and Abstract Volume

LPI Contribution No. 1685

Annual Meeting of the
Lunar Exploration Analysis Group

October 22–24, 2012 • Greenbelt, Maryland

Sponsor

National Aeronautics and Space Administration

Conveners

Charles Shearer
University of New Mexico

Jeffrey Plescia
The John Hopkins Applied Physics Laboratory

Clive Neal
University of Notre Dame

Stephen Mackwell
Lunar and Planetary Institute

Scientific Organizing Committee

Charles Shearer, *University of New Mexico*

Jeffrey Plescia, *John Hopkins University Applied Physics Laboratory*

Clive Neal, *University of Notre Dame*

Michael Wargo, *NASA Headquarters*

Stephen Mackwell, *Lunar and Planetary Institute*

Dallas Bienhoff, *The Boeing Corporation*

Noah Petro, *NASA Goddard Space Flight Center*

Kurt Sacksteder, *NASA Glenn Research Center*

Greg Schmidt, *NASA Lunar Science Institute/NASA Ames Research Center*

George Tahu, *NASA Headquarters*

Lunar and Planetary Institute 3600 Bay Area Boulevard Houston TX 77058-1113

LPI Contribution No. 1685

Compiled in 2012 by

Meeting and Publication Services
Lunar and Planetary Institute
USRA Houston
3600 Bay Area Boulevard, Houston TX 77058-1113

This material is based upon work supported by NASA under Award No. NNX08AC28A. Any opinions, findings, and conclusions or recommendations expressed in this volume are those of the author(s) and do not necessarily reflect the views of the National Aeronautics and Space Administration.

The Lunar and Planetary Institute is operated by the Universities Space Research Association under a cooperative agreement with the Science Mission Directorate of the National Aeronautics and Space Administration.

Abstracts in this volume may be cited as

Author A. B. (2012) Title of abstract. In *Annual Meeting of the Lunar Exploration Analysis Group*, p. XX. LPI Contribution No. 1685, Lunar and Planetary Institute, Houston.

ISSN No. 0161-5297

Preface

This volume contains abstracts that have been accepted for presentation at the Annual Meeting of the Lunar Exploration Analysis Group, October 22–24, 2012, Greenbelt, Maryland.

Administration and publications support for this meeting were provided by the staff of the Meeting and Publication Services Department at the Lunar and Planetary Institute.

Technical Guide to Sessions

Monday, October 22, 2012

8:30 a.m.	Conference Room W150	Lunar Missions from the Apollo Program to Artemis and Beyond
1:30 p.m.	Conference Room W150	Exploring the Solar System: Updates from NASA
5:30 p.m.	Conference Room W120	Poster Session: Exploration of the Moon
6:45 p.m.	Visitor's Center	NASA Goddard's Visitors Center Open House for LEAG Attendees Featuring a Brand-New Exhibit on the Lunar Reconnaissance Orbiter

Tuesday, October 23, 2012

8:30 a.m.	Conference Room W150	Lunar Missions: The Next Generation
1:45 p.m.	Conference Room W150	The Cold-Hearted Orb that Rules the Night

Wednesday, October 24, 2012

8:30 a.m.	Conference Room W150	Human Exploration of the Moon and Gaps in our Strategic Knowledge

Contents

Program

Monday, October 22, 2012
LUNAR MISSIONS FROM THE APOLLO PROGRAM TO ARTEMIS AND BEYOND
8:30 a.m. Conference Room W150

A celebration of Apollo 17 and the Apollo program:
The role of missions in shaping our view of the Moon and our place in the solar system

Chairs: **Charles Shearer**
Michael Wargo

8:30 a.m. Shearer C. *
Welcome to the LEAG Meeting

8:40 a.m. Scolese C. *
Welcome: Goddard Space Flight Center and the Moon

8:55 a.m. Schmitt H. *
Field Geology at Taurus-Littrow: 40 Years and Counting

9:25 a.m. Head J. *
Apollo Mission Contributions to the Understanding of the Moon as Exemplified by the Apollo 17 Mission to Taurus-Littrow

9:55 a.m. Shearer C. K. *
The Return of Samples by the Apollo Program Shaped our Understanding of the Solar System **[#3048]**

10:15 a.m. BREAK

10:30 a.m. Vondrak R. R. * Keller J. W. Chin G. Garvin J. B. Petro N. E.
The Lunar Reconnaissance Orbiter: Plans for the Extended Science Mission and Next Steps for Lunar Science and Exploration **[#3054]**

11:00 a.m. Smith D. *
GRAIL Update

11:30 a.m. Halekas J. *
ARTEMIS: Results from the First Year

12:00 p.m. Shearer C. and Neal C.
Discussion: Lessons Learned for Future Missions

Monday, October 22, 2012
EXPLORING THE SOLAR SYSTEM: UPDATES FROM NASA
1:30 p.m. Conference Room W150

NASA updates to the lunar and planetary community

Chairs: **Charles Shearer**
Jeff Plescia

1:30 p.m. Garver L. *

2:00 p.m. Gerstenmaier W. *
Human Exploration and Operations Mission Directorate

2:30 p.m. Green J. *
Science Mission Directorate/Planetary Science Division

3:00 p.m. Reuther J. *
Enabling both Precursor Robotic Missions that Could fill Strategic Knowledge Gaps and Human Activities Beyond Low Earth Orbit

3:30 p.m. BREAK

3:50 p.m. Laurini K. *
Overview of the GLEX Meeting, Global Exploration Activities, and How the Moon Fits into this Vision

4:20 p.m. Friedensen V. *
Joint Robotic Precursor Activities

4:40 p.m. Martinez R. *
International Architecture Working Group

5:00 p.m. Pendleton Y. *
NASA Lunar Science Institute — Going Forward

Monday, October 22, 2012
POSTER SESSION: EXPLORATION OF THE MOON
5:30–6:30 p.m. Conference Room W120

Mall U. Bugiolacchi R. Woehler C. Grumpe A.
Mineral Investigation Through the Combined Analysis of NIR and Image-Based 3D Shape Reconstructed Topographic Data **[#3016]**

Patterson G. W. Raney R. K. Cahill J. T. S. Bussey D. B. J. Mini-RF Team
Characterization of Lunar Crater Ejecta Deposits Using m-chi Decompositions of Mini-RF Radar Data **[#3017]**

Jolliff B. L. Robinson M. S. Watters T. R.
LROC Observations in the LRO Extended Mission **[#3052]**

Su J. J. Khachatryan R. Sagdeev R. Usikov D. Milikh G. Chin G.
Monte Carlo Simulations in Support of Orbital Neutron Detection by the LEND Instrument On Board of LRO Spacecraft **[#3021]**

Usikov D. McClanahan T. Sagdeev R. Khachatryan R. Milikh G. Chin G. Su J. J.
LEND: Going Beyond Nominal Angular Resolution **[#3031]**

McClanahan T. P. Chin G. Livengood T. LEND Team LOLA Team
Is Drygalski Crater Wet? Joint Analysis of Lunar Epithermal Neutrons from the LRO LEND and Lunar Prospector Neutron Spectrometers **[#3028]**

Wilson J. K. Spence H. E. Case A. W. Blake J. B. Golightly M. J. Kasper J. Looper M. D. Mazur J. E. Schwadron N. Townsend L. W. Zeitlin C.
Cosmic Ray Albedo Proton Yield Correlated with Lunar Elemental Abundances **[#3014]**

Zimmerman M. I. Farrell W. M. Jackson T. L. Stubbs T. J.
Toward Understanding the Lunar Electrostatic Environment in the Vicinity of Complex Polar Topography **[#3035]**

Mest S. C. Dworzanczyk A. R. Calzada-Diaz A. Bleacher J. E. Petro N. E. Yingst R. A.
Update on the Scientific Characterization of Lunar Regions of Interest **[#3042]**

Merkowitz S. M. Preston A. M.
Next Generation Lunar Laser Ranging **[#3022]**

Petro N. E. Votava J. E.
ArcGIS Digitization of Apollo Surface Activities: A Spatial Database of Traverses, Samples, and Images **[#3036]**

Speyerer E. J. Lawrence S. J. Stopar J. D. Burns K. N. Robinson M. S.
Traverse Planning Using Lunar Reconnaissance Orbiter Narrow Angle Camera Digital Elevation Models **[#3044]**

Clark P. E. Rilee M. L. Curtis S. A.
Frontier: Towards Onboard Intelligence for More Capable Next Generation Space Assets **[#3002]**

Colaprete A. Elphic R. Heldmann J. Ennico K. Mattes G. Sanders J.
Near Real-Time Prospecting for Lunar Volatiles: Demonstrating RESOLVE Science in the Field **[#3038]**

Malespin C. A. Glavin D. P. ten Kate I. L. Franz H. B. Mumm E. Getty S. Southard A. Mahaffy P.
Volatile Analysis by Pyrolysis of Regolith for Planetary Resource Exploration **[#3013]**

Crosby K. M. Werlink R. Mathe S. Lubick K.
Modal Evaluation of Fluid Volume in Spacecraft Propellant Tanks **[#3005]**

Farrell W. M. Killen R. M. Delory G. T.
DREAM Center for Lunar Science: A Three Year Summary Report **[#3027]**

Mahanti P. Robinson M. S. Boyd A. Speyrer E.
Informed Line-of-Sight Communications on the Lunar Surface Using LRO NAC DEMs **[#3006]**

Spence H. E. Schwadron N. A. Gorby M. Joyce C. Quinn M. LeVeille M. Smith S. Wilson J. Townsend L. Cucinotta F.
PREDICCs: A Radiation Prediction Tool for Lunar, Planetary, and Deep Space Exploration **[#3032]**

Gorby M. J. Schwadron N. A. Linker J. A. Spence H. E. Townsend L. W. Cucinotta F. A. Wilson J. K.
From CMEs to Earth/Lunar Radiation Dosages: A First in Heliospheric End-to-End Coupling **[#3043]**

Deans M. C. Smith T. Lees D. S. Scharff E. B. Cohen T. E. Lim D. S. S.
Ground Data Systems for Real Time Lunar Science **[#3045]**

Chi P. J.
A Revisit to Apollo Magnetic Field Records for Sounding of the Lunar Interior **[#3039]**

Karachevtseva I. Zubarev A. Nadezhdina I. Kozlova N. Gusakova E.
Mapping of Luna-17 Landing Site and Reconstruction of Lunokhod-1 Stereo Panoramas **[#3024]**

Jin Y.-Q.
Simulation of Radar Sounder Echoes and Inversion of Lunar Subsurface **[#3003]**

Monday, October 22, 2012
NASA GODDARD VISITOR'S CENTER OPEN HOUSE FOR LEAG ATTENDEES
FEATURING A BRAND-NEW EXHIBIT ON THE LUNAR RECONNAISSANCE ORBITER
6:00–8:00 p.m. NASA Goddard Visitor's Center

Recent renovations to Goddard's Visitors Center include a brand-new exhibit featuring the full-scale Structural Verification Unit for LRO, which has been upgraded to resemble LRO in its launch configuration. During the event, the Science On a Sphere (SOS) will be showcasing lunar content.

We encourage all attendees to come and enjoy good company and hospitality.

Tuesday, October 23, 2012
LUNAR MISSIONS: THE NEXT GENERATION
8:30 a.m. Conference Room W150

Updates on the next generation of lunar missions and innovative approaches to returning to the Moon

Chairs: **Ben Bussey**
Richard Elphic

8:30 a.m. Elphic R. C. * Delory G. T. Grayzeck E. J. Colaprete A. Horanyi M. Mahaffy P. Hine B. Salute J. Boroson D.
The Lunar Atmosphere and Dust Environment Explorer (LADEE): T-Minus One Year and Counting **[#3033]**

8:45 a.m. Stiles A. *
Google Lunar X Prize

9:00 a.m. Whittaker R. *
Astrobiotic

9:15 a.m. Doswell J. *
JURBAN

9:30 a.m. Bourgeois F. *
Frednet

9:45 a.m. Richards B. *
Moon Express

10:00 a.m. Ghafoor N. *
Recent Preparatory Activities for Future Lunar Exploration: Towards a Robotic Precursor

10:15 a.m. Rocha G. *
Angelicum

10:30 a.m. BREAK

10:45 a.m. Neal C. *
Network Science on the Moon: Missions that also Inform Exploration

11:00 a.m. Jolliff B. L. * Shearer C. K. Cohen B. A.
Sampling South Pole-Aitken Basin: The Moonrise Approach **[#3047]**

11:15 a.m. Mitrofanov I. G. * Zelenyi L. M. Tret'yakov V. I.
Upgraded Program of Russian Lunar Landers: Studying of Lunar Poles **[#3025]**

11:30 a.m. Peterson K. M. * Thornton J.
Commercial Models for Lunar Landing and Exploration **[#3050]**

11:45 a.m. Clark P. E. * MacDowall R. Cox R. Vasant A. Schaire S. Malphrus B.
LunarCube: Payload Development for Enhanced Yet Low Cost Lunar Exploration **[#3001]**

12:00 p.m. DISCUSSION

Tuesday, October 23, 2012
THE COLD-HEARTED ORB THAT RULES THE NIGHT
1:45 p.m. Conference Room W150

Examination of results from previous and ongoing lunar missions

Chairs: **Mark Robinson**
Clive Neal

1:45 p.m. Robinson M. S. * LROC Team
LROC Exploration of the Moon **[#3051]**

2:00 p.m. Klima R. L. * Cahill J. T. S. Hagerty J. Lawrence D.
Bullialdus Crater: A Rare Window into Lunar Plutonism and Late-Stage Magma Ocean Fluids **[#3015]**

2:15 p.m. Bussey D. B. J. * Schulze R. Wahl D. E. Patterson G. W. Nolan M. Jensen J. R. Turner F. S. Yocky D. A. Cahill J. T. S. Jakowatz C. V. Raney R. K. Mini-RF Team
Bistatic Radar Observations of the Moon Using the Arecibo Observatory and Mini-RF on LRO **[#3010]**

2:30 p.m. Greenhagen B. T. * Paige D. A. Diviner Science Team
Thermal, Thermophysical, and Compositional Properties of the Moon Revealed by the Diviner Lunar Radiometer **[#3049]**

2:45 p.m. Retherford K. D. * Stern S. A. Gladstone G. R. Cook J. C. Egan A. F. Miles P. F. Parker J. Wm. Kaufmann D. E. Greathouse T. K. Tsang C. C. C. Versteeg M. H. Mukherjee J. Davis M. W. Bayless A. J. Feldman P. D. Hurley D. M. Pryor W. R. Hendrix A. R.
Scientific Breakthroughs from the LRO-Lyman Alpha Mapping Project (LAMP) **[#3026]**

3:00 p.m. Sanin A. B. * Mitrofanov I. G. Litvak M. L. Malakhov A. Boynton W. V. Chin G. Droege G. Evans L. G. Garvin J. Golovin D. V. Harshman K. McClanahan T. P. Milikh G. Mokrousov M. I. Sagdeev R. Z. Starr R. D.
Searching for Water Ice Permafrost: LEND Results for About Three Years of Observations **[#3020]**

3:15 p.m. BREAK

3:30 p.m. Boynton W. V. * Droege G. F. Harshman K. Schaffner M. A. Mitrofanov I. G. McClanahan T. P. LEND Team
Latitudinal Enrichment of Hydrogen in the Lunar Polar Regions: Constraints on Hydrogen Mobility **[#3029]**

3:45 p.m. Livengood T. A. * Chin G. Mitrofanov I. G. Boynton W. V. Sagdeev R. Litvak M. McClanahan T. P. Sanin A. B.
Hydrogen-Bearing Volatiles at the Lunar Equatorial Terminator **[#3040]**

4:00 p.m. Glenar D. A. * Stubbs T. J. Farrell W. M. Keller J. W. Vondrak R. R.
The Search for a High Altitude Dust Exosphere: Observational Status and Dust Upper Limits **[#3008]**

4:15 p.m. Singer S. F. *
Questions About Lunar Origin **[#3004]**

4:30 p.m. Sasaki S. * Kikuchi F. Matsumoto K. Noda H. Araki H. Hanada H. Yamada R. Goossens S. Kunimori H. Iwata T. Kawaguchi N. Kono Y.
Exploration of Deep Interior of the Moon from Measurements of Changes of Long-Wavelength Gravity and Rotation **[#3018]**

4:45 p.m. Stubbs T. J. * Glenar D. A. Jordan A. P. Wang Y. Vondrak R. R. Collier M. R. Farrell W. M. Zimmerman M. I. Schwadron N. A. Spence H. E.
Interplanetary Conditions During the Apollo Missions: Implications for the State of the Lunar Environment **[#3019]**

5:00 p.m. DISCUSSION

Wednesday, October 24, 2012
HUMAN EXPLORATION OF THE MOON AND GAPS IN OUR STRATEGIC KNOWLEDGE
8:30 a.m. Conference Room W150

Examination of architectures for the human exploration and strategic knowledge gaps for a Moon first scenario

Chairs: **Kurt Retherford**
Rachel Klima

8:30 a.m. Shearer C. K. * Members of the GAP-SAT Teams I and II
Results of the Lunar Exploration Analysis Group GAP-SAT (Specific Action Team) I and II Examination of Strategic Knowledge Gaps for the Moon First Scenario for Human Exploration of the Solar System **[#3030]**

8:45 a.m. Connelly J. *
Alternative Lunar Architectures

9:00 a.m. Rask J. C. * Zeidler-Erdely P. C. Meighan T. Barger M. W. Wallace W. T. Cooper B. Porter D. W. Tranfield E. M. Taylor L. A. McKay D. S. Castranova V. Liu Y. Loftus D. J.
The Chemical Reactivity of Lunar Dust Influences Its Biological Effect **[#3037]**

9:15 a.m. Taylor L. A. *
Water, Water, Everywhere: But How to Find and Use It on the Moon! **[#3023]**

9:30 a.m. Sanders G. B. * Baird R. S. Rogers K. N. Larson W. E. Quinn J. W. Smith J. E. Colaprete A. Elphic R. C. Picard M.
RESOLVE Lunar Ice/Volatile Payload Development and Field Test Status **[#3046]**

9:45 a.m. Heldmann J. L. * Colaprete A. Elphic R. Mattes G. Ennico K. Fritzler E. Marinova M. McMurray R. Morse S. Roush T. Stoker C.
RESOLVE: Real-Time Science Operations to Support a Lunar Polar Volatiles Rover Mission **[#3034]**

10:00 a.m. Cardiff E. H. *
Volatile Extraction and In Situ Resource Utilization for the Moon Applied to Near Earth Objects **[#3041]**

10:15 a.m. BREAK

10:30 a.m. Lester D. F. Valinia A. * Thronson H. Schmidt G.
The First Exploration Telerobotics Symposium — Telepresence: A New Paradigm for Human-Robotic Cooperation **[#3012]**

10:45 a.m. Klaus K. * Post K. Lawrence S. J.
A Sustainable Architecture for Lunar Resource Prospecting from an EML-Based Exploration Platform **[#3009]**

11:00 a.m. Alkalai L. * Solish B. Wlliott J. O. Mueller J. McElrath T. Parker J.
ORION/MoonRise: A Human and Robotic Sample Return Mission Concept from the South Pole-Aitken Basin **[#3053]**

11:15 a.m. Cox R. * Clark P. Vasant A. Meinke R.
Gateways to the Solar System: Innovative Advanced Magnet Lab Mass Driver Launch Platforms at L1 and L2 **[#3007]**

11:30 a.m. Kelso R. M. * Hamilton J. C. Andersen C.
Lunar Concrete — Using Analogue Test Sites on the Big Island of Hawai'i for "Dust-to-Bricks": Demonstration of Technologies Associated with Basalt/Regolith Material Processing/Fabrication/Construction **[#3011]**

11:45 a.m. DISCUSSION

ORION/MoonRise: A Human & Robotic Sample Return Mission Concept from the South Pole-Aitken Basin.

L. Alkalai[1], Ben Solish[1], John O. Elliott[1], Juergen Mueller[1], Timothy McElrath[1], and Jeffrey Parker[1],

[1]Jet Propulsion Laboratory, California Institute of Technology, 4800 Oak Grove Drive, Pasadena, CA 91109, Tel. (818) 653 9274, leon.alkalai@jpl.nasa.gov

Introduction: A new mission concept is proposed for a joint human/robotic mission to return samples from the Lunar South Pole-Aitken Basin (SPAB). The mission concept combines architectural elements under development by NASA's Human Exploration & Operations Mission Directorate (HEOMD): the SLS launch vehicle, the ORION Muti-Purpose Crew Vehicle (MPCV), and a human habitat spacecraft potentially located at the Earth Moon Lagrange point-2 (EML-2). It also utilizes NASA's scientific robotic capabilities funded by NASA's Space Mission Directorate (SMD) including: the MoonRise lunar robotic sample return capabilities [1], [2], the AXEL or ATHLETE mobility capabilities [3], [4], [5], and the Atonomus Landing and Hazard Avoidance Technology (ALHAT) [6]. We present a preliminary mission concept, the trade space that was considered during the study, as well as a detailed discussion of the mission design parameters.

The mission concept envisions separate launches of the human crew using the (crewed) SLS launch vehicle with the Orion MPCV to take the astronauts to an existing spacecraft that was previously launched with the (cargo) SLS and parked in the Earth-Moon Lagrange point-2 (EML-2). Separately from these two lauches, the MoonRise robotic lander and sample return system is launched on an EELV to a lunar parking orbit (EML-1). After the astronauts reach EML-2, the robotic lander descends from EML-1 to a designated landing site within the SPAB. The astronauts in the human-rated spacecraft and the docked MPCV in EML-2 are strategically located to monitor the landing and also to provide the essential communication relay service to Earth. Upon landing, the robotic lander, tele-operated by the astronauts, will collect, sieve and cache samples into a canister located on the Lunar Ascent Vehicle (LAV). Once the sample acquisition is completed, the LAV will lift-off from the lunar surface and deliver the sample canister to the vicinity of the human spacecraft parked in EML-2. The astronauts will capture and return the samples to Earth. The capture strategy may involve proximity navigation and docking including a robotic arm to capture the sample canister. This new and innovative sample return mission concept has multiple features worth noting:

First, given that the MoonRise system does not have to return samples to Earth and does not need a communication relay satellite, the mass savings can be translated into delivering more samples to astronauts located in EML-2 and ultimately for their return to the science community on Earth. Preliminary calculations indicate that at least an order of magnitude more samples can be returned, e.g. 10 kg instead of the 1 kg required by the New Frontiers Program. This has a tremendous value to the science community both in the USA and the potential international partners participating in such a mission. Second, the mission concept that demonstrates the capture of samples in lunar orbit has a clear path forward to future sample return missions at Mars. Third, this mission concept gives a significant role to the astronauts to perform in EML-2 including: i) providing critical relay coverage for the Lander landing in the SPAB; ii) tele-operations of the robotic system on the surface of the Moon, and iii) technology demonstration of the sample capture in lunar orbit.

Finally, there is an opportunity to add a mobility system to the MoonRise lander that could have at least two additional functions: i) Collect samples from beyond the immediate vicinity of the lander, and ii) use the rover to deploy another science instrument such as a low-frequency radio antenna to perform an astrophysics experiment [7].

References:

[1] Jolliff, B. L., C. Shearer, D. Papanastassiou, L. Alkalai, R. Jaumann, G. Osinski, and the MoonRise Science Team (2010), *Lunar Exploration Analysis Group (LEAG) Annual Meeting*, Sep. 14-17, Washington, DC.

[2] Jolliff, B. L., L. Alkalai, C.M. Pieters, J. W. Head III, D. A. Papanastassiou, and E. B. Bierhaus, (2010) *Sampling the South Pole- Aitken Basin: Objectives & site selection criteria*. LPS 41, #2450.

[3] I. A. Nesnas et. al., "Axel and DuAxel Rovers for the Sustainable Exploration of Extreme Terrains," accepted for the *Journal of Field Robotics.*

[4] P. Abad-Manterola, et. al., "Axel: A Minimalist Tethered Rover for Exploration of Extreme Planetary Terrains," *IEEE Robotics and Automation Magazine*, Special Issue on Space Robotics, 2009.

[5] B. Wilcox, *ATHLETE: A Limbed Vehicle for Solar System Exploration*, IEEE Aerospace 2011.

[6] C. D. Epp et. al., *Autonomous Landing and Hazard Avoidance Technology (ALHAT),* IEEE Aerospace 2008.

[7] J. O. Burns, et. al., *A Lunar L2-Farside Exploration and Science Misson Concept with the Orion Multi-Purpose Crew Vehicle and a Teleoperated Lander/Rover*, GLEX-2012.

LATITUDINAL ENRICHMENT OF HYDROGEN IN THE LUNAR POLAR REGIONS: CONSTRAINTS ON HYDROGEN MOBILITY. W. V. Boynton[1], G. F. Droege[1], K. Harshman[1], M. A. Schaffner[1], I. G. Mitrofanov[2], T. P. McClanahan[3], and the LEND team. [1]The University of Arizona, Tucson, AZ USA, wboynton@lpl.arizona.edu, [2]Institute for Space Research, 117997 Moscow, Russia, [3]NASA Goddard Space Flight Center, Greenbelt, MD USA

Introduction: The Clementine mission suggested that deposits of water ice might exist in the permanently shadowed regions (PSRs) near the lunar south pole [1]. Subsequent data of the Lunar Prospector Neutron Spectrometer (LPNS) showed suppression of epithermal neutrons at both poles above 70° latitude, which were interpreted to indicate enhancement of hydrogen, predominantly within PSR areas [2]. More recently the Lunar Exploration Neutron Detector (LEND) onboard the NASA Lunar Reconnaissance Orbiter (LRO) showed, when viewed with its high spatial resolution, that the regions of neutron suppression were not closely related to the PSRs [3]. Two of the PSRs, those associated with the Cabeus and Shoemaker craters, showed significant suppression of neutrons, but others did not. In this work we shall focus not on the neutron suppressed regions (NSRs); rather we are concerned with the hydrogen content of the region between the NSRs.

Methods: A map of the epithermal neutron counting rate was made by binning the LEND counts from the four collimated epithermal neutron detectors using HEALPix [4] bins of size 1.7 km. We first made a plot of epithermal neutron count rate as a function of latitude in one-degree latitude bands between -82° and -90° after excluding the NSRs. A general decrease in count rate (increase in H content) is observed toward the poles.

Discussion: We found that the count rates decrease linearly and nearly identically at both poles. The decrease in epithermal-neutron flux is due to an increase in the H content of the regolith. This distribution of H is very different from the much higher H content of the strong flux depressions seen in the NSRs. The cause of the high H content in the NSRs is not well understood, but this work will discuss what the observed increase in H with latitude can tell us about H mobility on the lunar surface.

There are two obvious sources of hydrogen found on the moon: H_2O from impacts of volatile-rich comets or meteorites and hydrogen from the sun associated with the solar wind or solar particle events (SPEs). By a large margin, the solar wind accounts for the bulk of the lunar H [5].

The H implanted by the solar wind, as well as H_2O deposited from impact sources, can be mobilized by a variety of processes, but all them that rely on external sources, e.g. solar wind sputtering, solar photons, or impacts, are either isotropic or have at most a cosine dependence on latitude [5]. What we observe, however, is that the decrease in count rate at the poles is much steeper than that expected based on cosine dependent processes.

Because the solar-wind deposited H in the grains is saturated, we consider the H in the lunar regolith to be determined by differences between the rates of steady-state gain and loss mechanisms. As shown above, cosine dependent mechanisms cannot by themselves account for the steep decrease in count rate observed in the polar regions. The rate of loss of species due to diffusion of implanted H out of the grains or thermal vaporization, however, are expected to show a very strong dependence on temperature. We suggest the decrease in epithermal-neutron count rate (and increase in H content) is due to much slower vaporization of H in the polar regions.

Before we try to semi-quantitatively model the migration of H, we must first convert the count-rate data into concentrations of H (in all species). To do this we calculate an epithermal-neutron suppression value. The suppression is defined as the ratio of the background-adjusted count rate in an area of interest to that of a reference flux expected for an area containing no H.

Following a procedure like that used by [3], we find an average background-adjusted count rate of 1.6938 ± 0.0012 cps. We then take the average H content in Apollo 16 soils of 45 ppm from [6] as our best estimate of the H content in this area. Using Figure S-1 in the supplementary on-line material of [3], we calculate a reference count rate of 1.79 cps.

Based on the above model-dependent assumptions and the data in Figure 3, we calculate a H content of 120 ppm at 82° latitude and 200 ppm at 89° latitude. The bulk of the excess H above the 45 ppm assumed for that typical of lower latitudes must reside on the surface of the grains since it is difficult for an H_2O molecule on a ballistic trajectory to be imbedded into a grain. The implications of this conclusion will be discussed.

References: [1] P. D. Spudis *et al.*, *Solar Syst. Res.* 32, 17 (1998). [2] W. C. Feldman *et al.*, *Science* 281, 1496 (1998). [3] I.G. Mitrofanov, *et al. Science*, 330, 483–486 (2010). [4] Hierarchical Equal Area isoLatitude Pixelization, http://healpix.jpl.nasa.gov. [5] Boynton *et al.*, *JGR*, (under revision, 2012). [6] Bustin *et al.*, *Proc. Lunar Sci. Conf.* (1984)

Bistatic Radar Observations Of The Moon Using The Arecibo Observatory & Mini-RF On LRO. D. B. J. Bussey[1], R. Schulze[1], D. E. Wahl[2], G. W. Patterson[1], M. Nolan[3], J. R. Jensen[1], F. S. Turner[1], D. A. Yocky[2], J. T. S. Cahill[1], C. V. Jakowatz[2], R. K. Raney[1], and the Mini-RF Team, [1]Applied Physics Laboratory, Laurel MD 20723, [2]Sandia National Laboratory, Albuquerque NM, [3]Arecibo Observatory, Arecibo PR.

Introduction: The Mini-RF team is acquiring bistatic radar measurements that will test the hypothesis that permanently shadowed areas near the lunar poles contain water ice. Additionally these measurements can be used for studies of the composition and structure of pyroclastic deposits, impact ejecta and melts, and the lunar regolith. These bistatic observations (where the Arecibo Observatory Planetary Radar (AO) transmits a 12.6 cm wavelength signal, which is reflected off of the lunar surface and received by the Mini-RF instrument on LRO) have produced the first lunar non beta-zero radar images ever collected.

Rationale: Typically, orbital radar observations use the same antenna to both transmit and receive a signal. The angle between the transmitted and received signals (the bistatic, or beta angle) for these observations is therefore zero, and they are referred to as monostatic observations. By using the AO radar as the transmitter and Mini-RF as the receiver, we have the opportunity to collect data for the Moon with beta angles other than zero. These measurements provide a new and unique test of the water ice hypothesis for the Moon.

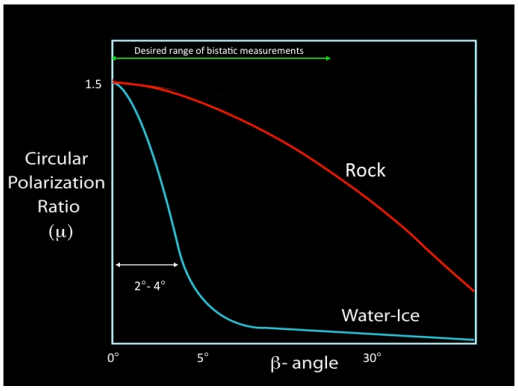

Figure 1. Predicted behavior of CPR versus beta angle for both rock terrains and an ice/regolith mixture.

A common science product produced using planetary radar is the Circular Polarization Ratio [1] (CPR). CPR is the ratio of the powers of received signal in the same sense transmitted divided by the opposite sense. Typical dry lunar surface has a CPR value less than unity [2]. Higher CPR signals can result from multiple-bounce backscatter from rocky surfaces or from the combined volume scattering and coherent backscatter opposition effects (CBOE) from an ice/regolith mixture [2]. The physics of radar scattering predict that high CPR caused by a rocky surface will be relatively insensitive to the beta angle, whilst high CPR caused by ice will be very sensitive to beta, with elevated CPR values dropping off abruptly at beta angles greater than about 1-2° (figure 1).

Figure2. Bistatic image of a portion of the south polar region. Shackleton crater is visible in the top right.

Mini-RF monostatic data shows many craters with high CPR values. Most of these features are associated with fresh, young craters and display elevated CPR both inside and outside their rims. Some permanently shadowed craters near both poles show elevated CPR inside the crater rims but low CPR outside the crater rim. This has been interpreted as being consistent with RF backscatter caused by surface roughness in the former case and water ice in the latter [2].

Planned Observations: We are imaging both polar, and non-polar targets that have high monostatic CPR values (figure 2). By acquiring non beta zero data of equatorial high-CPR regions (which we can safely assume have high CPR due to the presence of surface rocks) we can confirm the hypothesis that high CPR caused by rocks is reasonably invariant to the beta angle (red curve in Figure 1). We are looking to see if monostatic high-CPR polar craters have high or low values in the bistatic data. If we find areas that become low only in the bistatic data then this provides strong supporting evidence that these are ice deposits.

Conclusions: Using Arecibo and Mini-RF we are acquiring the first ever planetary bistatic radar images at non β=0 angles. These data provide a unique new piece of evidence to determine if the Moon's polar craters contain ice.

References: [1] Campbell B. et al., Nature, 2006 [2] Spudis P. D. et al., GRL 2010.

Volatile Extraction and *In Situ* Resource Utilization for the Moon applied to Near Earth Objects. E. H. Cardiff, NASA GSFC, Building 11 Room E135, Greenbelt, MD 20771. Eric.H.Cardiff@nasa.gov.

Introduction: Most *In Situ* Resource Utilization (ISRU) development has been done with respect to either the Moon or Mars, with relatively little applicable to Near Earth Objects (NEOs). Since NASA is now pursuing a "flexible path" strategy for exploration, it behoves the community to look at the application of ISRU that can work at either the Moon or NEOs.

One technique that is applicable for resource extraction at the Moon and on an asteroid is vacuum pyrolyis. The thermal extraction of volatiles is the most promising technique for volatile extraction and scientific measurement of critical volatile species, and has been well demonstrated. Vacuum pyrolysis has also been demonstrated to produce substantial volatiles from regolith stimulants, including oxygen [1].

Solar Heating: A mobile platform (shown in Figure 1) has been developed at NASA GSFC to sinter and melt simulated lunar regolith. It has been demonstrated (as illustrated in Figure 2 for two samples), and the melting rates have been quantified. The vehicle consists of a chassis that supports a $1m^2$ lens used to focus the solar flux. The position of the vehicle and of the lens is determined remotely by radio control.

Figure 1: The NASA GSFC Fresnel lens vehicle [2].

The melting volumetric rate produced by the Fresnel lens vehicle was 2.6 cm^3 / min [2] (or 7.5 g/min for JSC-1A). By manipulating the lens, the focal area and intensity can be altered – thus allowing the production of volatiles with different release patterns.

Resistive Heating: A vacuum chamber has been used at NASA GSFC to study multiple configurations of crucibles to resitively heat regolith stimulants. A custom zirconia crucible with embedded tungsten resistive heating elements is used to pyrolyze the simulant. The resistive heating element connects to a power input from the bottom, delivering up to 160 DC volts and over 2000 W. The crucible and stands are surrounded by several layers of tungsten foil shields heat shields.

The improved crucible and shielding in this configuration required 200 W.hr to take 0.1 g of JSC1A to 1600 degrees C.

Near Earth Objects: The high temperature of 1600 C is not required to extract volatiles from cometary material, but cometary material is the least likely to be collected as a bulk resource. It is expected that for Near Earth Asteroids (NEAs) that may have undergone substantial heating cycles, there will be a multi-modal release pattern with low temperature volatiles or solar wind volatiles releasing at low temperatures, and residual volatiles from when the minerals were formed being released by high and prolonged temperatures. Because the density of NEAs is not well known, potential exploration targets may vary in mass by factor of 2. Typical 7 m diameter asteroids may vary from 300 T to 600 T of material.[3]

Scaling: At current rates, it would take a 1 m^2 Fresnel lens 76 years to process a 300 T asteroid. While that might meet current utilization rates on orbit, the rate could be accelerated linearly. Accordingly, a 100 m^2 Fresnel lens (which is within current state of the art processing capabilities for etched surfaces) could process the entire asteroid in less than a year.

Scaling the resistive process is merely a matter of power. At the current processing rates, an 83 kW power system (similar to the International Space Station) could process the same 300 T asteroid in a little over 825 years.

Scaling: Direct solar heating is clearly advantageous in terms of processing capability, but also imposes significant difficulties. Resistive heating is much easier to contain. Without significant precautions, direct solar heating can cause condensation of the released volatiles on cooler processing optics, leading to failure of the optics. However, resistive elements are much more susceptible to thermal shock, and thereby limit the processing rate.

It should be noted that the processing capability should be driven by the demand for the volatiles. The scaled resistive heating system would supply over 300 kg of material per year, which is a significant material stream, with a relatively high value.

References: [1] E. Cardiff, B. Pomeroy, I. Banks, and A. Benz, *Vacuum Pyrolysis and Related ISRU Techniques*, STAIF, 2007. [2] 5. E.H. Cardiff, and Hall, B. C., *A Dust Mitigation Vehicle Utilizing Direct Solar Heating*, Space Resources Roundtable X, October, 2008. [3] *Asteroid Retrieval Feasibility Study*, April 2012, Keck Institute for Space Studies, JPL.

A REVISIT TO APOLLO MAGNETIC FIELD RECORDS FOR SOUNDING OF THE LUNAR INTERIOR.

P. J. Chi[1,2], [1]Institute of Geophysics and Planetary Physics, University of California, Box 951567, Los Angeles, California 90095; E-mail: pchi@igpp.ucla.edu, [2]Space Weather Laboratory, Heliophysics Division, Goddard Space Flight Center, Greenbelt, Maryland 20771.

Introduction: Between 1969 and 1975 three Apollo missions collected a unique set of magnetic field records measured on the surface of the Moon and in orbit at about 100 km above the surface. One of the important uses of these magnetic field records is to detect the lunar interior, such as a metallic core, by electromagnetic sounding methods. The popular approach is the use of an orbiting Apollo sub-satellite and a Lunar Surface Magnetometer (LSM) to measure respectively the input to the Moon and the sum of the input and the response [1,2]. Studies using this approach suggest either no evidence of a core with an upper limit of about 360 km [3] or a paramagnetic Moon [4]. Another approach probes the deep interior of the Moon using a low-altitude orbiting sub-satellite magnetometer to measure the induced dipole moment of the Moon in the magnetictail lobes [5,6]. The Apollo sub-satellite meausrements detected an induced magnetic field of $-4.2\pm0.6\times10^{22}$ Gauss-cm^3 per Gauss of applied field, suggesting an electrically conducting core with a radius of slightly more than 400 km [7]. The two approaches did not necessarily yield the same result.

Revisit to Apollo Magnetic Field Data: The two-instrument studies depend crucially on the accurate intercalibration of the magnetometers, and some of these earlier studies might have suffered from the differences in the gain of the magnetometers [8] that worth re-analysis with a careful calibration across different instruments. For over two decades, the format of the Apollo magnetic data had become obsolete, and the data were difficult to study. Only until recently are we able to restore the Apollo sub-satellite magnetometer data and a small portion of the LSM data. We selected a few intervals in 1971 where both Apollo 15 sub-satellite and LSM were operational, and we compared the two measurements in the solar wind, in the magnetosheath, and in the magnetotail for the intercalibration of the instruments as well as the sounding of the lunar interior. The comparison between the two Apollo instruments has not been made in the past, and we will assess how the results are compared with those obtained in early studies using Explorer 35 for upstream measurements.

Looking Forward: The revisit to the Apollo magnetic field records reminds us that for more than 37 years we have not been making magnetic field measurements on the surface of the Moon. Surface measurements have their unique role that cannot be replaced by orbital measurements. The resolution of Apollo magnetic observations may be coarse, and the intercalibration of the Apollo measurements made several decades ago may be more difficult today. Nevertheless, the lessons learned from revisits to the Apollo magnetic observations can provide useful references for planning future lunar surface experiments.

References: [1] Wiskerchen M. J. and Sonnett C. P. (1977) *PLSC IX*, 3113-3124. [2] Dyal P. et al. (1976) *JGR, 84*, 3313-3326. [3] Hood L. L. et al., (1981) *Lunar Science XII*, 457-459. [4] Parkin C. W. et al. (1973) *PLSC IV*, 2947-2961. [5] Goldstein B. E. et al. (1976a) *GRL, 3*, 289-292. [6] Goldstein B. E. et al. (1976b) *PLSC 7*, 3321-3341. [7] Russell C. T. et al. (1981) *PLPS 12B*, 831-836. [8] Daily W. D. and Dyal P. (1979) *PLSC VII*, 3313-3326.

LunarCube: Payload Development for Enhanced yet Low Cost Lunar Exploration;
P.E. Clark, CUA; R. MacDowall, NASA/GSFC; R. Cox, A. Vasant, Flexure Engineering; M.L. Rilee, RST; S. Schaire, NASA/WFF; B. Malphrus, Morehead State University

We are proposing LunarCube, a space architecture that extends the affordable and successful CubeSat approach, to facilitate access to the Moon. CubeSat provides standards for bus design and operation for low–cost, focused–objective, Earth orbital missions via open access documentation and even online purchasable kits, facilitating the implementation process, and reducing development costs, risks, and time. The bus provides standardized interfaces and shared access by guest 'instruments' to all subsystems using CubeSat protocols. Four key aspects of specified design are: 1) profile: short duration, low earth orbit; 2) form factor: multiple 10 cm cubes (U), typically varying from 0.5 to 3 U; 3) technology impact: low, incorporating off the shelf electronics and software; 4) risk: Class D, based on the rationale that CubeSat standards have been improved and demonstrated with use, and failures have far less impact, in terms of expenditures and size of groups involved, than conventional government sponsored 'missions'. Part of its appeal is that CubeSat afforded universities access for hands on student education. After a decade of development, this approach is beginning to yield scientifically useful monitoring of Earth's atmosphere and climate through combined experiments (e.g., CINEMA, CubeSat for Ions, Neutrals, Electron, and Magnetic Fields). Most recently CubeSat has been proposed as a model for a lunar swirl study mission.

LunarCube deals with risk analogously by bus standardization and modularization, still keeping costs low, while extending the current CubeSat concept in stages to include additional capability required for deep space operation in five key areas: 1) profile: increase duration from months to years; 2) form factor: grow to at least 6U as needed; 3) control: active attitude control and propulsion, made sustainable with onboard intelligence for routine multi-platform operation; 4) information transfer: more robust communication and C&DH to support onboard processing, made sustainable with onboard intelligence for routine multi-platform operation, and 5) thermal/mechanical design: greater hardness to deep space radiation and ruggedness for extreme thermal variation, potentially using MilSpec components initially, but ultimately requiring state of the art cold temperature electronics and power developments for deep cryo operation. Accomplishment of these, with some degree of onboard intelligence, would allow multiple platform operation in cis-lunar space, as well as survival and operation for at least a limited duty cycle on, the lunar surface. More robust and larger 6U CubeSat concepts exist. Stage 2 would require fully implementing onboard intelligence (3 and 4) and deep cryo design in electronics, power systems, mechanisms (moving parts), precision navigation and control, and advanced payload integration. Full operation on the lunar surface would be possible. At this stage, the LunarCube could be a virtual 'smart phone' with a 'nano–rack' representing a variety of experiments, as open access software applications.

A critical need for LunarCube development is obtaining inputs on required resources (Mass, power, bandwidth, volume) for the broad range of instruments required to do cutting edge science, and continuing the development of onboard intelligence to support processing for highly selective data return as well as guidance, navigation and control without 'ground control', allowing temporally and spatially distributed measurements of 3D systems from distributed platforms with minimal bandwidth.

Frontier: Towards Onboard Intelligence For Next Generation Space Assets; P.E. Clark, CUA; M.L. Rilee, Rilee Systems Technologies; S.A. Curtis, Tetrobotics

We are working toward development of Frontier, a highly adaptable, stably reconfigurable, web–accessible intelligent decision engine that will be capable of optimizing the design and simulating the operation of, and ultimately operating complex systems, ranging from instruments to multi-platform distributed assets, in response to evolving needs and environments. The most innovative aspect of Frontier is what makes it truly unique, capable of absorbing and utilizing lessons learned and thus evolving from a tool to a tool user: an adaptable framework consisting of a decision engine with evolving intelligence based on a genetic algorithm–driven evolving neural interface with an evolving synthetic neural system consisting of neural basis functions for the human (to the Stakeholder GUI) and tool (to the modeling support environment) interfaces and a specially designed stability algorithm to balance rule– and choice–driven inputs originating from either side facilitate the design evaluation and selection process. The adaptable framework will be increasingly capable of dynamic reconfiguration of parameters and rules associated with tools and resources, as well as selection of tools most optimally matched to stakeholder needs through pattern recognition in response to 'lessons learned'. Frontier is built on an open source, web services oriented environment. Through web–based interfaces, it will support distributed, multi–user, concurrent access to resources and tools, including the human and tool interfaces, modeling and development services, databases, simulation, scenario development, analysis, and evaluation.

In our NASA Edison SmartSat proposal, we apply Frontier in the demonstration of autonomous close proximity operations critical for deep space operation, including knowledge and control of orientation and position to support formation flying, close approach, stationkeeping, changing orbital parameters, and active/passive object interactions, with progressively greater onboard intelligence drive by Frontier intelligent decision engine (IDE). Morehead State University provides the 3 3U standard cubesat buses with 1) IDE based on GSFC patented Synthetic Neural System Nervous Net Attitude Control and Neural Net Target Discrimination, Tracking, and Prediction leveraged from previously supported developments in support of NASA ST-8 choice driven system for an autonomous navigation demonstration, and DARPA System F6 intelligent decision engine; 2) Morehead State University 60GHz RF System with omni-antennas for distance and direction determination, inter-spacecraft communication, and atmospheric sounding (science mode); 3) Honeywell Dependable Multiprocessor (DM), with GPS determination capability leveraged from NASA ST-8 and the DOD SMDC TechSat; 4) In-Space primary propulsion utilizing Busek resistojet thrusters leveraged from developments in support of the Air Force NanoSat Program and demonstrating sufficient Delta-V and ISP to support our proximity operations.

SmartSat has three levels of autonomy, from lowest level health & safety and control software baseline flight software (BFS) mainly on the standard C&DH platform, and two higher levels associated with the Synthetic Neural System Neural Basis Functions running as a DM application and consisting of low-level controllers to drive spacecraft behaviors through command sequences and high-level controllers to deal with more complex or symbolic tasks, for example, selecting between safing alternatives or collision avoidance trajectories.

Near Real-Time Prospecting for Lunar Volatiles: Demonstrating RESOLVE Science in the Field A. Colaprete[1], R. Elphic[1], J. L. Heldmann[1], G. Mattes[2], K. Ennico[1], E. Fritzler[1], M. Marinova[1], R. McMurray[1], S. Morse[1], T. Roush[1], C. Stoker[1], Jerry Sanders[2], Jackie Quinn[3], Bill Larson[3], M. Picard[4], [1]NASA Ames Research Center, Moffett Field, CA, [2]NASA Johnson Space Center, Houston, TX, [3]NASA Kennedy Space Center, FL, [4]Candian Space Center, Québec, Canada.

Introduction: The Regolith and Environment Science and Oxygen & Lunar Volatile Extraction (RESOLVE) project aims to demonstrate the utility of "in situ resource utilization". In situ resource utilization (ISRU) is a way to rebalance the economics of spaceflight by reducing or eliminating materials that must be brought up from Earth and placed on the surface of the Moon for human use. RESOLVE is developing a rover-borne payload that (1) can locate near subsurface volatiles, (2) excavate and analyze samples of the volatile-bearing regolith, and (3) demonstrate the form, extractability and usefulness of the materials. Such investigations are important not only for ISRU but are also critically important for understanding the scientific nature of these intriguing lunar polar volatile deposits.

Temperature models and orbital data suggest near surface volatile concentrations may exist at briefly lit lunar polar locations outside persistently shadowed regions. A lunar rover could be remotely operated at some of these locations for the 4-7 days of expected sunlight at relatively low cost.

RESOLVE Field Test: In July 2012 the RESOLVE project conducted a full-scale field demonstration. In particular, the ability to perform the real-time measurement analysis necessary to search for volatiles and the ability to combine the various measurement techniques to meet the mission measurement and science goals. With help from the Pacific International Space Center for Exploration Systems (PISCES), a lunar rover prototype (provided by the Canadian Space Agency) was equipped with a suite of prospecting instruments (neutron spectrometer and near-infrared spectrometer), subsurface access and sampling tools, including both an auger and coring drill (provided by CSA) and subsurface sample analysis instrumentation, including a sample oven system, the Oxygen and Volatile Extraction Node (OVEN), and Gas Chromatograph / Mass Spectrometer system, the Lunar Advanced Volatile Analysis (LAVA) system. This paper will discuss how the RESOLVE science was demonstrated during the field campaign.

Real-time Prospecting and Combined Instrument Science: Given the relatively short time period this lunar mission is being designed to, prospecting for sites of interest needs to occur near real-time. The two instruments which are being used for prospecting are the neutron and NIR spectrometers (Fig. 1). In the flight mission the neutron spectrometer would sense hydrogen down to concentrations as low as 0.5WT% to a depth of approximately 80 cm. This instrument is the principle instrument for identifying buried volatiles. In flight the neutron source is the integration of galactic rays with the lunar regolith. In the field demo a small radioactive source provided the neutron flux. The NIR spectrometer, which includes its own light source, looks at surface reflectance for signatures of bound H2O/OH and general mineralogy. The RESOLVE flight instrument will work between 1.7-3.4 um; however for the field demonstration a LCROSS NIR spectrometer engineering unit was used which operates between 1.2-2.4 um. Once an area of interest was identified by the neutron and/or NIR spectrometer (what was referred to as a "hot spot") the option to drill was considered. The drill could either auger or core. The auger drill worked to a depth of 50 cm and is monitored with a drill camera and the NIR spectrometer. As cuttings are brought up the NIR spectra is monitored. If a particular location is considered of high-interest then the decision to core could be made. The coring drill (a push-tube) allowed a 1-meter sample to be acquired and then processed by the OVEN/LAVA system. This presentation will provide details as to how these instruments worked together and how and if the planned measurements and science was obtained.

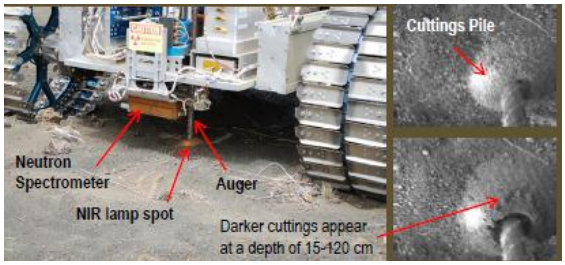

Figure 1. The RESOLVE Payload on the Artemis Jr. rover: Shown is an augering activity with the NIR lamp illuminating the drill spot the view from the Dril Camera.

Gateways to the Solar System: Innovative Advanced Magnet Lab Mass Driver Launch Platforms at L1 and L2

Cox, Clark, Vasant, Meinke

Lagrange points 1 and 2, each about 1.5 million kilometers from the Earth, are potential gateways to the solar system. From either point, many deep space destinations, including the Moon, Mars, or asteroids, would be accessible at much lower Delta-V than a direct transfer would require. At either gateway, an efficient, reusable launch platform, such as the Advanced Magnetics Lab mass driver discussed here, would provide further reduction in resources required to reach these destinations. The advanced magnet lab offers unique technology solution for a low mass launch tube driven by magnetic levitation, through the use of superconducting materials, 3D simulation and control of conductor placement and coil geometry, and automated manufacturing of multi-layered coils. This combination generates the highly stable double helix field with unprecedented robustness, reliability, and radiation tolerance, all of which lower production costs. L1 or L2 Gateways are reachable from a Geosynchronous Transfer Orbits (GTO) through a small hop. Although such weak stability transfers require more time, they require much less energy. Many Geosynchronous communications satellite insertions have unused "Launch Performance" such that as much as 5,000 pounds could ride along and be placed in a GTO at very low cost. Thus, from those gateways, many smallsats, including Interplanetary CubeSats or LunarCube-based missions could be sent to many destinations throughout the solar system. As an example, let's assume, conservatively, we have placed a 2,000 kg 'ride along' payload into a GTO as a ride along payload, where, conservatively, 1,000 kg represents the vehicle needed to get to the gateway, and 1,000 kg the remainder, including a 500 kg payload consisting of tens of 10 to 15 kg 2x2x2 or 2x2x3 U cubesats bound for another destination, and a reusable launch platform. The launch platform would be comprised of the spacecraft bus mass, solar arrays, long duration power storage, a rapid discharge power system and launch control electronics, all of which will support an Advanced Magnetics Lab Mass Driver launch tube with conventional or superconducting coils. Once the chemical or other conventional propulsion system has placed the Launch Platform near the L1 or L2 Gateway the approximately 50 free flying spacecraft would be transferred to the AML Mass Driver and launched, one at a time, to their final destinations throughout the solar system. To calculate the efficiency of this launch sequence you would divide the total mass at the gateway by the number of launches. The kinetic energy is being provided by the "massless " solar flux at 1 AU. This architecture could offer a very low cost, flexible, and thus effective mechanism for solar system exploration.

Modal Evaluation of Fluid Volume in Spacecraft Propellant Tanks

Kevin M. Crosby[1], Rudy Werlink[2], Steven Mathe[1], Kevin Lubick[1], [1]Carthage College, Kenosha, WI, USA (kcrosby@carthage.edu), [2]NASA Kennedy Space Center, Florida, USA (rudy.werlink-1@nasa.gov)

Introduction: Low gravity propellant mass gauging is identified in NASA's Exploratory Systems Architecture Study as a primary research challenge. The future of manned spaceflight beyond LEO relies in part on the development of accurate and robust methods of mass gauging in both settled and unsettled propellant states.

In the present study, we describe the use of experimental modal analysis (EMA) to infer fluid levels in model spacecraft propellant tanks in a microgravity environment provided by parabolic flights.

Modal Analysis Technique: EMA involves the application of acoustic forces to test structures. Natural resonances of the test structure are excited by the applied force, and sensors affixed to the structure record the amplitude of the acoustic response across the range of resonating frequencies.

Typically, EMA involves the computation of frequency response functions (FRF) to determine the resonant frequencies present at each sensor location. The FRF shows peaks at the frequencies where a sensor records a strong resonance that is not present in the spectrum of the input signal. Modal techniques can therefore be used as real-time diagnostics of structural properties. Fluid loading increases the effective mass of the loaded structure, resulting in a decrease in the structure's resonant frequencies.

Experimental Design: Our experimental rig consists of cylindrical steel tanks of diameter 15.3 cm, and total length including two spherical end caps of 48.3 cm. The tanks each have a capacity of two gallons. PZT sensors affixed to the surface of each tank record the vibrational response to the white noise signal presented to the tank surface via a PZT actuator. Fluid fill levels are independently calculated by means of both a flow totalizer and PVT methods. Water is used as the propellant simulant in all tests.

Results: The fundamental resonance at representative fill fractions with a settled fluid under 1-g lab testing is illustrated in Fig. 1. The structure's effective mass increases with fluid load, resulting in a continuous decrease in the frequencies of tank resonances.

In the reduced gravity of parabolic flight, fluid instabilities cause the fluid to slosh resulting in continual variation of the contact area between fluid and tank wall. As a result, the frequencies of resonant modes drift around their means with periods on the order of the average slosh period of 1-2 seconds. To compensate for this effect, we average over multiple 1.0 second FRF data windows. A set of sample averaged FRFs is shown in Fig. 2.

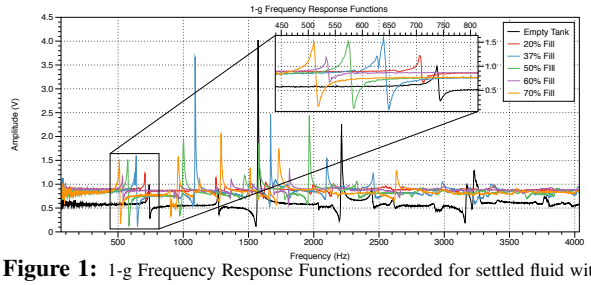

Figure 1: 1-g Frequency Response Functions recorded for settled fluid with tank in vertical position. Inset shows blow-up of fundamental mode and demonstrates the decrease of mode frequency with increasing fill-fraction.

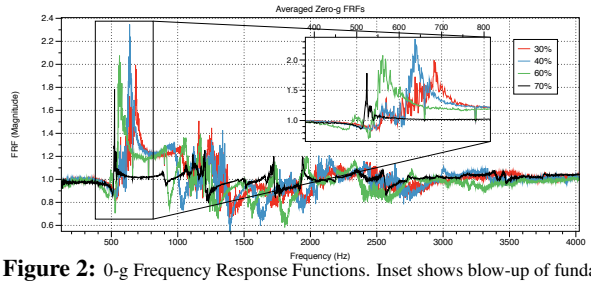

Figure 2: 0-g Frequency Response Functions. Inset shows blow-up of fundamental mode and demonstrates the decrease of mode frequency with increasing fill-fraction.

The resolution of the EMA technique in discriminating between fill fraction can be estimated from the summary data presented in Fig. 3.

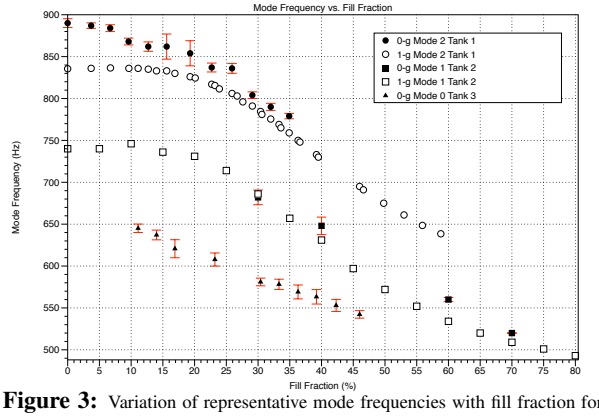

Figure 3: Variation of representative mode frequencies with fill fraction for both 1-g settled fluid configurations and 0-g slosh-averaged fluid. Error bars on the flight data represent standard error in the data, while error bars for the 1-g data are not depicted, but would be smaller than the data symbol.

The flight data in Fig. 3 have a typical frequency resolution that is better than 5% across fill fractions between 10% and 70%. Nodes in the tank structure near tank weld seams correlate well with a loss of resolution between fill-fractions.

GROUND DATA SYSTEMS FOR REAL TIME LUNAR SCIENCE. M. C. Deans[1], T. Smith[2], D. S. Lees[2], E. B. Scharff[3], T. E. Cohen[3], D. S. S. Lim[4], [1]NASA Ames Research Center, Moffett Field, CA, USA, matthew.deans@nasa.gov, [2]Carnegie Mellon Silicon Valley, Moffett Field, CA, USA, [3]Stinger-Ghaffarian Technologies, Moffett Field, CA, USA, [4]SETI Institute, Mountain View, CA, USA.

Introduction: We designed, developed, and tested science operations support software using our Exploration Ground Data System (xGDS) framework[1] for the Regolith and Environmental Science, Oxygen and Lunar Volatiles Exploration (RESOLVE)[2] field test, culminating in the test on Mauna Kea in July of 2012.

Background: xGDS has been developed under the Human Robotic Systems (HRS) project[3]. The architecture and core system are designed to be flexible to scientific field work and mission operations, covering planning, operations, and post-mission data analysis. Instances of xGDS have been tailored to the K10 rover [4], piloted submersibles [5,6] and surface vehicles[7], and now RESOLVE. These represent analogs to human and robotic planetary missions, with different constraints on objectives, operations concepts, comms, *a priori* knowledge, goals, etc.

System Architecture: xGDS core systems include a map content management system, a traverse planner, plots, a data product archive, a console log and search tools. Our system is designed to be flexible, modular and based on open standards. Supporting multiple different field tests has helped our team to keep the software modular since any one deployment may use a distinct subset of the core capabilities.

We built xGDS using Python and the Django web framework backed by a MySQL database. xGDS was designed to be accessed primarily through web browsers and Google Earth, so that we could focus on data management and dynamic content while leveraging familiar user interfaces. This minimizes our development time and users' training time.

The RESOLVE project included 5 operations centers and about 100 simultaneous users. Rover and payload telemetry used two different protocols and information was integrated in xGDS on the ground. xGDS was required to produce real time plots and maps of data that would be immediately visible to any users.

xGDS Tools for RESOLVE: We deployed several xGDS tools for the RESOLVE mission.

Planning: The xGDS traverse planner uses the Google Earth web plug-in embedded in a web page to enable map-based editing of traverse plans with other plan parameters, such as distances, time estimates, range and bearing reflected in the same page.

Monitoring: We added real-time 2D plotting and grid-based mapping to xGDS specifically for RESOLVE. These tools generate plots of 1-D quantities to show temporal variations and correlations in measurements vs. time, and 2-D heatmaps of measurements vs. vehicle location (Fig. 1) to aid in localizing geographic points of interest for prospecting.

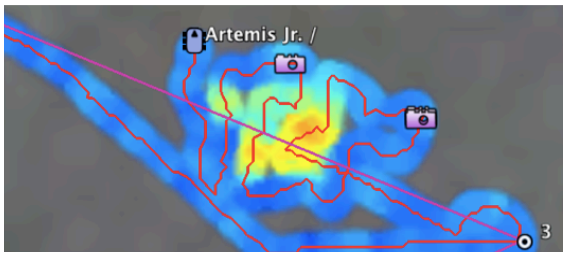

Fig 2. xGDS raster map of Neutron Spectrometer data.

Console Log: Every console operator kept their own time-tagged log by entering free-form text and twitter-style hashtags. All consoles could browse entries chronologically or search by text or hashtag to find entries related to events, observations, etc.

Archive: xGDS supported browsing or search of discrete data products, such as images, in a paginated chronological list and in a map containing georeferenced links in context with satellite images, plans, rover tracks, and any other map content available.

Assessment: We also established a means of assessing the utility of our software for the operations team, primarily in the Ames science back room. The approach leveraged the metrics developed and used at PLRP[4] over several field seasons.

Results: Field testing showed that real time science is feasible with fast diagnostics (esp. band depth plots) and visualizations, that xGDS tools and capabilities are valuable assets for a science team to make decisions quickly, and revealed improvements we can make to the system for a flight mission.

References: [1] M. Deans, et al. (2011) LPSC XLII #2765 [2] B. Larson et al. (2012) GLEX-2012.11.1.8 [3] R. O. Ambrose (2012) ICAPS [4] T. Fong et al. (2009) IAC-09.A5.2.-B3.6.7 [5] D. Lim, et al. (2011) GSA Special Papers 2011, v.483, p.85-115 [6] A. Abercromby, et al. (2012) Acta Astronautica [7] S. Lee, et al. (2012) Acta Astronautica

Acknowledgments: This work was funded by OCT Game Changing Technologies, SMD LASER, and HEOMD AES program. We thank the HRS, RESOLVE, and AES Analogs projects for support, and the RESOLVE team for help defining requirements, testing systems, and providing valuable feedback.

THE LUNAR ATMOSPHERE AND DUST ENVIRONMENT EXPLORER (LADEE): T-MINUS ONE YEAR AND COUNTING. R. C. Elphic[1], G. T. Delory[2], E. J. Grayzeck[3], A. Colaprete[1], M. Horanyi[5], P. Mahaffy[4], B. Hine[1], D. Boroson[6], and J. S. Salut[3], [1]Planetary Systems Branch, NASA Ames Research Center, MS 245-3, Moffett Field, CA, 94035-1000, [2]Space Sciences Laboratory, University of California, Berkeley CA 94720, [3]Planetary Science Division, Science Mission Directorate, NASA, Washington, DC 20546, [4]NASA Goddard Space Flight Center, Greenbelt, MD, 20771, [5]Laboratory for Atmospheric and Space Physics, University of Colorado, Boulder, CO 80309, [6]Lincoln Laboratory, Massachusetts Institute of Technology, Lexington MA 02421

Introduction: 40 years have passed since the last Apollo missions investigated the mysteries of the lunar atmosphere and the question of levitated lunar dust. The most important questions remain: what is the composition, structure and variability of the tenuous lunar exosphere? What are its origins, transport mechanisms, and loss processes? Is lofted lunar dust the cause of the Surveyor and astronaut horizon glow observations? How does such levitated dust arise and move, what is its density, and what is its ultimate fate?

Past National Research Council decadal surveys, and the "Scientific Context for Exploration of the Moon" (SCEM) report have identified studies of the pristine state of the lunar atmosphere and dust environment as among the leading priorities for future lunar science missions. These measurements have become particularly important since recent observations by the Lunar Crater Observation and Sensing Satellite (LCROSS) mission point to significant water and other volatiles sequestered within polar lunar cold traps. Moreover, Chandrayaan M^3/EPOXI/Cassini VIMS identifications of H_2O and OH on surface regolith grains hint at variability in time and space; these species are likely present in the exosphere, and thus constitute a source for the cold traps.

The LADEE Mission: The Lunar Atmosphere and Dust Environment Explorer (LADEE) is currently in integration and test, aiming for launch in August of 2013. LADEE will determine the composition of the lunar atmosphere and investigate the processes that control its distribution and variability, including sources, sinks, and surface interactions. LADEE will also determine whether dust is present in the lunar exosphere, and reveal its sources and variability. These investigations are relevant to our understanding of surface boundary exospheres and dust processes occurring at many objects throughout the solar system, address questions regarding the origin and evolution of lunar volatiles, and have potential implications for future exploration activities.

The LADEE Payload: LADEE employs a high heritage instrument payload: a Neutral Mass Spectrometer (NMS) from Goddard Space Flight Center, an Ultraviolet/Visible Spectrometer (UVS) from Ames Rsearch Center, and a dust detection experiment (LDEX) from the University of Colorado/LASP. It will also carry the Lunar Laser Communications Demonstration (LLCD) as a technology demonstration. The LLCD is funded by the Space Operations Mission Directorate (SOMD), managed by GSFC, and built by the MIT Lincoln Labs.

The LADEE NMS instrument for LADEE draws its design from the MSL/SAM, CONTOUR and MAVEN projects, and covers the 2-150 Dalton mass range. The UVS instrument is a next-generation, high-reliability redesign of the LCROSS UV-Vis spectrometer, spanning 250-800 nm wavelength, with high (<1 nm) spectral resolution. UVS will also perform dust occultation measurements via a solar viewer optic. LDEX senses dust impacts in situ, at LADEE orbital altitudes, with a particle size range of between 100 nm and 5 μm. Dust particle impacts on a large spherical target surface create electron and ion pairs. The latter are focused and accelerated in an electric field and detected at a microchannel plate. The overall LADEE payload configuration is shown below.

Status of LADEE Mission: LADEE is currently in I&T, with the immiment integration of the first two payload instruments, UVS and LDEX. Integrated observatory testing will continue until LADEE is shipped to Wallops for launch processing in June 2013. The first launch opportunity is currently August 10, 2013.

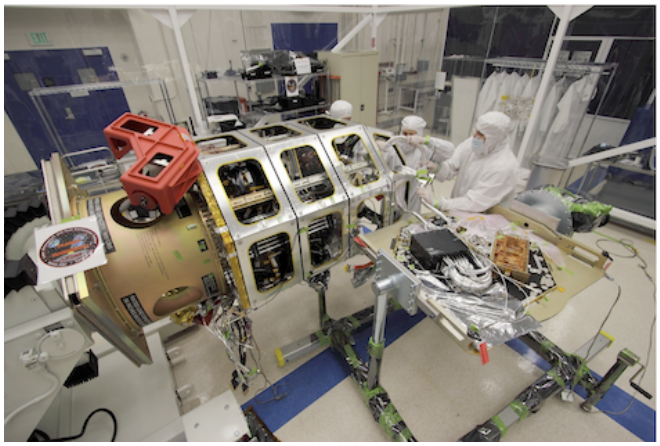

Fig. 1. LADEE in integration and test within its clean tent.

DREAM CENTER FOR LUNAR SCIENCE: A THREE YEAR SUMMARY REPORT. W. M. Farrell[1,3], R. M. Killen[1,3], and G. T. Delory[2,3], [1]Solar System Exploration Division, NASA/Goddard Space Flight Center, Greenbelt, MD, [2]Space Science Laboratory, University of California, Berkeley, CA, [3]NASA's Lunar Science Institute, NASA/Ames Research Center, Moffett Field, CA.

Abstract. In early 2009, the Dynamic Response of the Environment At the Moon (DREAM) lunar science center became a supporting team of NASA's Lunar Science Institute specifically to study the solar-lunar connection and understand the response of the lunar plasma, exosphere, dust, and near-surface environments to solar variations. DREAM especially emphasizes the effect extreme events like solar storms and impacts have on the plasma-surface-gas dynamical system.

One of the center's hallmark contribution is the solar storm/lunar atmosphere modeling (SSLAM) study that cross-integrated a large number of the center's models to determine the effect a strong solar storm has at the Moon. The results from this intramural event will be described herein.

A number of other key studies were performed, including a unique ground-based observation of the LCROSS impact-generated sodium plume, exo-atmosphere modeling studies, and focused studies on the formation and distribution of lunar water. The team is supporting ARTEMIS lunar plasma interaction studies via modeling/data validation efforts, especially examining ion reflection from magnetic anomalies and pick-up ions from the Moon.

Special emphasis has been on simulating the ambipolar-driven inflow of solar wind into polar craters, and the sputtering effect on any near-surface volatiles. DREAM models predict that this sputtering and impact vaporization may effectively 'dry out' the upper surface – not by submlimation but by the more-violent space weathering process.

The team has also produced a set of works in support of the 2013 LADEE mission. Light scattering models have been developed for predicting the horizon glow expected from high altitude dust in support of the UVS and LDEX instruments. Exospheric models have been developed to estimate the atomic and molecular gas UV florescence values and to bound expected UVS measurements.

DREAM successfully advanced the understanding of the solar-driven lunar environment from the Apollo era to the Altair era and has direct applications to other exposed rocky bodies in our new target-independent, flexible era of exploration.

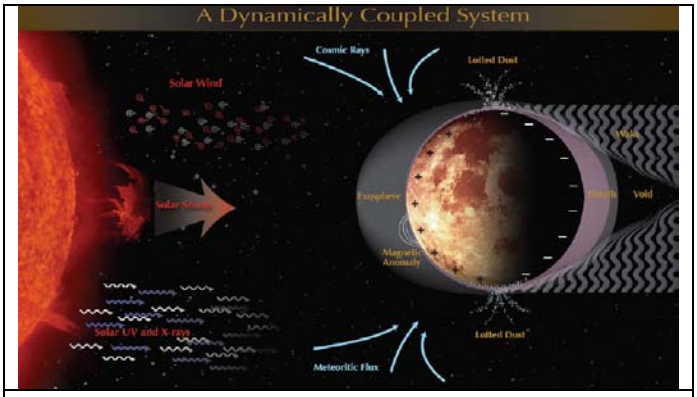

The Solar-Lunar Connection studies by DREAM. Solar energy and matter stimulate the lunar surface, resulting in an exosphere, exo-ionosphere, lifted dust, and plasma flow layers.

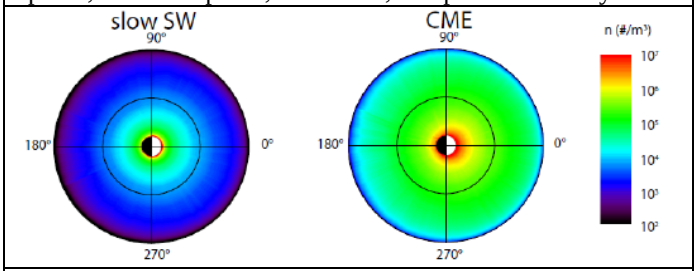

A model of the enhancment expected of the sodium exosphere during the passage of a dense cool CME driver gas. Models like this were key output from the SSLAM study.

DREAM supports E/PO objective, including Maryland Day activities shown here.

THE SEARCH FOR A HIGH ALTITUDE DUST EXOSPHERE: OBSERVATIONAL STATUS AND DUST UPPER LIMITS. D. A. Glenar[1,2], T. J. Stubbs[3,4,2], W. M. Farrell[4,2], J. W. Keller[4,2], R. R. Vondrak[4,2], [1]New Mexico State University (dglenar@nmsu.edu), [2]NASA Lunar Science Institute, [3]University of Maryland, Baltimore County, [4]NASA Goddard Space Flight Center.

Introduction: Strong evidence for a lunar dust exosphere appeared during Apollo-era optical observations (see below). Additional confirmation has been much anticipated as a baseline for the upcoming LADEE mission[1], but so far, no confident detection of a dust exosphere has been made since that time. Dust is detected optically via single-scattering of sunlight, and would appear from orbit as faint horizon glow (HG) near the limb, a consequence of its small expected scale height (5-10 km). At near-UV/VIS wavelengths, HG would also be superimposed on the coronal-zodiacal light (CZL) background, which brightens rapidly at small solar elongation angle[2] and complicates the measurements. Line-of-sight (LOS) dust optical depth is expected to be very small ($< 10^{-5}$) with dust concentration < 0.01 cm^{-3} at a few km altitude, although these numbers are sensitive to grain size and illumination altitude. We summarize the search results that have so far been reported, and use these to estimate dust concentration and upper limits.

Searches for High Altitude Horizon Glow:

Apollo Era. Excess limb brightness was observed in Apollo 15 coronal photographs, and analyzed in terms of dust at altitudes of a few km or higher[3],[4]. The notion of a measurable dust exosphere was further supported by Apollo 17 astronaut observations[5] of horizon glow with apparent radial crepuscular rays, dubbed "streamers", as well as measurements of sky brightness by uplooking photometers on the Lunokhod-2 lander, acquired shortly after surface sunset[6].

Clementine Star Trackers. Portions of 25 orbits were allocated to limb searches for horizon glow using the Clementine navigational star trackers[7]. Four of the image sequences were made at small solar elongation angles and free of earthshine at the limb, which lessens the chance of stray light contamination. No obvious HG appears in these data sets above the detection limit of 2-3 x 10^{-12} B_{Sun} (with B_{Sun} the mean solar disk brightness), although this analysis is still in progress.

Limb Searches by LRO Instruments. Dust searches are being carried out at far-UV wavelengths by the LRO Lyman Alpha Mapping Project, LAMP[8] and also at VIS wavelengths by the LROC Narrow Angle Camera (NAC)[9]. Dust scattering has not yet been detected, although LAMP established firm upper limits at the times and locations of the measurements. Because the NAC was designed for imaging of the sunlit surface, it is rather insensitive to low brightness scenes[10].

Dust Estimates: The figure compares the resulting LOS dust estimates and observational upper limits for a tangential viewing geometry. Brightness was converted to LOS concentration using Mie scattering theory and a broadband model for lunar dust optical constants[11], assuming a narrow size distribution of dust grains, with r_{peak}= 0.10 μm. Tangent height is 5-10 km, but that is not tightly constrained in this comparison. The uplooking Lunokhod measurements are converted to limb viewing geometry using a dust distribution model with scale height of 5 km. Predicted LADEE UVS detection limits (at λ≅ 400 nm) are shown for comparison.

Were the Apollo-era observations in error? Upcoming measurements should provide needed aswers.

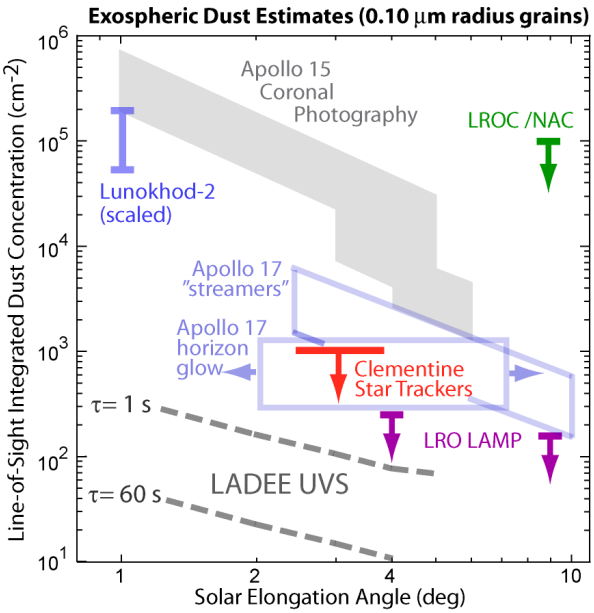

References: [1] Delory et al. (2010) *41st LPS*, Abstract #2459. [2] Hayes A. P. et al. (2001) *Astrophys. J., 548*, 1081-1086. [3] McCoy J. E. (1976) *Proc. Lunar Sci. Conf. VII*, 1087-1112. [4] Glenar et al. (2011) *Planet. Space Sci., 59*, 1695-1707. [5] McCoy J. E. and Criswell D. R. (1974) *Proc. Lunar Sci. Conf. V*, 2991-3005. [6] Severny A. B. et al. (1975) *The Moon, 14*, 123-128. [7] Zook H. A. et al. (1995) *LPS XXVI*, 1577-1578. [8] Gladstone G. R. et al. (2010) *Space Sci. Review, 150*, 161-181. [9] Robinson M. et al. (2010) *Space Sci. Rev., 150*, 81-124. [10] Mahanti P. et al., (2012) *43rd LPS*, Abstract #1638. [11] Shkuratov Y. et al. (1999) *Icarus, 137*, 235-246.

From CMEs to Earth/Lunar Radiation Dosages: a First in Heliospheric End-to-End Coupling. M. J. Gorby[1], N. A. Schwadron[1], J. A. Linker[2], H. E. Spence[1], L. W. Townsend[3], F. A. Cucinotta[4], and J. K. Wilson[1], [1]University of New Hampshire, [2]Predictive Science, Inc., [3]University of Tennessee, [4]National Aeronautics and Space Administration

We have taken fundamental, new steps in coupling MHD simulations to our fully 3D Lagrangian code allowing us to accurately model CMEs and SEP events, and to attain flux and dosage rates out to 1AU. The Earth-Moon-Mars Radiation Environment Module (EMMREM) is a collection of tools based on the output of the Energetic Particle Radiation Environment Model (EPREM) [1]. We feed resulting flux from EPREM into the Baryon Transport (BRYNTRYN) code developed at NASA to calculate dose rates and accumulated dosages.

Recently we have coupled EPREM to Magnetohydrodynamics Around a Sphere (MAS) developed at Predictive Science Inc.. The MAS / EPREM couplings allow us to move past a constant solar wind solution and to realistically model the impact of evolving CMEs on the acceleration of SEPs. Results from both a weak and severe SEP event will be presented, along with a comparison of the results with CraTer and Goes data. Validation of the coupling and the implications for predicting dose rates at 1AU will also be discussed.

Predicting radiation dosages for humans and instruments is vitally important for both current and any future Lunar missions. This critical step in the evolution of code coupling enables us to explore, discover, and ultimately predict connections between SEP events and their effects on the space environment through the inner heliosphere.

[1] Schwadron, N. A. and A. L. Townsend, et al. (2010) Space Weather Journal, Vol. 8, S00E02

THERMAL, THERMOPHYSICAL, AND COMPOSITIONAL PROPERTIES OF THE MOON REVEALED BY THE DIVINER LUNAR RADIOMETER. B. T. Greenhagen[1], D. A. Paige[2], and the Diviner Science Team; [1]Jet Propulsion Laboratory, California Institute of Technology, Pasadena, CA, USA; [2]Dept. of Earth and Space Sciences, University of California, Los Angeles, CA, USA. Email: Benjamin.T.Greenhagen@jpl.nasa.gov

Introduction: The Diviner Lunar Radiometer is the first multispectral thermal instrument to globally map the surface of the Moon. After over three years in operation, this unprecedented dataset has revealed the extreme nature of the Moon's thermal environment, thermophysical properties, and surface composition.

Diviner Lunar Radiometer: The Diviner Lunar Radiometer is a nine-channel, pushbroom mapping radiometer that was launched onboard the Lunar Reconnaissance Orbiter in June 2009. Diviner measures broadband reflected solar radiation with two channels, and emitted thermal infrared radiation with seven infrared channels [1]. The two solar channels, which both span 0.3 to 3 μm, are used to characterize the photometric properties of the lunar surface. The three shortest wavelength thermal infrared channels near 8 μm were specifically designed to characterize the mid-infrared "Christiansen Feature" emissivity maximum, which is sensitive to silicate composition [2]. Diviner's longer wavelength thermal infrared channels span the mid- to far-infrared between 13 and 400 μm and are used to characterize the lunar thermal environment and thermophysical properties [3,4].

In more than three years of operations, Diviner has now acquired observations over six complete diurnal cycles and three complete seasonal cycles. Diviner daytime and nighttime observations (12 hour time bins) have essentially global coverage, and more than 75% of the surface has been measured with at least 6 different local times. The spatial resolution during the mapping orbit was ~200 m and now ranges from 150 m to 1300 m in the current elliptical orbit. Calibrated Diviner data and global maps of visible brightness temperature, bolometric temperature, rock abundance, nighttime soil temperature, and silicate mineralogy are available through the PDS Geosciences Node [5,6].

Thermal Environment: The lunar thermal environment is complex and extreme. Surface temperatures in equatorial regions such as the Apollo landing sites are close to 400K at noon and less than 100K at night, with annual average temperatures at depth of approximately 250K [7]. Diviner has mapped the poles at diurnal and seasonal temperature extremes and the data show that large areas within permanently shadowed craters have annual average temperature less than 50K [3]. The coldest multiply-shadowed polar craters have temperatures low enough to put constraints on lunar heat flow [8]. Diviner data have also been used to estimate the thermal properties of non-polar permanently shadowed regions [9].

Thermophysical Properties: Diviner is directly sensitive to the thermophysical properties of the lunar surface including nighttime soil temperature, rock abundance, and surface roughness. Although much of the Moon has uniform regolith thermal properties, some fresh impact craters cool to lower than normal temperatures. Hundreds of these "cold spots" have been observed distributed across all lunar terrain types and may indicate a fluffier surface layer [4]. By modeling the higher thermal inertia of rocks, which stay warmer than lunar soil at night we have demonstrated the ability to quantify the areal rock fraction [4]. Diviner is also sensitive to surface roughness on the mm scale and the multispectral nature of the dataset has been used to model RMS surface slopes and show that on these scales the maria are generally rougher than the highlands (Figure 4).

Compositional Properties: Diviner was designed to characterize the Christiansen Feature (CF) and constrain lunar silicate mineralogy [2]. The CF is tied to the fundamental SiO_2 vibrational band and shifts to shorter wavelengths with increasing silicate polymerization. Leveraging the relatively restricted geochemistry of the lunar surface, we have used Diviner observations of Apollo sites, and laboratory measurements of Apollo soils to infer some geochemical abundances (e.g. FeO) [10]. Diviner is sensitive to the presence of high silica minerals such as quartz or alkali feldspar and has been used to localize these minerals on the lunar surface [11,2]. Diviner data also provided an important constraint on plagioclase abundance that can be used to infer the amount of country rock mixing [2] and when combined with near-infrared datasets can reveal more than either dataset individually.

References: [1] Paige D.A. *et al*. (2010) *SSR, 150*. [2] Greenhagen B.T. *et al*. (2010) *Science, 329*, 1507. [3] Paige D.A. *et al*. (2010) *Science, 330*, 479. [4] Bandfield J.L. *et al*. (2011) *JGR, 116*. [5] Paige D.A. *et al*. (2011) LPSC XLII, #2544. [6] Greenhagen B.T. *et al*. (2011) LPSC XLII, #2679. [7] Vasavada A.R. *et al*. (2012) *JGR, 117*. [8] Siegler M.A. *et al*. (2012) *NLSI LSF*. [9] McGovern J.A. *et al*. (2012) *JGR*, submitted. [10] Allen C.C. *et al*. (2012) *JGR*, in press. [11] Glotch T.D. *et al*. (2010) *Science, 329*, 1510.

RESOLVE: REAL-TIME SCIENCE OPERATIONS TO SUPPORT A LUNAR POLAR VOLATILES ROVER MISSION. J. L. Heldmann[1], A. Colaprete[1], R. Elphic[1], G. Mattes[2], K. Ennico[1], E. Fritzler[1], M. Marinova[1], R. McMurray[1], S. Morse[1], T. Roush[1], C. Stoker[1], [1]NASA Ames Research Center, Moffett Field, CA, [2]NASA Johnson Space Center, Houston, TX

Introduction: The Regolith and Environment Science and Oxygen & Lunar Volatile Extraction (RESOLVE) project aims to demonstrate the utility of in situ resource utilization (ISRU). ISRU is a way to rebalance the economics of spaceflight by reducing or eliminating materials that must be brought up from Earth and placed on the surface of the Moon (or Mars) for human use. RESOLVE is developing a rover-borne payload that (1) can locate near subsurface volatiles, (2) excavate and analyze samples of the volatile-bearing regolith, and (3) demonstrate the form, extractability and usefulness of the materials. Such investigations are important not only for ISRU but are also critically relevant for understanding the scientific nature of these intriguing lunar polar volatile deposits.

Temperature models and orbital data suggest near surface volatile concentrations may exist at briefly lit lunar polar locations outside persistently shadowed regions. A lunar rover could be remotely operated at some of these locations for the 7-10 days of expected sunlight at relatively low cost. Such a mission is unique and requires a new concept of operations. Due to the limited operational time available, both science and rover operations decisions must be made in real time, requiring immediate situational awareness, data analysis, and decision support tools.

RESOLVE Field Test: In July 2012 the RESOLVE project conducted a full-scale field demonstration for testing of both technologies required to enable this mission and concepts of operations. With help from the Pacific International Space Center for Exploration Systems (PISCES), a lunar rover prototype (provided by the Canadian Space Agency) was equipped with a suite of prospecting instruments (neutron spectrometer and near-infrared spectrometer) and volatile characterization instruments (drill and auger for subsurface sample collection plus the ISRU-specific instruments LAVA (Lunar Advanced Volatile Analysis) and OVEN (Oxygen and Volatile Extraction Node)). The rover was operated at a lunar analog site on the upper slopes of Mauna Kea, Hawaii with a mission operations center co-located in Hawaii, rover navigation center in Canada, and a Science Backroom at NASA Ames Research Center in California.

Real-time Science Operations: In Hawaii, several console positions within the flight mission operations hierarchy reflected the need for timely science decision-making including an overall Science Lead, a Real-Time Science Lead, and Neutron and Near-infrared Spectrometer Leads. Supporting these console positions was the Science Backroom that was tasked with monitoring the data, conducting in-depth data analysis to support mission decision-making, and conducting any rover traverse replanning as required (Figure 1).

Strict communications protocols were invoked to ensure efficient and effective communication in real-time. For example, the Science Backroom at NASA Ames conversed with the two Spectrometer Leads (located in the flight control center in Hawaii) on a dedicated voice loop, Spectrometer Leads and the Real-Time Science position conversed with the overall Science Lead, and the Science Lead relayed all science-related operational information to the Flight Director responsible for the overall mission. RESOLVE also utilized customized exploration ground data system software (xGDS) to monitor navigation telemetry, spectrometer data feeds, etc. in real-time to support mission decision-making.

Conclusions: The envisoned lunar mission requires highly efficient, real time, remotely operated rover operations to enable low cost, scientifically relevant exploration of the distribution and nature of lunar polar volatiles. The RESOLVE field demonstration illustrated the need for science operations personnel in constant communictions with the flight mission operators and the Science Backroom to provide immediate and continual science support and validation throughout the mission. The RESOLVE field campaign demonstrated that this novel methodology of real-time science operations is possible and applicable to providing important new insights regarding lunar polar volatiles for both science and exploration.

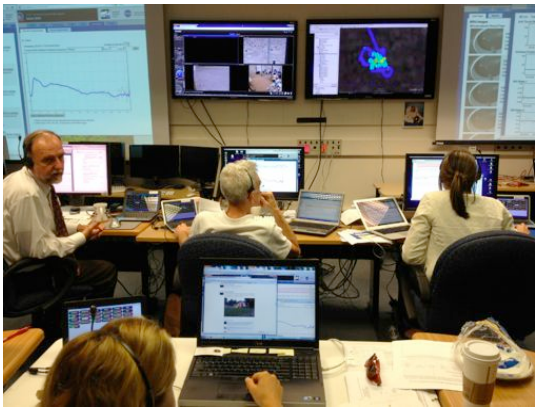

Figure 1. RESOLVE Science Backroom at NASA Ames Research Center during the July 2012 campaign.

SIMULATION OF RADAR SOUNDER ECHOES AND INVERSION OF LUNAR SUBSURFACE. Y. Q. Jin, Key Lab of Wave Scattering and Remote Sensing Information, Fudan University, Shanghai 200433, China, Email: yqjin@fudan.edu.cn.

Introduction: Numerical simulation of radar sounder echoes from Moon cratered surface and subsurface, and inversion of the lunar subsurface, e.g. layering thickness and dielectric properties, are developed. Subsurface detection is utilized based on the nadir echoes time delay and intensity difference from the media interfaces. According to Moon surface feature, the cratered topography is numerically generated, and the triangulated network is employed to make digital elevations of the whole surface. Based on the Kirchhoff approximation of rough surface scattering and the ray tracing of geometric optics, radar range echoes at 5~50 MHz from lunar layering structure is numerically simulated. Then, inversions of the regolith layer thickness and dielectric permittivities are designed.

Scattering from Layered Media: Scattering from layering media is derived using the Stratton-Chu integral formula in the KA method [1-4].

In numerical calculation, the surface is divided into discrete meshes. The surface topography at each node of the grid with given mesh dimension (resolution of original DEM) are created.

Summing up all scattering fields from those meshes, whose ranges fall in the range bin r_n (the n-th range bin), the total scattered field received from the lunar surface (sur) $\mathbf{E}_{\text{sur}}(r_n)$ and subsurface (sub) $\mathbf{E}_{\text{sub}}(r_n)$ received by a radar sounder is then

$$\mathbf{E}(r_n) = \mathbf{E}_{\text{sur}}(r_n) + \mathbf{E}_{\text{sub}}(r_n) \quad (1)$$

To make enough range resolution and transmitted energy, linear frequency modulation (LFM) pulse is usually employed as the transmission signal [4,5].

Simulations of Radar Range Echoes: Based on statistics of Moon craters, a DEM of a Moon cratered surface is simulated using a Monte-Carlo method.

We selected a bandwidth of 5~50 MHz to design the most feasible frequency for probing lunar subsurface with good resolution and penetration depth.

In simulation of 5, 20 and 50 MHz, the whole scene is 35×25 km^2. Due to computation limitation, the illumination area for the 50 MHz case is reduced. A flat subsurface is assumed to be at 200 m depth.

Simulations of radar range echoes at 5, 20 and 50 MHz are presented for two cases of basalt ε_1=7.1(1+i0.015) and water-ice ε_1=3.15(1+i0.005). It can be seen from comparison between the cases of basalt and water-ice that due to the complex dielectric constant of basalt being larger than that of water-ice, attenuation through the basalt layer is larger.

Also, due to the different dielectric constants of basalt and water-ice in the layer 1, radar ranges for the cases of basalt and water-ice look different because of range change with $1/\sqrt{\varepsilon_1}$.

As frequency increases from 5 MHz to 50 MHz, the echoes from the top surface become stronger and those from the subsurface become much weaker through attenuation. At 50MHz, scattering and reflection from ranges larger than the subsurface almost cannot be seen.

As a real example, a lunar area of the crater taking from the DTM (digital topography model) data is given.

Suppose that the radar at the altitude 100 km is flying across a flat subsurface located at -1850 m. Thus, along the flight, a cross profile shows the layer thickness from 26 m to 486 m. The images of radar range echoes at 5, 20 and 50MHz are simulated for basalt ε_1 and water-ice ε_1, respectively.

This simulation program provides a tool for analysis of radar echoes, and inversions of the layer structures, such as the layer thickness and dielectric properties of the media [6,7].

Inversion of Layer Thickness: The layer thickness d_1, and dielectric properties of two media, ε_1, ε_2, from radar range echoes image are inverted.

Let the radar power I_0 be incident upon the top surface. Then, the radar range echo from top surface can be measured. Comparing this echo with the reflected echo from plat surface based on scattering theory of rough surface, the real part of ε_1 can be first determined. Then, the radar range can be used to determine the layer depth d_1. In radar ecoes, two neighboring locations, S and S′, are specifically chosen, and the height difference between these two locations has been the known δ. The subsurface underlying below these locations is assumed as flat. Comparing these two echoes, the imaginary part of ε_1 and ε_2 can be inverted.

References: [1] Phillips R J, et al. (1973), *Apollo Technical Report*, NASA.[2] Porcello L J et al. (1974), *Proceeding of the IEEE, 62*: 769–788. [3] Ono T, Oya H. (2000), *Earth Planets Space, 52*: 629–637. [4] Kobayashi T et al. (2002), *Earth Planets Space, 54*: 983–991. [5] Nouvel J F et al. (2004), *Radio Science 39*: RS1013. [6] Jiang J S and Jin Y Q (2011). *Selected Papers on Microwave Lunar Exploration in Chinese Cheng′E-1 Project*, Beijing: Science Press 2011. [7] Fa W and Jin Y Q (2009). *Science in China (F), 52*: 559–574.

LROC OBSERVATIONS IN THE LRO EXTENDED MISSION. B. L. Jolliff[1], M. S. Robinson[2], and T. R. Watters[3], [1]Washington University, St. Louis, MO 63130, blj@wustl.edu; [2]School of Earth & Space Exploration, ASU, Tempe, AZ; [3]National Air and Space Museum, Smithsonian Institution, Washington, DC.

Introduction: In the Lunar Reconnaissance Orbiter (LRO) extended science mission (ESM), the LRO Cameras (LROC) will continue exploring the Moon using targeted Narrow Angle Camera (NAC) observations that optimize opportunities afforded by the ESM orbit and Wide Angle Camera (WAC) coverage that will continue to improve knowledge of lunar photometry, surface composition, and mineralogy.

LROC ESM Themes: During the ESM, LROC will continue to fill in gaps in NAC coverage from the primary mission, and will focus on observations that improve coverage of (1) south polar targets, (2) tectonic features such as lobate scarps, graben, etc., (3) impact-related features, including impact melt deposits and processes, uplift structures, and degradation processes, and (4) volcanic features, including the identification and characterization of small, previously undetected structures. The 30×200 km elliptical orbit with south polar periselene will enable the NACs to obtain high spatial resolution observations of southern hemisphere and south polar targets while obtaining broad areal coverage of northern hemisphere targets.

Polar Illumination. Using LROC images, regions at the poles have been identified that are illuminated for nearly 95% of the year [1]. Lighting conditions vary from year to year as the lunar orbit precesses with an 18.6 year period. Further LROC WAC observations will improve illumination maps and the ability to predict lighting conditions for future polar missions. Increased NAC coverage will enable meter scale mapping of illuminated terrain, which will support planning and operations of future polar landers and rovers. Targeting LROC imaging of permanently shadowed regions (PSR) use Diviner models and LOLA topography to determine when secondary lighting is optimal in regions that receive no direct sunlight. The PSR images provide data on albedo and regolith properties.

Tectonic Features. The discovery of young, widely distributed tectonic features during from LROC images changed the existing view of the Moon as a geologically inactive body [2]. Our understanding of the current stress state of the crust and the age of the tectonic features, however, is incomplete because the total population of young structures is not yet known. A goal of the ESM is to determine the global distribution of the contractional lobate scarps and the extensional small-scale graben. Topographic data is critical in analyzing the tectonic landforms, characterizing morphometry in detail to constrain the geometry of faults, and modeling the kinematics and mechanics of faulting. Another goal of the ESM is to compare Apollo Pan photos and LROC images from throughout the mission to determine if any faults are currently active. The goal of these efforts is to better understand: (1) the spatial distribution, distribution of orientations, and morphometry of tectonic landforms; (2) the evolution of tectonic stresses with time; and (3) the origin of tectonic stresses and their relationship to the origin and thermal evolution of the Moon, and comparison to other terrestrial planets.

Impact craters and phenomena. New NAC stereo images, derived DEMs and the improved WAC-derived GLD100 [3] calibrate models for impact melt volume that is produced, ejected, and retained in crater formation, and test theoretical calculations against crater size, terrain, impact angle, and impactor properties. Properly calibrated cratering models are important to cratering studies on other planetary bodies, such as Vesta, Mercury, and Mars. The photometry and composition of impact products currently are not well characterized. Impact products may include flat-lying ponds and dark stringers that extend over the crater rim, but it is not clear if these materials were emplaced as melt or granular deposits. Impact products have a wide range in reflectance that may represent different degrees of melting and glass content. New photometric analysis using repeat NAC imaging in various lighting conditions will provide the needed phase function for high-priority targets. Repeat imaging will also be used to investigate the recent impact flux.

Volcanic Features. LROC images will be used to investigate emplacement mechanisms by characterizing composition, morphology, slope, flow features, and volumes. These data provide the basis for new investigations and discoveries of volcanic centers [e.g., 4], including unusual features such as the enigmatic volcanic caldera known as "Ina-D" [5], which is among the youngest volcanic features on the Moon. In the ESM, LROC will continue to search for and image similar young volcanic features, with NAC image resolution to better understand the distribution of the Moon's most recent volcanic activity. NAC observations of volcanic features, especially imaging to obtain geometric stereo pairs, will address the conditions of formation. Young volcanic features will be located and characterized to better understand the nature and distribution of the Moon's most recent volcanic activity.

References: [1] Speyerer & Robinson (2011) LPSC 42, #2540. [2] Watters, et al. (2012) Nat. Geosci. [3] Scholten et al. (2012) JGR Papers in Press. [4] Spudis et al. (2011) JGR 116. [5] Robinson et al. (2010) LPSC 41, #2592.

SAMPLING SOUTH POLE-AITKEN BASIN: THE MOONRISE APPROACH. B. L. Jolliff[1], C. K. Shearer[2], and B. A. Cohen[3], [1]Dept. of Earth & Planetary Sciences, Washington University, St. Louis, MO 63130, blj@wustl.edu; [2]Institute of Meteoritics, University of New Mexico, Albuquerque, NM 87131; [3]NASA Marshall Space Flight Center, 320 Sparkman Dr., Huntsville AL 35805.

Introduction: The South Pole-Aitken basin (SPA) is the largest of the giant impact basins in the inner Solar System, and its location on Earth's Moon makes it the most accessible. Exploration of SPA through direct collection and analysis of representative materials addresses issues as fundamental as the characteristics of the chemical reservoir from which the Moon originated, early differentiation and production of crust and development of global asymmetry, relationships between magmatic activity and internal thermal evolution, and effects of giant impact events on the terrestrial planets.

Owing to its great size and superposition relationships with other lunar impact basins, SPA is the oldest and as such anchors the lunar chronology. Moreover, numerous large impact craters and basins are contained within it such that materials (rocks) of the SPA basin contain a record of the early impact chronology, one less likely to have been affected by the large, late nearside basins (*e.g.*, Imbrium). Understanding the early basin chronology is key to deciphering the sequence and effects of early giant impact bombardment of the inner Solar System. That record exists on the Moon, and materials of the SPA basin will allow us to read that record. Knowledge of the early bombardment history will test – and may reshape – a key paradigm relating to early Solar System evolution. Did the planets form with the alignment of today, or was there a major reorientation of the giant planets that led to destabilization of asteroid orbits, and a cataclysmic bombardment of the inner Solar System hundreds of millions of years after accretion of the planets? Implications include understanding environments for early life-supporting habitats on Earth and Mars, and relationships to new observations of extra-solar planetary systems.

Scientific Priority: The 2003 NRC Decadal Survey listed sample return from SPA as among the highest priorities for Solar System science. This priority was reaffirmed in 2007 by the NRC (SCEM Rpt.) and again in the 2012 Decadal Survey. The high priority stems largely from the idea that the 'cataclysm' can be tested by determining ages of impact-melt from an SPA sample that would include rock materials produced or affected by the impact event. SPA is far distant from the nearside Apollo and Luna landing sites where all of the samples of known origin were collected. Materials excavated and reset by late nearside basin impacts, especially Imbrium, dominate those samples. A sample from the interior of SPA will be dominated by materials formed in the SPA event, with contributions from smaller basins and large craters that occur within it, thus providing a fresh and independent record of ages associated with the early parts of the lunar heavy bombardment record.

Sample return and investigation of the diversity and distribution of materials within SPA will address other issues of high science priority as well. Analysis of materials derived from the deep crust and upper mantle will enable new tests of models for lunar differentiation, especially as linked to GRAIL results. Knowing the age and characteristics of the impact that produced SPA basin will help illuminate the basin-impact forming process and the role it played in modifying early planetary crusts. Volcanic rocks also occur within SPA, some of which are ancient volcanics covered by later crater deposits. Knowing their age and composition is key to the thermal history of the Moon, the composition of the deep interior, and relationships between basin formation and later volcanism. Because of impact-ejecta redistribution, fragments of these rocks will be found mixed in the regolith at most locations within the SPA interior.

MoonRise Approach: Determining the age of the SPA Basin is a primary goal, but selecting an area that will allow determination of the ages of other large impact events (*i.e.*, more recent basins or craters within SPA) will provide additional dates to anchor the chronology. The MoonRise sampling strategy leverages the "natural" sampling mechanism afforded by the impact cratering process, which delivers diverse rock samples from the surroundings to the regolith where they can be accessed from a surface lander at a single point. Regolith samples from Apollo missions provide ample statistics on the rock content, diversity, and representativeness relative to local and regional geology that can be expected in a given location. Recent remote sensing missions provide sufficient geologic and topographic information to enable a sound site geology determination as well as landing-site safety assessment.

The MoonRise approach leverages the small rock content of lunar regolith by scooping and sieving a sufficient volume of regolith to collect >1 kg of rock fragments, which are needed for age determinations. Using modern, state-of-the-art analytical techniques, capabilities exist now to analyze very small quantities of rock samples and determine not only their chemical and mineral compositions, but also their ages and petrologic history. Larger fragments can even be split, and portions of the samples retained for future analyses.

MAPPING OF LUNA-17 LANDING SITE AND RECONSTRUCTION OF LUNOKHOD-1 STEREO PANORAMAS. I. Karachevtseva[1], A. Zubarev[1], I. Nadezhdina[1], N. Kozlova[1], E. Gusakova[1], and J. Oberst[1,2,3]
[1]Moscow State University of Geodesy and Cartography (MIIGAiK), MIIGAiK Extraterrestrial Laboratory (MExLab). Gorokhovskiy per., 4, 105064, Moscow, Russia; [2]German Aerospace Center (DLR); [3] Technical University of Berlin, Germany

Introduction: Unmanned interplanetary probe Luna 17 was launched from the Earth towards the Moon on 10 November 1970 and entered the lunar orbit on 15 November 1970. The spacecraft successfully landed on the Moon 17 November 1970 and Lunokhod-1 descended to the lunar surface. During the operation Lunokhod-1 sent to the Earth 211 lunar panoramas and 25 thousands images [1, 2].

Sources: Based on results of LRO image data processing we have carried out mapping of the Luna-17 landing site area [3]. We have reconstructed the Lunokhod-1 traverse and identified coordinates of surveying points from which panoramic images were obtained. New DEM, based on LRO NAC images was generated using PHOTOMOD software [4]. Bundle block adjustment was performed using tie-points, determined by automatic correlation of LRO NAC stereo pairs. Afterwards 2-pixels (1.1 meters) step detailed DEM was derived. Ground sample distance (GSD) is 0.55 m. Results of GIS-mapping and new DEM will be used for 3D reconstruction of the Lunokhod-1 stereo panoramas.

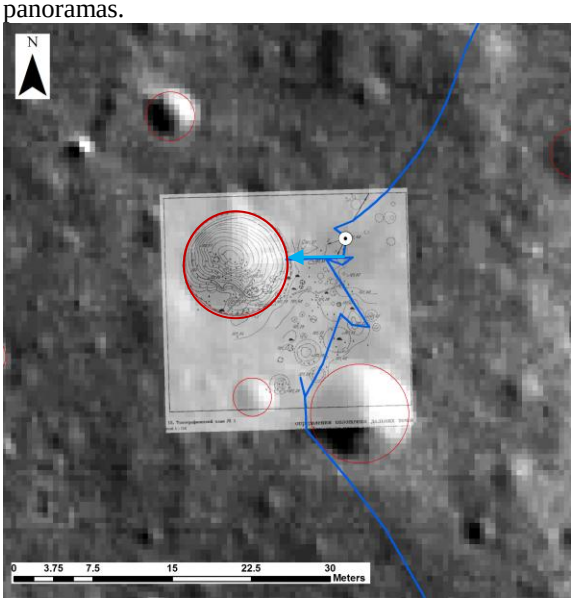

Figure 1. Large-scale map № 5, derived from Lunokhod-1 panoramas stereo-processing [1, 2] and integrated into GIS with traverse and crater data (background – LRO NAC orthomosaic)

Methodology: We have done GIS-analyses of the Lunokhod-1 traverse area using high resolution DEM, LRO NAC orthomosaics and large-scale maps (Fig. 1), derived from Lunokhod-1 panoramas [2]. We identified Lunokhod-1 wheel tracks and coordinates of surveying points from where stereo panoramas (Fig. 2) were acquired by Lunokhod-1 cameras.

Lunokhod-1 panoramic images were obtained from the Moscow State Archive. We have selected some stereo panoramas of Lunokhod-1 from which the previous large-scale maps were derived. While final results of Lunokhod-1 mission mapping were published in the form of 7 individual maps [2], other data and descriptive camera information probably have been lost, unfortunately. So Lunokhod-1 panoramas were reconstructed as 3D free model without referencing (Fig.3). We expected that the model will be reference to new LRO NAC DEM and the high detailed DEM will be derived with panoramas which were obtained by Lunokhod-1 camera from the lunar surface.

Figure 2. Example the original stereo panorama image We presuppose that the crater indicated with red circle and the part of track indicated with blue arrow are the same on the map № 5 (see Fig. 1)

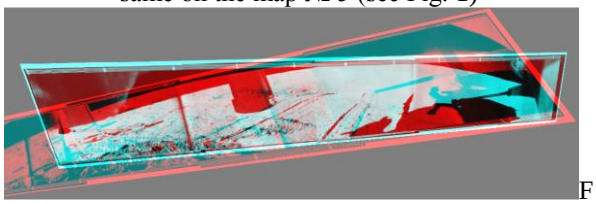

Figure 3. Example of Lunokhod-1 stereo panoramas processed without referencing. 3D reconstruction for map № 5 (anaglyph image)

References: [1] Vinogradov A.P. ed. Mobile laboratory on the Moon Lunokhod-1, Volume 1 (Peredvijnaya laboratoriya na Lune Lunokhod-1, I) – Moscow, Nauka, 1971 (in Russian). [2] Barsukov V.L. et. al. (1978) Peredvijnaya laboratoriya na Lune Lunokhod-1, Vol. 2. Nauka (in Russian). [3] Gusakova E. et al. (2012) Mapping and GIS-Analyses of the Lunokhod-1 Landing. Abstracts of 43 LPSC, # 1750. [4] http://www.racurs.ru/?lng=en&page=634

Acknowledgements: This work has been supported by a grant from the Ministry of Education and Science of the Russian Federation (Agreement № 11.G34.31.0021 dd. 30/11/2010).

LUNAR CONCRETE - Using Analogue Test Sites on the Big Island of Hawai'i for "Dust-to-Bricks": demonstration of technologies associated with basalt/regolith material processing/fabrication/construction.

R. M. Kelso[1] ; J. Hamilton and C. Andersen[2],
[1]Kelso Aerospace Consulting, rmkelso54@gmail.com, [2]PISCES , jch@hawaii.edu, canderse@hawaii.edu

Introduction: The Big Island of Hawai'i is perhaps the premier site in theworld to test Lunar and Martian surface systems (robot rovers, human transport and habitation).

The Big Island's volcanic terrain and basaltic geology are nearly identical in many aspects to the Moon and Mars. The Pacific International Space Center for Exploration Systems (PISCES) facility will allow onsite development of multiple technologies (many not traditionally associated with space…such as construction, clean energy, recyling). These advancements can then be rapidly tested in the field at many of the analog sites around the island.

PISCES and the State of Hawai'i are in the process of establishing a new analogue research park for collaborative/partnership work in analogue testing of robotic systems and resource utilization technologies that have both 'beyond-LEO' and earth-based applications. A key piece of this effort is toward the investigation and demonstration of technologies associated with basalt / regolith material processing, fabrication, and construction. We intend to demonstrate these technologies for both lunar surface stabilization and preparation of landing pad surfaces by first testing these technologies on the volcano of the Big Island of Hawai'i. Further, the State of Hawai'i has parallel interest in using similar processes for basalt construction materials (ala 'lunar bricks') from the volcanic basalt located on the Big Island for bricks, slabs/foundations, roads and houses.

This paper/presentation will brief the latest updates in Hawaii's efforts to revamp PISCES and establish these world class analogue test sites for lunar testing. Further, this presentation will outline upcoming efforts within PISCES in the area of "lunar concrete"on the Big Island through technology demonstration and the establishment of a pilot plan for industrial construction using basalt materials from the volcanoes.

A Sustainable Architecture for Lunar Resource Prospecting from an EML-based Exploration Platform. K.Klaus[1], K, Post[1] and S.J. Lawrence[2], [1]The Boeing Company (13100 Space Center Blvd, Houston, TX 77059; kurt.k.klaus@boeing.com, kevin.e.post@boeing.com), [2]School of Earth and Space Exploration (Arizona State University, samuel.lawrence@asu.edu).

Introduction: We present a point of departure architecture for prospecting for Lunar Resources from an Exploration Platform at the Earth – Moon Lagrange points. Included in our study are launch vehicle, cis-lunar transportation architecture, habitat requirements and utilization, lander/rover concepts and sample return.

In our current point of departure architecture, we envision the use of the NASA Space Launch System to launch large elements of the system directly to an EML camp once it has been deployed.

Transport to L2: The benefits derived by integrating high and low energy transfers range from system design and support to overall mission design mass savings and re-supply strategies. Different transfer design techniques can be explored by mission designers, testing various propulsive systems, maneuvers, rendezvous, and other in-space and surface operations. Understanding the availability of high and low energy trajectory transfer options opens up the possibility of exploring the human and logistics support mission design space and deriving solutions never before contemplated. For sample return missions from the lunar surface, low-energy transfers could be utilized between EML platform and the surface as well as return of samples to EML-based spacecraft.

Human Habitation at the Exploration Platform: Telerobotic and telepresence capabilities are considered by the agency to be "grand challenges" for space technology. We invite the lunar science community to consider the priority scientific tasks that such on-orbit operations might enable. While human visits to the lunar surface provide optimal opportunities for field geologic exploration, on-orbit telerobotics may provide attractive early opportunities for geologic exploration, resource prospecting, and other precursor activities in advance of human exploration campaigns and ISRU processing.

The Exploration Platform provides a perfect port for a small lander which could be refueled and used for multiple missions including sample return. This reuse of expensive spaceflight hardware is an essential element of a sustainable space program. The EVA and robotic capabilities of the EML Exploration Platform allow the lander to be serviced both internally and externally, based on operational requirements. The placement of the platform at an EML point allows the lander to access any site on the lunar surface, thus providing the global lunar surface access that is commonly understood to be required in order to enable a robust lunar exploration program. Designing the sample return lander for low-energy trajectories would reduce the overall mass and potentially increase the sample return mass. Of course, following the commencement of ISRU production, locally-derived resources could be leveraged to refuel the lander, further reducing the fuel supply chain from Earth.

The Initial Lunar Mission: Building upon Apollo sample investigations, the recent results of the LRO/LCROSS, international missions such as Chandrayaan-1, and legacy missions including Lunar Prospector, and Clementine, among the most important science and exploration goals is surface prospecting for lunar resources and to provide ground truth for orbital observations. Being able to constrain resource production potential will allow us to estimate the prospect for reducing the size of payloads launched from Earth required for Solar System exploration. Flight opportunities for something like the NASA RESOLVE instrument suite to areas of high science and exploration interest could be used to refine and improve future Exploration architectures, reducing the outlays required for cis-lunar operations. Mobile explorers are the required next missions to explore polar regions (volatiles) and non-polar regions (e.g., mature Ti-rich soil for solar wind implanted H, pyroclastic deposits for indigenous volatiles, etc.). These prospectors will incrementally address science, exploration, technology, commercial and public outreach objectives by:

- Defining the composition, form, and extent of lunar resources;
- Characterizing the environment in which the resources are found;
- Defining the accessibility/extractability of the resources;
- Quantifying the geotechnical properties of the lunar regolith in the areas where resources are found;
- Identifying resource-rich sites for targeting future missions,
-Offering immersive and unparalleled opportunities for public engagement and citizen science.

Summary: EML points are excellent for placement of a semi-permanent human-tended Exploration Platform both in the near term, while providing important infrastructure and deep-space experience that will be built upon to gradually increase long-term operational capabilities for deep space exploration.

BULLIALDUS CRATER: A RARE WINDOW INTO LUNAR PLUTONISM AND LATE-STAGE MAGMA OCEAN FLUIDS. Rachel L. Klima (Rachel.Klima@jhuapl.edu)[1], Joshua T. S. Cahill[1], Justin Hagerty[2] and David Lawrence[1], [1]Johns Hopkins University Applied Physics Laboratory, Laurel, MD 20723, USA; [2]USGS Astrogeology Science Center, Flagstaff, AZ, USA.

Introduction: The central peak of Bullialdus Crater has long been recognized as having a reflectance spectrum dominated by a strong noritic signature (e.g., 1-4). Results of spectral fits to the central peak of Bullialdus suggest a relatively high Mg# (>Mg_{75}) in the low-Ca pyroxenes (5), within the range of values observed for Mg-suite lunar samples (e.g., 5). Centered at -20.7°, 337.5° in Mare Nubium, Bullialdus Crater lies within the high-thorium Procellarum KREEP Terrane (e.g., 6). In fact, based on orbital gamma-ray data, Bullialdus is the location of a clear thorium (Th) enhancement, which is important because Th commonly serves as a proxy for detecting KREEP-rich materials on the lunar surface (e.g., 6-8). We examine the mineralogy of Bullialdus crater and the spatial distribution of the Th signature associated with it to investigate the character and composition of the excavated pluton.

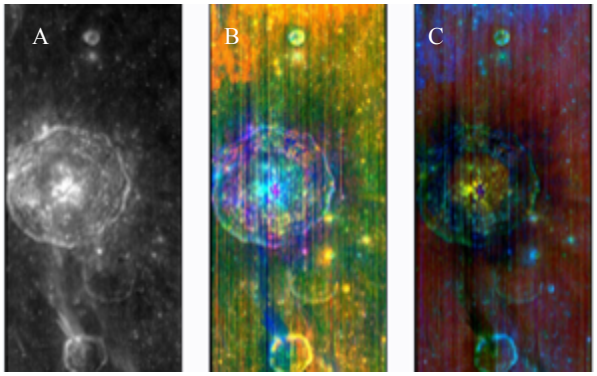

Fig. 1. Mineral diversity in Bullialdus crater. (A) 0.75 µm albedo map. (B) Mafic mineralogy depicted using an RGB composite where R=integrated 1 µm band depth; G=integrated 2 µm band depth, and B=reflectance at 1.5 µm. In this color scheme, fresh material appears bright, with deep blue generally indicating feldspathic material, red indicating an enhancement in olivine, and orange and yellow indicating pyroxenes. Low-Ca pyroxene often appears as cyan, due to the overall brightness and narrow 1 µm band. (C) Pyroxene diversity map depicted using an RGB composite where R = 1.9 µm band depth, G = integrated 2 µm band depth, and B = integrated 1µm band depth. This color scheme highlights low-Ca pyroxene as yellow, and fresh high-Ca pyroxene as cyan. Anorthositic material and highly space-weathered material appear as black.

Bullialdus Region Mineralogy: Bullialdus crater and the local mineralogy are shown in Fig. 1. Strong pyroxene bands indicative of a noritic composition dominate the central peak. Anorthositic material, excavated by Bullialdus, is exposed in the crater rim and proximal ejecta (Fig. 1). Portions of the walls exhibit a gabbroic signature, potentially olivine-bearing. Fresh craters in Mare Nubium exhibit a typical basaltic spectral signature, while both mare and highland soils in the region are generally spectrally featureless.

There is a clear Th enhancement (~6-7 ppm Th) centered on Bullialdus crater and its northern wall outer flanks (9). However, if the source of the Th is only the material excavated in the central peak, the Th content is higher, and closer to the range of Alkali suite norites (10). Observations of the central peak of Bullialdus crater indicate that the pyroxenes exhibit a distinctive 2.8 µm band absorption that is significantly stronger than the immediate surroundings, indicating the presence of a hydroxyl component. The hydroxyl signature persists through multiple viewing geometries and illumination conditions, suggesting that it is not transient, like the lunar surface water previously observed (11-13). The correspondence between KREEP and hydroxyl within Bullialdus suggests that hydroxyl might have been concentrated in late stage magma ocean fluids. However, KREEP-rich Apollo samples exhibit lower hydroxyl contents than mare basalts (14-16), suggesting that Bullialdus crater may sample materials not represented in our sample collection.

Acknowledgements: We are extremely grateful to the M^3 and Chandrayaan-1 teams for providing reflectance data for this project. We also thank the APL NSLI node and LASER grant #NNX10AH62G for supporting mapping and lab work for this project. PMDAP grant #NNH09AL42I provided support for JJH.

References: [1] C. M. Pieters, 1991, GRL 18, 2129. [2] S. Tompkins et al., 1994, Icarus 110, 261. [3] J. T. Cahill and P. G. Lucey, 2007, JGR 112, E10007, doi:10.1029/2006JE002868. [4] Cahill et al., 2009, JGR 114, 9001. [5] Klima et al., 2011, JGR 116, E00G06, doi:10.1029/2010JE003719. [6] Papike et al., 1998, in Planetary Materials, 5-1. [7] B. L. Jolliff et al., 2000, JGR 105, 4197. [8] D. J. Lawrence et al., 2003, JGR 108, 5102. [9] Lawrence et al., 2007, GRL 34, 3201. [10] Klima et al., 2012, submitted. [11] R. N. Clark, 2009, Science 326, 562. [12] C. M. Pieters et al., 2009, Science 326, 568. [13] J. M. Sunshine et al., 2009, Science 326, 565. [14] A. E. Saal et al., 2008, Nature 454, 192. [15] F. M. McCubbin et al., 2010, PNAS 107, 11223. [16] E. H. Hauri et al., 2011, Science 333, 213.

THE FIRST EXPLORATION TELEROBOTICS SYMPOSIUM – TELEPRESENCE: A NEW PARADIGM FOR HUMAN-ROBOTIC COOPERATION. D. F. Lester[1], A. Valinia[2], H. Thronson[2], and G. Schmidt[3], [1]Dept. of Astronomy, University of Texas, Austin TX 78712, [2]NASA Goddard Space Flight Center, Greenbelt, MD 20771, [3]NASA Glenn Research Center, Cleveland OH 77573.

Introduction: We present findings and observations from the *Exploration Telerobotics Symposium* held at Goddard Space Flight Center, on May 2-3, 2012. This symposium was devoted to opportunities and challenges of telepresence for exploration. A hundred participants from science, robotics, and human space flight stakeholder communities attended, representing space agencies, industry, and academia.

Telepresence as an Exploration Strategy: Telepresence is the placing of human cognition telerobotically at an exploration site, which may be hazardous to humans. This strategy is now being used routinely for undersea science, oil and cable maintenance, high-dexterity surgery, the mining industry, and for surveillance and munitions in airborne drones. An important goal of the symposium was to bring representatives of these applications to share their perspectives.

The *Exploration Telerobotics Symposium* considered a strategy whereby human operators could be sent close enough to their telerobotic surrogates that high bandwidth and low-latency communication could be assured. In the case of the Moon, this could be from low lunar orbit, or Earth-Moon L1 or L2 [1]. For Mars, this could be done from martian orbit [2] possibly from martian moons. For asteroids, work could be done from a convenient stand-off site, in orbit, or formation flying. For a gravity well, EDL (as well as safe return) is an expensive and risky part of the trip, perhaps the hardest part of the journey. This strategy is enabling for contamination control (forward, for planetary protection, and backward, for human safety).

The L1 and L2 locations, about 50000 km over the near- and far-sides of the Moon respectively, offer two-way control latencies to the lunar surface of order 400 ms, *six times smaller than the control latency from the Earth*. This allows for a high degree of cognitive coupling and likely enables complex tasks that would otherwise require in situ humans [3].

Symposium Organization: The two-day symposium included plenary talks and panel discussions on the first day. These are available at the symposium website -- http://telerobotics.gsfc.nasa.gov. Four plenary sessions addressed several key themes; (1) The historical context of telepresence; human cognition, performance, and human factors; and the relationship of telepresence to exploration; (2) Field science: what it is, and how it differs fundamentally from remote sensing science; the value of "being there" at least cognitively; (3) State-of-art space telerobotics, and directions for expansion of capability; future expectations; (4) terrestrial telerobotics, and feed-forward to space exploration; sensory extension and dexterity for surgery, mining, undersea operations.

The second day was devoted to breakout sessions to produce actionable findings to be delivered to an integration panel, which would distill these findings and observations. These three breakout groups were (1) identification of priority goals in science enabled or enhanced by telepresence, (2) assessment of the relationship of telepresence and human exploration, and (3) identification of priority capabilities to enable telepresence: technologies and operations.

Breakout Session Findings: The science breakout group recognized strong potential for this strategy. New science is enabled at distant locations where very long communication latency is a serious handicap to efficient operations from Earth. For the Moon, science activities in permanently shadowed regions (in particular for access of volatiles) can be particularly enhanced. In addition, construction of far-side facilities by on-orbit control at EM L2 is of interest. Robotic telepresence could be an especially useful strategy in areas that might be hazardous to humans such as mare pits, escarpments, and fresh craters. Telepresence should provide improved access to better samples, perhaps in the South Pole Aitken basin. It was pointed out that the impact of communication latency on planetary field geology [4] is poorly understood, and analog efforts to understand natural breakpoints in communication latency for science task completion should be carried out.

Advantages for Mars are much more significant, because of the vastly longer two-way latency to Earth, but science advantages on the Moon have parallels on Mars. In this respect, telepresence control of science experiments on the Moon exercises capabilities that will be needed for Mars. Symposium results have been briefed at GLEX2012 and NASA HQ, and a report is in production. Follow-on activity is being planned.

References: [1] Lester, D. and Thronson, H. 116-RSA-7, AIAA Space 2011 Conference. [2] Schmidt, G., et al. AIAA-2010-0629, AIAA Aerospace Sciences Meeting. [3] Lester, D., and Thronson, H. 2011, *Space Policy 27, 89-93.* [4] Hodges, K.V. and Schmitt, H.H. Geological Society of America Special Papers, December 2011, v. 483, p. 17-31.

HYDROGEN-BEARING VOLATILES AT THE LUNAR EQUATORIAL TERMINATOR.

T. A. Livengood[1], G. Chin[2], I. G. Mitrofanov[3], W. V. Boynton[4], R. Sagdeev[5], M. Litvak[6], T. P. McClanahan[7], A. B. Sanin[8], [1]CRESST/UMD/GSFC, Planetary Systems Lab, NASA/GSFC, Greenbelt, MD 20771, timothy.a.livengood@nasa.gov; [2]Planetary Systems Lab, NASA/GSFC, gordon.chin@nasa.gov; [3]Institute for Space Research, Moscow 117997, Russia, mitrofanov@l503.iki.rssi.ru; [4]LPL, University of Arizona, wboynton@lpl.arizona.edu; [5]UMD, rsagdeev@gmail.com; [6]Institute for Space Research, Moscow 117997, Russia, mlitvak.iki@gmail.com; [7]Planetary Systems Lab, NASA/GSFC, timothy.p.mcclanahan@nasa.gov; [8]Institute for Space Research, Moscow 117997, Russia, sanin@mx.iki.rssi.ru

Introduction: We detect suppression of epithermal neutron detection rates at the Lunar Reconnaissance Orbiter (LRO) using the Lunar Exploration Neutron Detector (LEND) collimated detectors when the LRO spacecraft is near the dawn and dusk terminators at near-equatorial latitude (30°S to 30°N). The greatest neutron count rate (least flux suppression) is found at post-meridian local time, at about 14:30. Suppression of epithermal neutrons is consistent with the presence of hydrogen in the regolith near the terminator. Since the terminator moves across the surface as the Moon rotates, this implies a mobile population of hydrogenated volatiles that dwells near the terminator but resides only transiently in the regolith. The observed pattern of neutron flux suppression is consistent with the distribution of mineral hydration observed by Sunshine et al. (2009) in reflected light, if the inferred layer of transiently hydrated minerals extends to a depth of order 15 cm or greater into the regolith to accommodate the observed degree of neutron flux suppression.

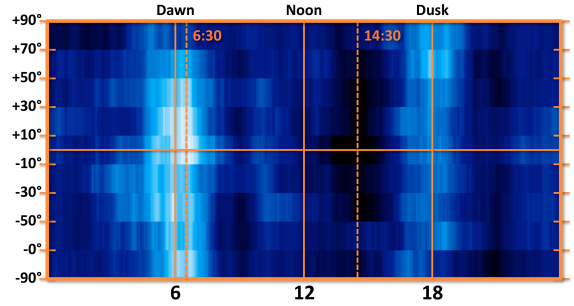

Cylindrical projection of water-equivalent hydrogen map transformed from a smoothed map of CSETN (epithermal+fast) neutron count rate, in units of local time (hortizontal) and latitude (vertical), north at the top. Local maxima in hydrogen content are found at dawn and at dusk over nearly the full range of latitude.

Modulated Neutron Flux: The CSETN detectors exhibit minima at dawn and dusk terminators, consistent with local enhancement of hydrogen/H_2O; count rate peaks in the afternoon sector, consistent with desiccated regolith with a phase lag for dehydration. Contrast between the maximum and minimum count rates implies ~0.075 wt% H_2O centered on dawn terminator, about 0.05 wt% H_2O at dusk. Comparison to the Sunshine *et al.* [1] extreme upper limit of ~0.5 wt% hydration, suggests relevant depth of hydrated surface layer is of order 15 cm or more.

Conclusions: Water group ions migrate from the warmest region to the terminator and pile up at the cold surface at the terminator. The dawn and dusk terminators are not identical: hydrated regolith at the dawn terminator rotates into sunlight and ions/molecules migrate back to the terminator along with fresh molecules migrating from the subsolar region. Dusk-side molecules always rotate and transport in the same direction, thus with less cumulative build-up. The diurnal hydration cycle appears to persist even at polar latitudes. Lawrence et *al.* [5] argue for a slight *increase* in epithermal flux from a thin hydrated layer on top of dry regolith. Different energy sensitivity between SETN and CSETN in presence of this effect is possible explanation for observed discrepancy, since SETN and CSETN sense somewhat different populations.

References: Use the brief numbered style common in many abstracts, e.g., [1], [2], etc. References should then appear in numerical order in the reference list, and should use the following abbreviated style:

[1] Sunshine, J. M. *et al.* (2009) *Science* **326**, 565–568. [2] Lawrence, D. J. *et al.* (2010) *Astrobiology* **10**, 183–200. [3] Mitrofanov, I. G. *et al.* (2010) *Space Sci. Rev.* **150**, 183–207. [4] Mitrofanov, I. G. *et al.* (2012) *JGR-Planets*, 10.1029/2011JE003956. [5] Lawrence, D. J. *et al.* (2011) *JGR-Planets* **116**, E01002.

INFORMED LINE-OF-SIGHT COMMUNICATIONS ON THE LUNAR SURFACE USING LRO NAC DEMs. Prasun Mahanti[1] , Mark S. Robinson[1], Aaron Boyd[1], Emerson Speyrer[1] ,[1]Lunar Reconnaissance Orbiter Camera Science Operations Center, Arizona State University, Tempe, AZ. (pmahanti@asu.edu)

Introduction: Short and long range line-of-sight communication on the lunar surface is of vital importance for both robotic and human extra-vehicular activity (EVA) [1,2,3]. While line-of-sight based data acquisition and transmission techniques remain the most potent form of communication between assets on the lunar surface, it also presents operational limitations [2]. Astronauts or robotic landers must have either the main lunar module (LM) or another rover in their line-of-sight to maintain com-munication for imaging or any other form of data acquisition. A-priori information mitigate this limitation, e.g. for the efficient placement of transmission modules or knowing the elevation required by an imaging device to be able to see required targets. Shadow maps can be used to acquire this information [2] to estimate LM/EVA line-of-sight for pre-mission planning and real-time EVA. Detailed elevation information can be used to form even better information maps and possible decision strategies well in advance before the actual mission as well as for real-time decision making. For example, in the NASA Mars Exploration Rover project [4] visibility analysis was done prior to landing to find how far the rover actually might see from the surface. Digital terrain models (DEMs) made from the Lunar Reconnaissance Orbiter Narrow Angle Camera (LRO NAC) stereo images offer high resolution elevation information with pixel scales down 2 meters. In this work we show some examples of how NAC DEMs can be utilized for exploration planning.

Viewsheds and maximum visibility analysis: A viewshed is a location (geographic/cell/pixel) specific visible area. Viewshed analysis uses the elevation information to determine interlocation visual connectivity based on observer and target positions. From the NAC DEMs, a rigorous viewshed analysis can be done; an example of such an analysis was performed for a DEM obtained at the Marius Hills (NAC images M111958993 and M111965782) showing (Figure1) the terrain area visible from the highest elevation point with the observer height set for 2 meters. A key result is that only a small percentage of the total surface area was 'visible' from this highest point. Similar analysis was done for all the cells for the DEM, and for each cell the corresponding viewshed area was recorded as a percentage of the total DEM area. We call the resulting matrix the maximum visibility map (Figure 2). Regions of high visibility are immediately evident from the map, with about 30% of the total terrain visible specific points. Also, smoother parts of the terrain show higher average levels of percentage visibility.

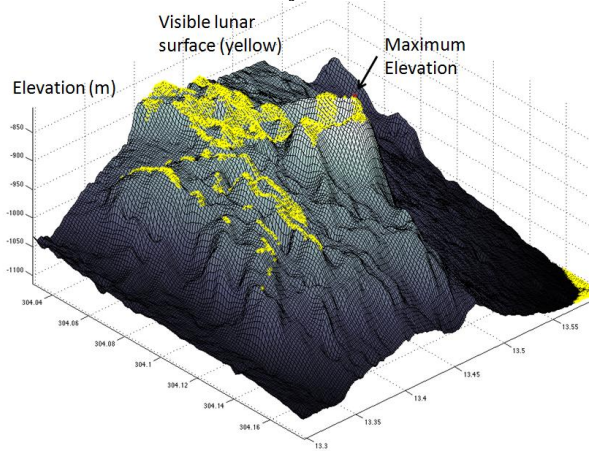

Figure 1: Viewshed at maximum elevation

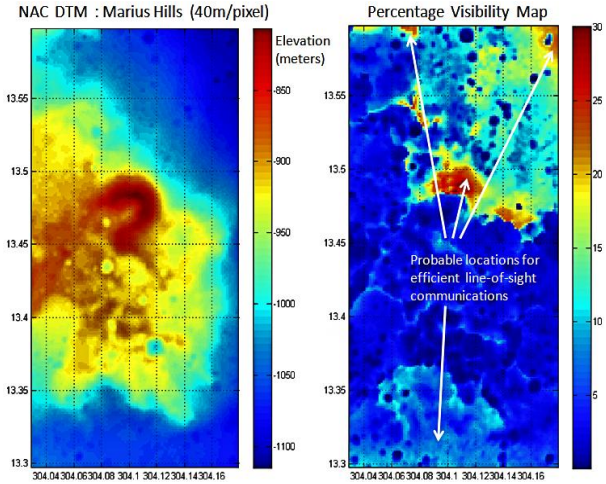

Figure 2 : DEM & maximum visibily map

Conclusions: The resolution of the NAC DEMs is highly adventagious for lunar viewshed analysis. Line-of-sight visibility conditions can be readily assessed with high accuracy. Multiple viewshed analysis results can be combined to generate more informative results, providing the basis for future lunar exploration planning.

References: [1] Kraus H. & Rosenblum I (1970) NASA-CR-110487[2] Hanson T. Markley. R. (1993) GLOBECOM'93 IEEE 929-933,2.[3] Cooper B.L. et al (2005) J. earth Syst. Sci., 815–822. [4] URL:http: // webgis.wr.usgs.gov/mer/viewshed_analysis.htm (2009)

Volatile Analysis by Pyrolysis of Regolith for Planetary Resource Exploration C.A. Malespin[1,2], D.P. Glavin[1], I.L. ten Kate[3], H. B. Franz[1,4], E. Mumm[5], S. Getty[1], A. Southard[1,2], and P. Mahaffy[1], [1]NASA Goddard Space Flight Center, 8800 Greenbelt Rd, Greenbelt, MD 20771, (charles.a.malespin@nasa.gov), [2]Universities Space Research Association, 10211 Wincopin Circle, Columbia, MD 21044, [3]Dept. of Earth Sciences, Faculty of Geosciences, Utrecht University, Budapestlaan 4, 3584 CD Utrecht, the Netherlands, [4]Center for Research and Exploration in Space Science and Technology, 5523 Research Park Drive, University of Maryland Baltimore County, Baltimore, MD 21228, [5]Honeybee Robotics, 460 34th Street, New York, NY 10001

Introduction: The extraction and identification of volatile resources that could be utilized by humans including water, oxygen, noble gases, and hydrocarbons on the Moon, Mars, and small planetary bodies will be critical for future long-term human exploration of these objects. Vacuum pyrolysis at elevated temperatures has been shown to be an efficient way to release volatiles trapped inside solid samples. In order to maximize the extraction of volatiles, including oxygen and noble gases from the breakdown of minerals, a pyrolysis temperature of 1300° C or higher is required, which greatly exceeds the maximum temperatures of current state-of-the-art flight pyrolysis instruments. Here we report on the recent optimization and field testing results of a high temperature pyrolysis oven and sample manipulation system coupled to a mass spectrometer instrument called Volatile Analysis by Pyrolysis of Regolith(VAPoR).VAPoR is capable of heating solid samples under vacuum to temperatures above 1300° C and determining the composition of volatiles released as a function of temperature. [1]

Instrument Description: The preliminary VAPoR flight instrument concept (Fig. 1) combines a sample carousel of up to six individually heated pyrolysis ovens with a reflectron time of flight mass spectrometer. [2]

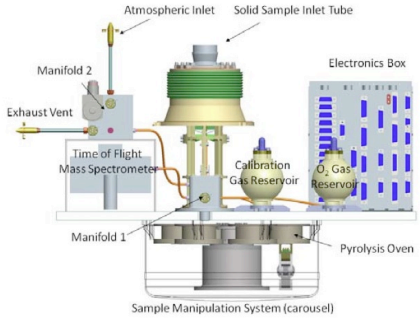

Figure 1. Cross sectional view of preliminary VAPoR flight instrument concept

The VAPoR gas processing system includes two gas manifolds, heated transfer lines, and two separate gas reservoirs containing calibration gas for the mass spectrometer and oxygen for combustion experiments. Powdered rock or soil samples collected from a rover or lander drill or scoop and delivered through the solid sample tube to one of the VAPoR ovens can then be heated by a controlled ramp from ambient to temperatures up to 1300° C to release the volatile constituents for direct measurement by the mass spectrometer.

Two independent units have been built and tested to understand the performance of the different instrument components. A laboratory breadboard was developed to test, optimize, and calibrate the reflectron time of flight mass spectrometer (TOF-MS) component of VAPoR inside a separate vacuum chamber. A separate portable field unit (Fig 2) consisting of a custom made pyrolysis oven coupled to a commercial RGA quadrupole mass spectrometer, vacuum manifold and turbomolecular pumping station, was built to demonstrate the feasibility of conducting vacuum pyrolysis evolved gas measurements in the field and has been discussed previously [3]

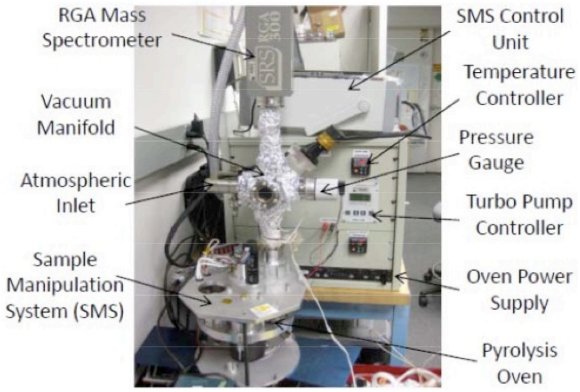

Figure 2. The VAPoR field instrument uses a new sample manipulation system and high temperature pyrolysis oven for evolved gas analysis of powdered solid samples.

Summary: Using the VAPoR instrument during NASA's 2011 Desert RATS field campaign at Black Lava Point, AZ and the 2012 MMAMA test in Apollo Valley, HI, we successfully demonstrated that high temperature vacuum pyrolysis of solid samples to temperatures exceeding 1300°C coupled with detection of volatiles by mass spectrometry can be used for the identification of resources including water and oxygen in surface samples. The inclusion of evolved gas analysis capability in the field and continued testing of instruments such as VAPoR in future field tests will be critical to the success of future robotic and human planetary resource exploration missions. The development of sample collection protocols designed to minimize or eliminate contamination from analyses such as those conducted by VAPoR are critical considerations for future space exploration architecture planning.

Acknowledgments: We wish to acknowledge support from the NASA ASTID, Goddard IRAD, and MMAMA programs for funding.

References: [1] ten Kate, et al, Planetary and Space Sciences, Vol 58, Issue 7-8, pp 1007-1017 [2] Getty et al, Int. J. Mass. Spec, Vol 295, pp 124-132, 2010 [3] Glavin et al, Aerospace Conference, 2012 IEEE, pp 1-11

MINERAL INVESTIGATION THROUGH THE COMBINED ANALYSIS OF NIR AND IMAGE-BASED 3D SHAPE RECONSTRUCTED TOPOGRAPHIC DATA. U. Mall[1], R. Bugiolacchi[1], C. Woehler[2] and A. Grumpe[2], [1]Max-Planck-Institute for Solar System Science, Max-Planck-Str. 2, 37191 Katlenburg-Lindau,Germany, mall@mps.mpg.de, [2] TU Dortmund University, Otto-Hahn-Str. 4, 44227 Dortmund, Germany.

Introduction: One of the most important objectives of lunar remote sensing remains the investigation of the abundance and distribution of the major minerals across the Moon's surface. Reflectance spectroscopy makes use of the fact that absorption bands in the reflectance spectra of planetary surfaces contain information on the mineralogy and petrology of the remotely sensed surface areas.The most prominent spectral variations that characterize lunar soils occur in the VIS-NIR part of the spectrum, and in particular, in the near-infrared. The strength and shape of measured infrared absorption bands of an irradiated mineral compound are a function of several variables, among them the abundance of the absorbing minerals. The precise measurements of the spectra allow an estimation of the quantitative mineralogical composition of the observed material.

Mineralogical Maps: Among the lunar minerals, pyroxenes' prominent spectral absorption features at one and two microns in the near-infrared (NIR) spectral region make them ideal targets for remote sensing investigations (i.e. [1], [2]). A variety of quantitative lunar pyroxenes maps have been produced in the past (among them, maps by [3], or more recently, by [4]).However, until recently, all those maps resulted from the measurements of absorption bands at very few selected wavelengths, always assuming a flat lunar surface.

Data Sets: By combining data measured withinstruments on more recent missions like Chandrayaan-1 and LRO, a more precise analysis of absorption spectra and the reflecting topography is becoming a reality.Within this paper, we use hyperspectral data from the SIR-2 and M3 instruments on Chandrayaan-1 to analyze and interpret the mineralogical composition of selected lunar areas with unprecedented high spectral and spatial resolution. The SIR-2 Near InfraRed (NIR) point spectrometer that orbited the Moon on board the Chandrayaan-1 mission in 2008 and 2009 [5], delivered spectra in the 0.9-2.4 µm spectral range with approx. 6 nm spectral resolution at an absolute constant temperature of ±0.1 degree K with a single detector, thus providing NIR reflectance measurements of slightly elliptical footprints of approximately 220 m diameter. The topographic information is obtained by the fusion of the GLD 100, which is derived from LROC WAC imagery and the photometric information from the analysis of M3 images. The GLD 100 is accurate at scales of about 1.5 km/px and lacks topographic features with extents less than 1.5 km[6] while the M3 data features a resolution of 140 m/px. The fusion results in topographic maps of the same lateral resolution as the M3 imagery and, more important, topographic maps which share the same pixel coordinates as the M3 images and are aligned to SIR-2 spectra taken simultaneously, thus allowing one to reference the spectra with absolute precision.

Methods: In order to improve the lateral resolution of the GLD 100, an extended photoclinometry and shape from shading algorithm is applied as proposed in [7]. The method can be described as the search for the surface that best matches the observed images if illuminated using the same light source and viewer positions and is still close to the original shape model. Furthermore, the shape reconstruction method is used to register M3 images from different orbits as proposed in [7]. The aligned images contain different photometric information and thus allow a better estimation of the reflectance behavior, such as the single-scattering albedo and single-scattering phase functions. Since the spectral range of the M3 reaches up to 3 µm the thermal emission is important. We estimate the surface temperature by the superposition of a linear extrapolation to the norm reflectance spectrum R62231 and a black body emission spectrum, as presented in [8]. Radiance values of the SIR-2 and M3 data are used to align the two data sets. Finally, the information derived from the M3 images, such as surface temperature and continuum slope of the absorption at 2 microns, can be applied to the SIR-2 spectra, resulting in high precision NIR reflectance measurements.

We report on the identification and abundance measurements of lunar minerals through the combined analysis and interpretation of NIR and image-based 3D shape reconstructed topographic data.

References:

[1] Hunt, G.R., Salisbury, J.W., 1970. *Modern. Geol. 1, 283-300*.[2] Rossman, G.R., 1980. *Rev. Miner. 7, 93-116*. [3] McCord, T.B., Clark, R.N., Hawke, B.R., McFadden, L.A., Owensby, P.D., Pieters, C.M., Adams, J.B., 1981. *JGR. 86, 10883-10892*. [4] Shkuratov, Yu. G., Kaydash, V. G. and Pieters C. M., 2005. *Solar System Research, Vol. 39, No. 4, pp. 255–266*. [5] Mall, U., Banaszkiewicz, M., Brønstad, K., McKenna-Lawlor, S., Nathues, A., Søraas, F., Vilenius, E. and Ullaland, K.2009. *CURRENT SCIENCE, VOL. 96, NO. 4, 25*. [6] Scholten, F., Oberst, J., Matz, K.-D.,Roatsch, T., Wählisch, M., Speyerer, E. J., and Robinson, M. S., 2012, In: *JGR, 117, E00H17*.[7] Grumpe, A. and Wöhler, C., 2011. In:*Proc. 7th IEEE Int. Symp. Image and Signal Processing and Analysis, 609–614.* [8] Wöhler, C. and Grumpe, A., 2012. In*: Innovations for Shape Analysis: Models and Algorithms. Rev. contrib. to Dagstuhl Seminar, to appear*

IS DRYGALSKI CRATER WET? JOINT ANALYSIS OF LUNAR EPITHERMAL NEUTRONS FROM THE LRO LEND AND LUNAR PROSPECTOR NEUTRON SPECTROMETERS. T.P. McClanahan[1], I.G. Mitrofanov[2], W.V Boynton[3], G. Chin[1], R.D. Starr[4], L.G. Evans[5], G. Droege[3], A. Sanin[2], M. Litvak[2], J. Garvin[1], R. Sagdeev[6], G. Milikh[6], Astrochemistry Laboratory, NASA Goddard Space Flight Center, Greenbelt, MD 20771, (timothy.p.mcclanahan@nasa.gov), [2]Institute for Space Research, RAS, Moscow 117997, Russia, [3]Lunar and Planetary Laboratory, Univ. of Arizona, Tucson AZ, [4]Catholic Univ. of America, Washington DC, [5]Computer Sciences Corporation, Lanham MD 20706, [6]University of Maryland, Space Physics Dept.

Introduction: We investigate the epithermal neutron fluxes observed over the near south-polar Drygalski crater using the Lunar Reconnaissance Orbiter's (LRO), Lunar Exploration Neutron Detector (LEND) detector systems and the Lunar Prospector Neutron Spectrometer (LPNS) [1-3]. We correlate these observations with the Lunar Orbiting Laser Altimeter (LOLA) [4]. These observations indicate the epithermal neutron fluences observed over Drygalksi are significantly low and the LEND results suggest the region may contain the highest-hydrogen concentrations in the Moon's southern hemisphere. These observations have important implications for lunar volatile research as Drygalksi's large-scale, geomorphology and lower latitude -78° may provide clues to the physics of the lunar hydrogen budget.

Initial Results: Recent studies of the Moon's south pole indicate little correlation between low-epithermal rates (high-hydrogen) and regions of permanent shadow [5,6]. Our initial results performed during July 2009 to May 2011 are depicted in the LEND south-polar epithermal count rate map in Figure 1. This map illustrates low-epithermals as purple to black patches. Permanent shadow regions are outlined in white delineating Cabeus (A) and Shoemaker (B), which suggest higher-hydrogen. Other permanent shadow regions are inferred to contain lower Hydrogen abundances. The *green*-boxes in Figure 1 and 2 encompass the 150km diameter and 5km deep Drygalski crater. The neutron suppression region overlies Drygalski's poleward-facing inner slopes and north of the permanent shadow region near daughter crater Drygalksi V (C). This region reflects minimal epithermal rates: 4.80±0.05 cps vs. 4.82±0.02 for Shoemaker and 4.83±0.03 for Cabeus. Also, of interest in this result is the symmetric crescent shape and position of the suppression region which is consistent with the high inner-slopes and concave side of the suppression region facing the pole. This result is consistent with illumination predictions for cratered geomorphology [7, 8]. This observation may suggest a correlation of epithermal neutron fluences to illumination condition.

However, During LRO station keeping LEND is turned off yielding lower observation time and counting statistics over the Drygalski region. We revisit this research and include an additional 1.3 years of LEND collimated data up to September 2012.

References: [1] Chin *et al.* (2007) *Sp. Sci. Rev.* #150 [2] Mitrofanov *et al.* (2007) *Sp. Sci. Rev.* #150 [3] Feldman *et al.* (1998) *Science,* #281 [4] Smith *et al.* (2007) *Sp. Sci. Rev.* #150 [5] Mitrofanov *et al.* (2011) *Science* [6] Boynton *et al.* (2012) *JGR.* [7] McClanahan *et al.* (2010) *LPSC* [8] Carruba *et al.* (1999) *Icarus* #142

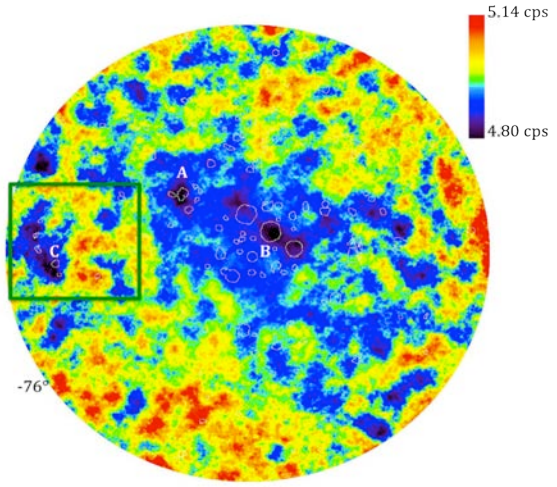

Figure 1: Initial Results: LEND South Polar Stereographic Epithermal Map with white permanent shadow regions A) Cabeus B) Shoemaker, *green*-box delineates C) Drygalski. Coverage from July 2009 to May 2011.

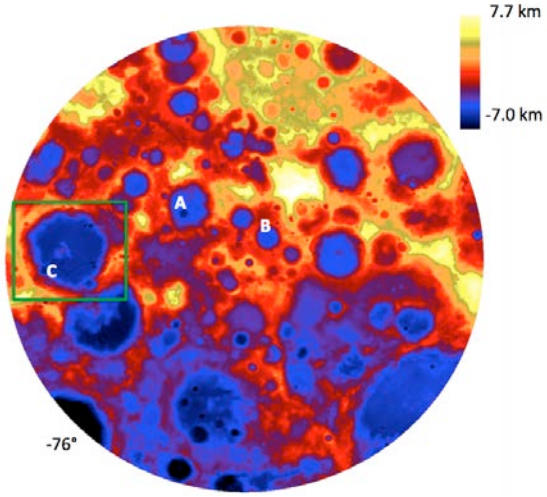

Figure 2: LOLA South Polar Stereographic DEM with white permanent shadow regions A) Cabeus B) Shoemaker, green-box delineates C) Drygalski region.

Next Generation Lunar Laser Ranging. S. M. Merkowitz and A. M. Preston, NASA Goddard Space Flight Center, Greenbelt MD 20771, Stephen.M.Merkowitz@nasa.gov

Lunar laser ranging (LLR) has been a workhorse for testing general relativity over the past four decades as well as dramatically increasing our understanding of Earth and Moon geophysics, geodesy, and dynamics [1]. The three retroreflector arrays put on the Moon by the Apollo astronauts and the French built arrays on the Soviet Lunokhod rovers continue to be useful targets, and have provided the most stringent tests of the Strong Equivalence Principle and the time variation of Newton's gravitational constant. The relatively new ranging system at the Apache Point 3.5 meter telescope now routinely makes millimeter level range measurements to these reflectors [2].

The precision of the range measurements has historically been limited by the ground station capabilities. With now routine millimeter level precision at Apache Point, future measurements are likely to be limited by errors associated with the Apollo retroreflectors. In addition, the clustering of the lunar arrays and similar latitudes of the available lunar ranging stations weakens our ability to precisely measure the lunar librations [3].

New retroreflectors placed at locations far from the Apollo sites (such as a pole or limb) would enable the study of additional effects, particularly those that rely on the measurement of the lunar librations. In addition, more advanced retroreflectors are now available that will reduce some of the systematic errors associated with using the current arrays, resulting in more precise range measurements. Retroreflectors are extremely robust, do not require power, and last for decades. This longevity is important for studying long-term effects such as a possible time variation in the gravitational constant. New retroreflectors with higher cross-sections would also enable more laser ranging stations to be used for lunar measurements.

We report here on the ongoing laser ranging development efforts at Goddard Space Flight Center as part of the NASA Lunar Science Institute's LUNAR team. At the heart of this effort is the development of next generation lunar retroreflectors. The recently completed LUNAR open cube assembly and testing facility is currently being used to design, assemble, and test large-scale open cube corners. Investigations into various bonding techniques, including the hydroxide bonding technique developed for Gravity Probe B, are underway and producing promising results. We are also investigating mirror coatings for the cubes that have dust mitigation properties.

[1] S. M. Merkowitz, "Tests of Gravity Using Lunar Laser Ranging," Living Rev. Relativity **13**, (2010).

[2] T. W. Murphy *et al.,* Publ. Astron. Soc. Pac. **120**, 20 (2008).

[3] S. M. Merkowitz *et al.,* Int. J. Mod. Phys. D **16**, 2151 (2007).

UPDATE ON THE SCIENTIFIC CHARACTERIZATION OF LUNAR REGIONS OF INTEREST. S.C. Mest[1,2], A.R. Dworzanczyk[3], A. Calzada-Diaz[4], J.E. Bleacher[2], N.E. Petro[2], and R.A. Yingst[1], [1]Planetary Science Institute, 1700 E. Ft. Lowell, Suite 106, Tucson, AZ 85719-2395 (mest@psi.edu); [2]Planetary Geodynamics Laboratory, Code 698, NASA GSFC, Greenbelt, MD 20771, [3]Regis High School, 55 E 84th Street, New York, NY 10028, [4]International Space University, Illkirch-Graffenstaden, France.

Introduction: NASA's Constellation Program Office (CxPO) has identified 50 Regions of Interest (ROIs) that represent scientifically high-value locations in preparation for our eventual return to the Moon [1] either by astronauts or robots. These ROIs are geologically diverse and spatially distributed, thus allowing each site to address a variety of scientific goals and objectives, such as those described by LEAG [2]. While the value of these ROIs relative to one another is a critical component, such as for landing site selection, detailed analyses of these sites have not been conducted in a comprehensive way that utilizes all available data or at the landing site scale.

In order to select an "ideal" landing site, preliminary detailed characterization of the surface properties of potential sites must be conducted. Analyses at this scale that incorporate geologic mapping, traverses, and evaluation of each ROI's scientific "value" (e.g., their potential for scientific return) have not been conducted since Apollo, and are necessary to accurately assess any potential landing site for the next series of human or robotic missions to the Moon. Here we present new LASER-funded work to evaluate the 50 ROIs.

Methodology: We have begun evaluating 7 of the 50 ROIs (Table 1) using a variety of LRO, Chandrayaan-1, Kaguya, Clementine, Apollo and Lunar Orbiter data to (1) characterize the geology, topography and surface morphology of each ROI and examine the spatial and temporal variability of geologic processes within a 40x40 km area around each ROI, and (2) assess the relative scientific "value" of each ROI with respect to their ability to address key scientific objectives identified by the lunar science and exploration community [2,3]. The relative scientific value of each ROI is be evaluated by constructing hypothetical traverses within the area defined by CxPO up to distances of 5, 10 and 20 km from the ROI location, and estimating the scientific return using the results from mapping. ESRI ArcMap Geographical Information System (GIS) software is being used to compile the datasets, and generate maps

Table 1. Five ROIs currently being studied.

Region of Interest	LAT	LON
Apollo 15	26.1	3.7
Aristarchus 1	24.6	-49.0
Copernicus	9.5	-18.9
Mare Moscoviense	26.2	150.5
North Pole	89.6	76.2
Orientale 1	-26.2	-95.4
South Pole	-89.3	-130.0

ROI Characterization:

Morphologic: Each ROI is being characterized using images and topography to identify and map structures (crater rims, ridges, faults, etc.), analyze surface morphologies and characterize geologic units, identify geologic contacts, and determine stratigraphic relationships. Geologic mapping and surface analyses are based primarily on LRO LROC (~50 cm/pixel), Kaguya Multi-band Imager (~20 m/pixel), Clementine UVVIS 750 nm (100-325 m/pixel) and HIRES (7-20 m/pixel) images, Lunar Orbiter IV and V images (~100 m/pixel), and Apollo MappingCam, Pancam, and Hasselblad images. In addition, we are using the most up-to-date lunar topographic data – LRO LOLA DEM (128 pixels/degree) and individual tracks – to characterize the topographic expression of the surface.

Spectral: We are utilizing currently released M^3 data, as well as Clementine UVVIS and NIR global mosaics (~100 m/pixel; 70ºN and 70ºS) to characterize surface materials at most of the 50 ROIs.

Digital Geologic Mapping: Geologic mapping of the lunar surface at the ROI-scale is important because it allows complex surfaces to be characterized based upon physical attributes, thereby allowing discrete material units to be defined. The distributions of these units are then mapped in order to identify the relative roles of impact cratering, volcanic, tectonic and gradational processes in shaping their surfaces.

ROI Traverse Development: For this research, hypothetical traverses from each ROI are being developed. Plotting the traverses is based primarily on the geologic assessment, that is, a traverse will be developed so that it maximizes its ability to observe and/or sample as many of the geologically significant features, units, etc. within an ROI area as possible. We are limiting our area of exploration to the maximum 40x40 km area identified by Cx [1], which is ultimately limited by current lunar exploration architecture.

References: [1] Gruener, J.E. and B.K. Joosten (2009) LRO Science Targeting Meeting, Abs. **#6036**. [2] LEAG (2009) The Lunar Exploration Roadmap, LPI. [3] NRC (2007) The Scientific Context for Exploration of the Moon, 121pp.

UPGRADED PROGRAM OF RUSSIAN LUNAR LANDERS: STUDYING OF LUNAR POLES. I. G. Mitrofanov[1] , L. M. Zelenyi[1] and V. I. Tret'yakov[1], [1]Institute for Space Research, Profsojuznaja 84/32, 117997 Moscow, Russia, imitrofa@space.ru.

The new program will be described of future Russian lunar landers. The main scientific goal of the program is studying of lunar South pole: volatiles in the regolith and polar exosphere. The main engineering goal is to develop the new space technology for lunar polar landing and surface operations.

The first lunar landing is scheduled on 2015, as part of the Luna-Glob project. The limited set of scientific instruments will be delivered to the Moon by this mission, which the primer goal is the testing of landing technology and surface operations. The next mission Luna-Resource will land on the Moon in 2017 with much larger payload. This mission will perform studies of lunar polar volatiles from the shallow subsurface.

Depending of results of these two landing missions, the third one of this sequence will be scheduled on 2019 or later for Lunar Polar Sample Return (LPSR).

CHARACTERIZATION OF LUNAR CRATER EJECTA DEPOSITS USING M-CHI DECOMPOSITIONS OF MINI-RF RADAR DATA. G.W. Patterson, R.K. Raney, J.T.S. Cahill, D.B.J. Bussey, and the Mini-RF Team. Johns Hopkins University Applied Physics Laboratory, Laurel, MD (Wes.Patterson@jhuapl.edu).

Introduction: Impact cratering is the dominant weathering process on the surface of the Moon and is largely the determining factor of material distribution on the lunar surface [1] Radar data provide unique information on both the horizontal and vertical distribution of impact deposits [2]. We introduce a new technique for analysis of polarimetric radar astronomical data, *m-chi*, derived from the classical Stokes parameters. Analysis of the crater Byrgius A demonstrates how *m-chi* can more easily differentiate materials within ejecta deposits and their relative thicknesses.

Background: The Miniature Radio Frequency (Mini-RF) instrument flown on the Lunar Reconnaissance Orbiter (LRO) is a Synthetic Aperture Radar (SAR) with an innovative hybrid dual-polarimetric architecture, transmitting (quasi-) circular polarization, and receiving orthogonal linear polarizations and their relative phase [3]. The four Stokes parameters that characterize the observed backscattered EM field are calculated from the received data. These parameters can be used to derive a variety of child products that include the circular polarization ratio (CPR) and the *m-chi* decomposition. The former provides an indication of surface roughness and the latter provides an indication of the scattering properties of the surface [4].

Analysis: Byrgius A is a 19 km diameter Copernican located in the lunar highlands east of the Orientale Basin and west of Mare Humorum. Visible image data of the region obtained by the Lunar Reconnaissance Orbiter Camera Wide Angle Camera (LROC WAC) [5] at a resolution of 100 m/pixel show optically bright ejecta deposits associated with the crater that extend to radial distances of 100s of km, with near continuous deposits observed to an average radial distance of 70 km (Fig. 1).

Mini-RF CPR information derived from S-band (12.6 cm) data of the region show an increased roughness for Byrgius A and its ejecta deposits relative to the surrounding terrain. This is a commonly observed characteristic of young, fresh craters and indicates that the crater and its ejecta have a higher fraction of cm- to m-scale scatterers at the surface and/or buried to depths of up to ~1 m. As observed with visible image data, the increased roughness associated with the ejecta of Byrgius A appears nearly continuous to a radial distance of ~70 km.

An *m-chi* decomposition of Mini-RF S-band data for Byrgius A suggests that the portion of ejecta that extends radially from ~10 to 70 km appears far less continuous than is suggested in both optical data and CPR information (Fig. 1). The implication is that we are observing properties of the ejecta and lunar background terrain in the top meter of the surface. In other words the thickness of the ejecta in this distance range is on the order of meters or less.

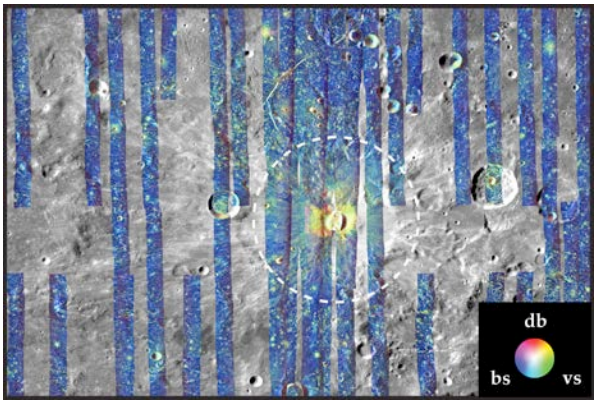

Figure 1. An m-chi decomposition showing the crater Byrgius A (19 km dia.; 24.5°S, 63.7°W) overlain on LROC WAC data (100 m/pixel). The color wheel highlights the m-chi scattering regimes (double bounce, db; single bounce, bs; volume scattering, vs).

Conclusions: The Mini-RF instrument on LRO is among the first polarimetric imaging radars outside of Earth orbit. Stokes information returned from the instrument can be used to create derived products such as CPR and *m-chi* decompositions. Using these products, we examine the crater Byrgius A and demonstrate the ability to differentiate materials within ejecta deposits and their relative thicknesses. This result suggests that the thickness of ejecta at radial distances > a crater radius differ significantly from estimates of ejecta thickness derived from models of ejecta emplacement [6,7].

References: [1] Melosh, H. J. (1989), Oxford Univ. Press, New York; [2] Ghent, R. R. et al. (2008), *Geology*, 36(5), 343-346; [3] Raney, R. K. et al. (2011), *Proc. of the IEEE*, 99(5), 808-823; [4] Raney, R.K. et al. (2012), *JGR,* 117, E00H21; [5] Robinson, M. S. et al. (2010), *Space Sci. Rev.*, 150, 81-124; [6] McGetchin et al. (1973), *EPSL*, 20, 226-236; [7] Pike (1974), *EPSL*, 23, 265-274.

COMMERCIAL MODELS FOR LUNAR LANDING AND EXPLORATION. K. M. Peterson[1] and J. Thornton[1], [1]Astrobotic Technology, 4551 Forbes Avenue #300, Pittsburgh, PA 15213, kevin.peterson@astrobotictech.com, john.thornton@astrobotictech.com

Introduction: Space agency costs for exploration and science missions can be reduced by combining fixed-price contracts with methods that enable commercial bidders to earn supplementary revenue. This non-agency revenue in many cases will feature novel methods of public involvement, transforming "public outreach and education" from a cost to the space agency into a revenue source for the commercial bidder. The space agency will get services at a fixed price that is lower than traditional cost-plus methods. Lower cost stems from several factors including commercial culture, where every dollar saved is profit so long as it doesn't materially impact mission success.

In the long term, select space endeavors will come to fruition solely with private funding. These endeavors will span prospecting, resource extraction, site preparation for human missions, and science goals from far-side radio astronomy to understanding the bombardment history of the early solar system. Many of these missions will be repetitive such as multiple prospectors to survey large areas, scrapers and dozers for resource extraction and site preparation and mobile rovers providing basic utilities like power, thermal control and communication for science payloads. Many of the same systems are common to each class of rover including power systems, drive-trains, communication systems, camera and antenna pointing mechanisms, navigation sensors and software. These factors argue for having the bulk of lunar robotic activity based in the cost effective private sector with governments as customers, rather than being carried out directly by government agencies.

However, further exploration is necessary to spur commercial activity on the moon. Financial models rely on presence of volatiles, precious metals, or sustained human activity. The uncertainty in these markets poses a significant barrier to investment. A public-private partnership to evaluate unknowns in these financial models is called for. The proposed partnership exploits commercial cost savings to advance lunar science and resolve financial uncertainty.

Astrobotic Technology, a spin-off from Carnegie Mellon University's Robotics Institute, has developed a lander and a prospecting rover for initial surface activities. A first expedition, Icebreaker, will launch from Florida in October 2015 to explore Polar regions in search of water. A SpaceX Falcon 9 will carry the lander and rover to trans-lunar injection. The lander

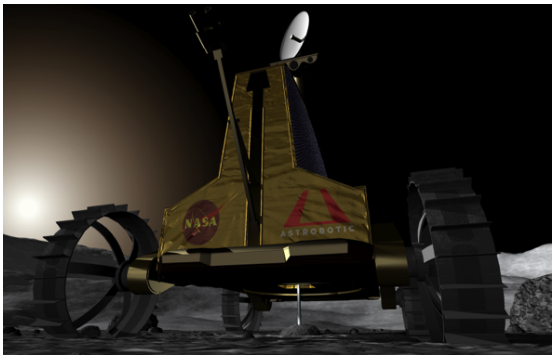

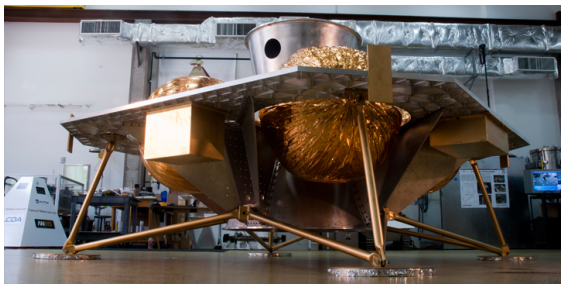

will cruise for three days, capture into orbit, descend and precisely land near the pole.

The rover is a self-sustaining lunar exploration platform designed for long-distance traverse. Freeze tolerant design enables unprecedented non-isotope operation through multiple day-night cycles. It features a U-shaped composite chassis allowing for large payloads up to 100-kg. Its navigation system provides better than two-meter global registration to terrain.

Subsequent missions will scout skylights - holes providing access to volcanic caves - and routes that circumnavigate the poles to stay perpetually in sunlight. Reuse of the chassis and lander designs will provide significant reduction in mission development cost.

ArcGIS DIGITIZATION OF APOLLO SURFACE ACTIVITES: A SPATIAL DATABASE OF TRAVERSES, SAMPLES, AND IMAGES. N. E. Petro[1] and J. E. Votava[1,2], [1]NASA Goddard Space Flight Center, Planetary Geodynamics Laboratory, Greenbelt, MD, 20771, [2]University of Minnesota Duluth. (email: Noah.E.Petro@nasa.gov)

Introduction: The Apollo surface activities are well documented [1-4] and an abundance of information associated with surface activities exists in multiple locations, both on paper and online [5-8]. With high-resolution data from LRO much of the routes taken by the Apollo crews can be digitized [9] along with corresponding sample and photograph locations. A centralized database of surface activities is being created in ArcGIS that places the traverses, sample sites, and other surface activities into a centralized spatial context [10]. The value of such a centralized database is that any feature (e.g., a traverse, a sample, or image) can have corresponding metadata (e.g., distance, time, compositions, web links) associated with it. The ArcGIS projects will be made available to the community and updated/revised as needed.

Thus far all of the J-Missions have been digitized, with Apollo 15 being the most mature of the group. We have digitized the published traverse maps [11], the planned traverse and contingency walking routes [12], traced paths visible in LROC NAC images, added the locations of each station, sample site, and panorama location (Figures 1,2). Accompanying each sample site are metadata containing sample description, mass, age information, compositional data (major elements and REE compositions), and a link to the corresponding descriptive curation document [7].

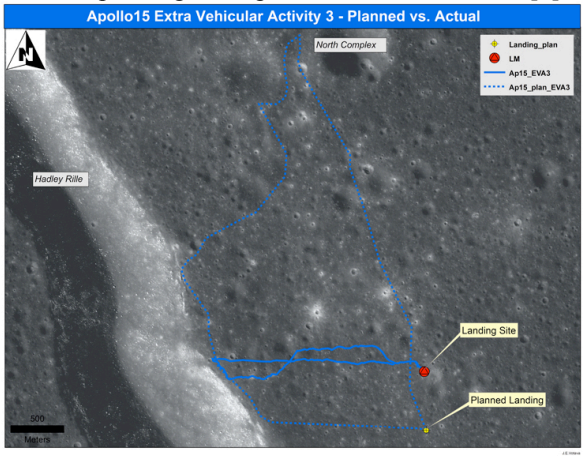

Figure 1. Apollo 15 EVA 3 planned traverse [12] versus actual traverse. Base image is LROC NAC frame M170538271.

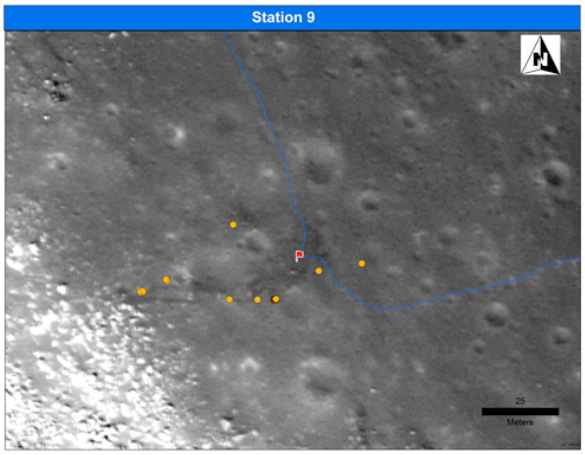

Figure 2. View of Station 9 from Apollo 15 EVA 3, showing sample locations [11]. Base image is LROC NAC frame M170538271.

Strengths of Digital Apollo Traverse Data: There are many benefits of creating a spatial database of Apollo surface activities. Of particular interest is the ability to easily display compositional or age data associated with samples [3, 13, 14], calculate derived values (times, distances, relative speeds) [4], and easily place Apollo samples in their proper sampled context. Additionally, this database can be easily mined for information to assist in planning of future surface activities (differences between planned and actual traverses in a variety of terrains).

We would appreciate suggestions for data and or products to include in the database or ways to make the digital product useable to the broader community.

Acknowledgements: Funding to NEP from the LASER program and the support of JEV by the Goddard Lunar and Planetary Science Academy is greatly appreciated.

References: [1] NASA, (1969) *NASA Special Publication*, 214. [2] Ulrich, G. E., et al., (1981) *Geology of the Apollo 16 area, Central Lunar Highlands*. [3] Robinson, M. S. and B. L. Jolliff, (2002) *Journal of Geophysical Research*, 107k, 20-21. [4] Orloff, R. W., (2004) *Apollo By The Numbers: A Statistical Reference*, 348 p. [5] Wolfe, E. W., et al., (1981) *The Geologic investigation of the Taurus-Littrow valley, Apollo 17 landing site*. [6] USGS Planetary GIS Web Server, (http://webgis.wr.usgs.gov/). [7] Astromaterials Curation at NASA JSC, (http://curator.jsc.nasa.gov/lunar/index.cfm). [8] Apollo Analyst's Notebook, (http://an.rsl.wustl.edu/apollo/). [9] Haase, I., et al., (2012) *J. Geophys. Res.* [10] Petro, N. E., et al., (2012) ArcGIS Digitization of Apollo Surface Traverses, 43, 2512. [11] (1972), *Apollo 15: Preliminary Science Report*,Abst. [12] NASA, (1971) *Apollo 15 FInal Lunar Surface Procedures*. [13] Votava, J. and N. Petro, (2012), *AGU Fall Meeting*,Abst. [14] Jolliff, B. L., (1999) *JGR*, 104, 14123-14148.

THE CHEMICAL REACTIVITY OF LUNAR DUST INFLUENCES ITS BIOLOGICAL EFFECT.

J. C. Rask[1], P. C. Zeidler-Erdely[2], T. Meighan[2], M. W. Barger[2], W. T. Wallace[3], B. Cooper[4], D. W. Porter[2], E. M. Tranfield[1], L. A. Taylor[5], D. S. McKay[4], V. Castranova[2], Y. Liu[5], D. J. Loftus[1], [1]Lunar Dust Biological Effects Laboratory, NASA Ames Research Center Moffett Field, CA 94035, jon.c.rask@nasa.gov, [2]Pathology and Physiology Research Branch, Health Effects Research Division, National Institute of Occupational Safety and Health, Morgantown, WV 26505, [3]Wyle Integrated Science and Engineering Group, Houston, TX 77058, [4]NASA Johnson Space Center, Houston, TX 77058, [5]Department of Earth and Planetary Science, University of Tennessee, Knoxville, TN 37996

Introduction We have investigated the relationship between the chemical reactivity of lunar dust and its biological effect in the lungs. Using authentic Apollo 14 lunar dust, we evaluated the responsiveness of rat lung macrophages after intratracheal instillation [1], using the zymosan-stimulated macrophage chemiluminescence assay. Three preparations of respirable-sized lunar dust were studied: ball-milled lunar dust, jet-milled lunar dust, and unground lunar dust. At 30 days post-exposure to lunar dust, macrophages from rats that received the most chemically reactive lunar dust exhibited greater responsiveness than macrophages from animals exposed to less chemically reactive forms of the same lunar dust. These results are analogous to the increased toxic effect of highly chemically-reactive mechanically-activated quartz dust [2]. Our results also show that Apollo 14 lunar dust is intermediate in toxicity, between TiO2 and quartz, and that lunar dust chemical reactivity may be a useful, measurable parameter in assessing *in situ* toxicity.

Acknowledgements We thank the NASA the Lunar Airborne Dust Toxicity Assessment Group for their support, and the NASA Human Research Program for funding this effort.

References: [1] P. A. Santana et. al. (2010), Modeling respiratory toxicity of authentic lunar dust, *NASA Technical Report JSC-CN-22387*. [2] D. W. Porter et al. (2002), Comparison of low doses of aged and freshly fractured silica on pulmonary inflammation and damage in the rat, *Toxicology* 175, 63.

Scientific Breakthroughs from the LRO-Lyman Alpha Mapping Project (LAMP). K. D. Retherford (1), S. A. Stern (2), G. R. Gladstone (1), J. C. Cook (2), A. F. Egan (2), P. F. Miles (1), J. Wm. Parker (2), D. E. Kaufmann (2), T. K. Greathouse (1), C. C. C. Tsang (2), M. H. Versteeg (1), J. Mukherjee (1), M. W. Davis (1), A. J. Bayless (1), P. D. Feldman (3), D. M. Hurley (4), W. R. Pryor (5), and A. R. Hendrix (6); (1) Southwest Research Institute, San Antonio, TX (kretherford@swri.edu), (2) Southwest Research Institute, Boulder, CO, (3) Johns Hopkins University, Baltimore, MD, (4) Johns Hopkins University Applied Physics Laboratory, Laurel, MD, (5) Central Arizona University, Coolidge, AZ, (6) Jet Propulsion Laboratory, Pasadena, CA.

Abstract. The Lunar Reconnaissance Orbiter (LRO) Lyman Alpha Mapping Project (LAMP)'s innovative nightside observing technique allows us to peer into the permanently shaded regions (PSRs) near the poles, and determine their UV albedos. LAMP measurements indicate ~1-2% surface water frost abundances in a few PSRs based on spectral color comparisons [1]. A strong water ice absorption edge near 160 nm within LAMP's bandpass presents itself as a relative reddening at the longest far-UV wavelengths. LAMP generally measures darker albedos within PSRs at Lyman-α and other far-UV wavelengths that are consistent with ~30% higher porosity, and consistent with "fairy-castle" structures previously suggested to exist there [1]. Nightside maps of far-UV albedo show relative brightnings associated with the peaks of crater rims and other features indicative of enhanced spaceweathering effects [2]. Dayside far-UV maps and spectra are also being produced using more traditional photometry techniques. Spectral analysis of dayside regions indicate far-UV signatures of surface hydration; this result complements the detections of OH/H_2O hydration at infrared wavelengths by the Chandryaan-1/M^3 team [3]. Lunar helium atmospheric emissions have been detected remotely for the first time, which enables new global investigations of its distribution and variability [4]. Initial variability studies show the lunar helium abundance to vary with solar wind conditions, as expected - including stoppages of helium in-flux during times of Earth magnetotail transits [5]. LCROSS impact plume observations with LAMP detected H_2, CO, Hg, Mg, and Ca constituents, which together with LCROSS shepherding satellite observations revealed a much richer mix of volatiles trapped within the PSRs than previously understood [6,7,8]. A lab study of the UV reflectance properties of lunar simulants and water ice samples is underway [9], and Apollo sample measurements are being planned to help us pioneer these new techniques in UV spectroscopy for investigating lunar volatiles.

Instrument. The LAMP UV spectrograph (Figure 1) covers the 57-196 nm bandpass [10]. Its 6°×0.3° slit, nominally pointed nadir, scans the surface in push-broom style, similar to other LRO instruments. LAMP routinely observes the Lunar nightside via reflected starlight and interplanetary medium illumination [11], and its mapping resolution of ~240 m x 240 m per pixel is similar to that for LROC/WAC and Diviner on LRO. The lunar dayside is also observed by switching to a pinhole mode after terminator crossings each orbit.

Figure 1: LAMP instrument prior to LRO integration.

References

[1] Gladstone, G. R. et al., Far-Ultraviolet Reflectance Properites of the Moon's Permanently Shadowed Regions, *J. Geophys. Res.*, 117, E00H04, doi:10.1029/2011JE003913, 2012.

[2] Retherford, K. D. et al., LRO/LAMP Far-UV Albedo Maps of the Lunar Poles, *in prep.*, 2012.

[3] Hendrix, A. R. et al. , The Lunar Far-UV Albedo: Indicator of Hydrated Materials and Space Weathering, *submitted to J. Geophys. Res.*, 2012.

[4] Stern, S. A. et al., Lunar atmospheric helium detections by the LAMP UV spectrograph on the Lunar Reconnaissance Orbiter, *Geophys. Res. Lett.*, 39, L12202, doi:10.1029/2012GL051797, 2012.

[5] Feldman, P. D. et al., "Temporal Variability of Lunar Exospheric Helium During January 2012 from LRO/LAMP," *submitted to Icarus*, 2012.

[6] Gladstone, G. R. et al., LRO-LAMP Observations of the LCROSS Impact Plume, *Science*, *330*, 472-476, 2010.

[7] Hurley, D. M. et al., "Modeling of the Vapor Release from the LCROSS Impact: II. Observations from LAMP," J. Geophys. Res., 117, E00H07, doi:10.1029/2011JE003841, 2012.

[8] Hurley, D. M et al., Two-dimensional distribution of volatiles in the lunar regolith from space weathering simulations, Geophys. Res. Lett., 39, L09203, doi:10.1029/2012GL051105.

[9] Retherford, K. D., et al., Lunar Ultraviolet Reflectance Experiment (LURE): Far-UV Signatures of Water Ice, *LPSC Meeting*, The Woodlands, TX 2012.

[10] Gladstone, G. R., and 15 coauthors, LAMP: The Lyman Alpha Mapping Project on NASA's Lunar Reconnaissance Orbiter Mission, *Space Sci. Rev.*, *150*, 161-181, 2010.

[11] Pryor, W. R. et al., Lyman-alpha Models for LRO LAMP based on MESSENGER MASCS and SOHO SWAN data, *ISSI book chapter*, 2012.

LROC EXPLORATION OF THE MOON. M.S. Robinson[1] and the LROC Team, [1]Arizona State University, School of Earth and Space Exploration, Box 871404, Tempe, AZ, 85287.

Since entering orbit in 2009 the Lunar Reconnaissance Orbiter Camera (LROC) has acquired over 700,000 Wide Angle Camera (WAC) and Narrow Angle Camera (NAC) images of the Moon. This new image collection is fueling research into the origin and evolution of the Moon (i.e. tectonism, volcanism, impact processes, photometry and space environment-surface interactions), unique advances in cartography, and provides the basis for stereo topography and mosaics. This abstract highlights a subset of LROC-based advances to date.

NAC images revealed an elevated silicic, nonmare volcanic complex 35 x 25 km (60˚N and 100˚E), between Compton and Belkovich craters (CB). The CB terrain sports numerous volcanic domes and irregular depressed areas interpreted to be caldera-like collapses. The volcanic complex corresponds to an area of high-silica content (Diviner) and high Th (Lunar Prospector). Volcanic constructs diameters range from 1 to 6 km in diameter with up to 800 m elevation and slopes >20˚. A low density of impact craters indicates that this volcanic complex is relatively young.

The LROC team mapped over 150 Marius Hills (MH) volcanic domes and 90 volcanic cones, many of which were not previously identified. Morphology and compositional estimates (Diviner) indicate that MH domes are not silica-rich, unlike most other lunar domes. These results indicate that the Marius Hills are a unique form of lunar volcanism and support the hypothesis that these landforms are products of low-effusion rate mare lavas.

Impact melt deposits are observed in most large Copernican impact craters (with diameters >10 km) in ponds and flows on exterior ejecta, the rim, inner wall, and crater floors. Preserved impact melt flow deposits are observed around craters as small as 2.4 km diameter, and the estimated melt volume is substantially higher than models predict. At small diameters (<5 km), the amount of melt predicted from modeling studies is small, and melt that is produced is expected to be ejected from the crater interior. However, we observe well-defined impact melt deposits on the floor of some highland impact craters as small as 200 m diameter. NAC digital elevation models (DEM) allow for a quantitative analysis of impact melt forms, from which properties such as viscosity, temperature, and clast content can be assessed. Observations show that melt deposits were highly fluid and superheated during emplacement.

A globally distributed population of previously undetected contractional and extensional structures were discovered in LROC images. Their crisp appearance, lack of superposed large-diameter impact craters, and crosscutting relations with small-diameter impact craters show that lobate scarps are relatively young landforms (<< 1 Ga). Because of their young age and wide distribution, the population of lobate scarps is interpreted as an expression of recent global radial contraction due to cooling of the lunar interior. NAC images also revealed small-scale extensional troughs or graben both in nearside mare and in the farside highlands. Crosscutting relations with small-diameter impact craters along with depths as shallow as 1 m indicate these pristine graben are <50 Ma old. The young, small-scale graben and lobate scarps place bounds on the amount of global radial contraction and the level of compressional stress in the lunar crust.

The polar orbit of LRO and the broad field of view of the WAC enable multi-temporal coverage of regions near the poles. From over 4000 WAC images several highly illuminated regions were discovered, including one site that remains illuminated for nearly 94% of the year, with its longest eclipse period lasting only 43 hours. Targeted NAC images provide higher resolution characterization of specific key sites with permanent shadowing and extended illumination.

Repeat imaging over a range of viewing and Sun angles revealed the presence of collapse pits both in the mare and impact melt deposits. For two of the mare pits LROC imaged into sublunarean voids with unknown extents.

The repeat WAC coverage provides an unparelled photometric dataset that allows spatially resolved solutions (currently 1°) to Hapke's photometric equation (7 bands, 300 to 700 nm) – data invaluable for photometric normalization and interpreting physical properties of the regolith. The WAC color also provides the means to better solve for titanium abundance within the mare, and distinguish subtle age differences within Copernican aged materials.

The longevity of the LRO mission allows follow up NAC and WAC observations of previously known and newly discovered science targets over a range of illumination and viewing geometries. Of particular merit is the continued acquisition of NAC stereo pairs and oblique sequences that provide amazing tools to unravel the complex and relatively unknown geologic history of the Moon. With the extended SMD phase, the LROC team is working towards the ultimate goal of imaging the whole Moon with pixel scales of 50 to 200 cm.

RESOLVE LUNAR ICE/VOLATILE PAYLOAD DEVELOPMENT AND FIELD TEST STATUS. G. B. Sanders[1], R.S. Baird[1], K. N. Rogers[1], W. E. Larson[2], J. W. Quinn[2], J. E. Smith[2], A. Colaprete[3], R. C. Elphic[3], and M. Picard[4], [1]NASA-JSC, 2101 NASA Parkway, Houston, TX, gerald.b.sanders@nasa.gov, [2]NASA-KSC, Kennedy Space Center, FL, [3]NASA-ARC, Moffet Field, CA, [4]Candian Space Center, Québec, Canada.

Introduction: Understanding the form, distribution, and content of water/ice and other volatiles at the lunar poles can have a profound effect on the scientific understanding of the Moon and solar system evolution, and on plans for utilizing the resources on the Moon for sustained human exploration and the commercial development of space. While orbital remote sensing and surface impact data has been obtained from lunar scientific spacecraft on the potential presence and distribution of water/ice on the Moon, the data collected provides only an initial understanding of its form and distribution which must be further refined. Since 2005, the National Aeronautics and Space Administration (NASA) and the Canadian Space Agency (CSA) have cooperated in developing an experiment package that could provide 'ground truth' measurements of water/ice and other volatiles at the lunar poles as well as demonstrate the feasibility of extracting oxygen from lunar regolith.

RESOLVE Overview: The Regolith & Environment Science and Oxygen & Lunar Volatile Extraction (RESOLVE) is a rover-based experiment that includes neutron and near infrared spectrometers to locate hydrogen-sources and water, a drilling system to collect samples down to one meter below the surface, and a sample analysis oven with a gas chromatograph/mass spectrometer to heat and analyze water and other volatiles released from subsurface samples. The same oven can be heated to 900 ºC with hydrogen gas to extract oxygen from iron-oxide minerals in the regolith. From 2005 to 2010, two generations of RESOLVE prototypes were built and tested, along with performing tests of RESOLVE on a rover at an analogue site in Hawaii in Nov. 2008 and Feb. 2010.

RESOLVE Design Reference Mission (DRM): In order to design the 3rd generation RESOLVE, a design reference mission (DRM) study was performed. Sites for the DRM had to meet four selection criteria: 1) high hydrogen concentrations, 2) good ice stability, 3) visibility from Earth so a relay satellite is not required to perform the mission, and 4) brief periods of sunlight to allow solar power to be utilized. Data from four instruments on LRO (LEND, DIVINER, LOLA, and LROC) were used in the study. Design requirements for RESOLVE are based on a 5-7 day sunlit mission near Cabeus crater.

RESOLVE 3rd Generation Flight Prototype: To meet mission DRM requirements, the 3rd Generation of the RESOLVE is being designed to operate both in sunlight as well as brief periods of shadowing (<100 K) and to perform 3 to 5 one-meter drill core sample collection and analyses operations in a 5 to 7 day period over a 1 to 3 km traverse. The 3rd Gen RESOLVE unit is being designed and built in two Phases. Phase I is a flight mass/power unit for lunar polar mission simulation analogue testing in July 2012, and Phase II is a flight mass/power unit for lunar environment testing in 2014.

Lunar Polar Mission Simulation: To validate both the design of the 3rd generation RESOLVE unit as well as the lunar polar RESOLVE DRM, an analogue field test mission simulation was performed in July 2012. The purpose was to demonstrate: i) integration of all the hardware necessary for flight on a single rover, ii) integrated operations of the RESOLVE and rover including roving/scanning, drilling/sample transfer, and sample processing/volatile measurement, iii) all mission operations and timelines to validate a short duration lunar mission, and iv) mission command and control with lunar time delays and bandwidth limitations.

To make the mission simulation as realistic as possible, polyethylene sheets were used to simulate ice/water concentrations and a mockup lander was utilized to 'deliver' the RESOLVE/rover to the mission start location and provide communication, situational awareness, and relative navigation to the RESOLVE/rover mission team. All operations were performed remotely with either the main RESOLVE/rover mission team near the test site, or by personnel at control centers at NASA Johnson and Kennedy Space Centers, CSA, or science support from NASA Ames Research Center using only data provided by the rover or mockup lander.

Before the field test, Category 1 (mandatory) to 4 (goals) objectives based on the RESOLVE lunar DRM were established. At the completion of the analogue mission simulation, almost all of the Category 1, 2, and 3 objectives were accomplished and 2 of 5 Category 4 objectives were accomplished.

Next Step in RESOLVE Development: With the completion of the Phase I RESOLVE buildup and mission simulation in Hawaii, the RESOLVE team is now focusing on Phase II development of the lunar vacuum/environment compatible flight prototype. Further testing of the Phase I RESOLVE unit will also be performed to provide more lessons learned going into Phase II. Lunar environment testing is planned for August, 2014.

SEARCHING FOR WATER ICE PERMAFROST: LEND RESULTS FOR ABOUT THREE YEARS OF OBSERVATIONS. A. B. Sanin[1], I .G. Mitrofanov[1], M. L. Litvak[1], A. Malakhov[1], W. V. Boynton[2], G. Chin[3], G. Droege[2], L. G. Evans[5], J. Garvin[3], D. V. Golovin[1], K. Harshman[2], T. P. McClanahan[1], G. Milikh[4], M. I. Mokrousov[1], R. Z. Sagdeev[4], R. D. Starr[6], [1]Institute for Space Research, RAS, Moscow 117997, Russia, sanin@mx.iki.rssi.ru, [2]Lunar and Planetary Laboratory, University of Arizona, Tucson AZ, USA, [3]NASA Goddard Space Flight Center, Greenbelt MD, 20771, USA, [4]Space Physics Department, University Maryland, College Park, MD, USA, [5]Computer Sciences Corporation, Lanham MD 20706, USA, [6]Catholic University of America, Washington DC, USA.

Introduction: More than 50 years ago, it was suggested that some areas near the lunar poles are sufficiently cold to trap and preserve for a very long time (~Gy) hydrogen bearing volatiles, either primordial or produced at the Moon via solar wind interactions or brought to the Moon as water ice by comets and meteoroids [1,2]. The results of observations made by radar onboard the Clementine spacecraft and by neutron (LPNS) and gamma-ray (LPGRS) spectrometers onboard the Lunar Prospector mission have been interpreted as an enhancement of hydrogen abundance in permanently shadowed regions (PSRs) [3]. Unfortunately, the spatial resolution of the LPNS was much broader than the size of any largest PSRs [4] requiring model dependent data deconvolution to reslve signal from PSRs itself.

Data Analysis: We would like to present updated results of analysis of Lunar Exploration Neutron Detector (LEND) data for about three years of lunar mapping. Data measured by collimated LEND detectors allows one to look at neutron flux distribution at Moon poles with much better spatial resolution then was achieved at previous space missions.

Using the LEND data we had tested the hypothesis that all PSRs are contain a large amount of water ice permafrost and test for hydrogen presents in regolith of regions outside of PSRs.

Discussion: Both analyses of individual PSRs and studies of groups of PSRs have shown that these spots of extreme cold at lunar poles are not associated with a strong effect of epithermal neutron flux suppression [5]. We found only three large PSRs, Shoemaker and Cabeus in the South and Rozhdestvensky U in the North, which manifest significant neutron suppression, from -5.5% to -14.9%. All other PSRs have much smaller suppression, no more than few percentages, if at all. Some PSRs even display excess of neutron emission in respect to sunlit vicinity around them. Testing PSRs collectively, we have not found any average suppression for them. Only group of 18 large PSRs, with area >200 km^2, show a marginal effect of small average suppression, ~2%, with low statistical confidence. A ~2% suppression corresponds to ~125 ppm of hydrogen taking into account the global neutron suppression near the lunar poles and assuming a homogeneous Hydrogen distribution in depth in the regolith [6].

Testing for hyfrogen presents in regolith of regions outside of PSRs has been done by detection of local spots of suppression and excess of epithermal neutron emission at the lunar poles. Found areas there named as Neutron Suppression Regions (NSRs) and Neutron Excess Regions (NERs). These NSRs may be identified with spots of water-ice rich permafrost on the Moon. It is shown that detected NSRs are include in both permanently shadowed and illuminated areas, and they are not coincident with Permanently Shadowed Regions (PSRs) at the bottom of polar craters, as has been commonly expected before LEND presented neutron data with high spatial resolution [7].

References: [1] Author A. B. and Author C. D. (1997) *JGR, 90,* 1151–1154. [2] Author E. F. et al. (1997) *Meteoritics & Planet. Sci., 32,* A74. [3] Author G. H. (1996) *LPS XXVII,* 1344–1345. [4] Author I. J. (2002) *LPS XXXIII,* Abstract #1402.

[1] Arnold, J. R. (1979) *JGR, 84,* 5659–5668. [2] Watson, K., Murray B. C. and Brown H. (1961) *JGR, 66,* 3033–3045. [3] Feldman W. C. et al. (2001) *JGR*, 106, 23231-23252. [4] Maurice S. et al. (2004) *JGR*, 109, E07S04, 40 PP. [5] Mitrofanov I. G. et al. (2010) *Science*, 330, 483. [6] Sanin A.B. et al. (2012) *JGR, 117*, E00H26. [7] Mitrofanov I. G. et al. (2012) *JGR, 117*, E00H27.

EXPLORATION OF DEEP INTERIOR OF THE MOON FROM MEASUREMENTS OF CHANGES OF LONG-WAVELENGTH GRAVITY AND ROTATION. S. Sasaki, F. Kikuchi[1], K. Matsumoto[1], H. Noda[1], H. Araki[1], H. Hanada[1], R. Yamada[1], S. Goossens[1,#], H. Kunimori[2], T. Iwata[3], N. Kawaguchi[1], Y. Kono[1] , [1]National Astronomical Observatory of Japan 2-12 Hoshigaoka, Mizusawa, Oshu 023-0861 Japan (sho@miz.nao.ac.jp), [2]NICT, Koganei, Japan, [3] ISAS/JAXA, Sagamihara, Japan, [#]Now at Goddard Space Flight Center/NASA, USA.

Introduction: Precise measurements of gravity and rotation of planets as well as seismic measurement are important for the discussion on their deep interior. The Moon revolves around the Earth once in a month synchronously with its rotation. It is tidally deformed by the Earth, which would excite irregular motion of the lunar rotation with small amplitude, which is called forced librations. Additionally, free libration is excited by impacts, liquid core, and orbital resonance. Dissipation of the libration terms of lunar rotation may depend on the interior structure of the Moon, especially the state of the core and lower mantle [1, 2]. Effect of tidal deformation can be detected by low-degree gravity change, although surface height change is as small as 10cm. Long-term (> a few months) gravity measurements can provide information of the lunar tidal deformation. One important scale of tidal deformation is degree 2 potential Love number k_2, which could constrain the state of the core (solid or liquid) and viscosity of the lower mantle of the Moon [3].

VLBI gravity measurement: In KAGUYA (SELENE) mission, multi-frequency differential VLBI observations (S/X bands) are used for the precise determination of orbits of satellites leading to increase in the accuracy of lunar gravity field [4]. However, the accuracy of low-order gravity and its change are limited. The same-beam VLBI observation is only possible when the separation angle between the two radio sources is smaller than the beamwidth of the ground antennas. The relatively large shape of Rstar's orbit (100 km x 2400 km) did not allow the same-beam observation all the time.

SELENE-2 is planed as a follow-on mission of KAGUYA. The spacecraft is to be launched in 2010's. SELENE-2 lands on the nearside of the Moon and investigates the surface and the interior of the moon. In SELENE-2 mission, we will have VLBI radio (VRAD) sources both in the lander and the orbiter. Vstar-like orbit (100 km x 800 km) will almost always keep the separation angle smaller than the S-band beamwidth of domestic VERA stations since one of the radio sources is fixed on the near-side lunar surface. Also, for continuous tracking of the orbiter both by S and X bands, we started development of two-beam S/X receivers which will allow larger separation angle between radiosources.

The k_2 is sensitive to the state of deep interior. When the core radius is 350 km, k_2 changes by about 5% between liquid and solid cores. Using same-beam (or two-beam) multi-frequency VLBI observation of , we will determine orbits of the orbiter precisely, measure low-order gravity changes, and estimate k_2 with uncertainty below 1%. If the core size is constrained by SELENE-2 seismometer, contributions of lower mantle and core on k_2 would separated.

LLR: We also propose a Lunar Laser Ranging (LLR) reflector on SELENE-2 lander. Instead of conventional corner cube reflector (CCR) array, we plan a larger single reflector in SELENE-2. The new reflector should be somewhere in the southern hemisphere on the nearside Moon. With pre-existed reflectors, latitudinal component of lunar libration and its dissipation can be measured precisely. The dissipation between the solid mantle and a fluid core was discussed. LLR observation has also provided information of moment of inertia and tidal Love number of the Moon. However, among LLR parameters, k_2 and core oblateness is coupled. Once k_2 is fixed, we can determine core oblateness, which would also constrain the core and lower mantle states.

ILOM (In-situ Lunar Orientation Measurement)
The ILOM is an experiment to measure the lunar physical librations on the Moon with a star-tracking small telescope [2]. Since observation of ILOM is independent of the distance between the Earth and the Moon, the effect of orbital motion is clearly separated from the observed data of lunar rotation. This is the advantage of ILOM over the ground-based methods such as LLR and VLBI. The crucial issue that should be overcome is the survival of lunar night and thermal effect of solar illumination on the zenith tube.

References: [1] J. G. Williams et al. (2001) *JGR* **106** 27933-27968. [2] H. Hanada et al. (2005) *Proc. Int. Ass. Geod.* Springer, pp.163-168. [3] K. Matsumoto et al., (2011) Geophysical Research Abstracts 13, EGU2011-2032-1. [4] S. Goossens, et al. (2011) J. Geodesy, 85, 205-228.

The Return of Samples by the Apollo Program Shaped Our Understanding of the Solar System. C.K. Shearer, Institute of Meteoritics, Department of Earth and Planetary Science, University of New Mexico, Albuquerque, NM 98122. (cshearer@unm.edu)

Introduction: The Apollo Program remains the only set of missions that enabled humans to land and explore the surface of a planetary body. Apollo 17 illustrated the powerful combination of mobility, science driven, sample site selection, human boots-on-the-ground geological observations, and sample collection that makes it a prototype for future human missions to planetary surfaces. One of the crowning achievements of the Apollo program was to collect and return approximately 381.7 kg of rock and soil from six landing sites located in the central part of the Moon's nearside. It is nearly impossible to decouple sample observations from observations made on the lunar surface and from orbit in examining the fundamental lunar science accomplished by the Apollo Program. Each type of observation provides a variety of perspectives that enrich all observations. For example, whereas samples provide ground truth for remotely sensed data, remotely sensed data provide a regional and planetary context to place returned samples. Here, I attempt to decouple these observations in order to illustrate the important role of samples in redefining how the solar system works and the scientific limitations of an Apollo Program if it did not return samples.

New Concepts of the Solar System derived from Apollo Program Sample: There were numerous concepts derived from the samples returned by the Apollo Program. Many of these concepts were initially proposed during the Apollo Program and continued to evolve over 40 plus years of sample analysis. This presentation explores the role of samples in defining mechanisms for early planetary differentiation, the origin of the Earth-Moon system, and the late, heavy bombardment of the inner Solar System.

Mechanisms for the differentiation of the terrestrial planets: Following the return of Apollo 11 samples, the concept of a lunar magma ocean (LMO) was first introduced based on the recognition that the lunar highlands are composed primarily of Ca-rich plagioclase. This concept was further tested and refined with other sample observations such as: (1) antiquity and geochemical uniqueness of the ferroan anorthosites, (2) complementary europium anomalies of ferroan anorthosites (primordial lunar crust) and mare basalts (derived from LMO cumulates), (3) ancient and variable mantle sources for mare basalts and (4) uniformity of incompatible trace-element ratios that may represent the last dregs of a LMO (i.e. KREEP). The early differentiation of the Moon via a lunar magma ocean has been viewed as an end-member differentiation process that has been extended to other terrestrial planets (Earth, Mars, asteroids).

Late, heavy bombardment of the inner Solar System. In the early-1970s, it was recognized that most highland samples exhibit a Pb-U fractionation that was essentially due to Pb volatilization during metamorphic events in the interval 3.85-4.00 Ga. It was proposed that highland samples from widely separated areas bear the imprint of a series of events in a narrow time interval which were identified with a cataclysmic impacting rate of the moon at ~ 3.9 Ga. This concept was further tested with chronological studies of impact derived lunar lithologies returned by the Apollo Program. This concept is further being tested and modeled to decipher the impact history of the inner solar system and link it to the alignment and potential reorientation of the giant planet hundreds of millions of years after accretion of the planets.

A giant impact origin for the Earth-Moon system: Numerous models had been proposed for the origin of the Earth-Moon system prior to the Apollo Program. However, dynamical constraints and celestrial mechanics were not sufficient to pin down the origin of this two planet system. Geochemical measurements of lunar samples provided some contrasts with materials from the Earth with regards to differences in Mg#, oxygen isotopes, refractory elements, and volatile elements. In the mid-1970s, combining the geochemical characteristics of lunar samples, and arguments for a LMO with other constraints led to the concept of the Giant impact model. The recent sample observation that the Moon is more H-rich than concluded after the Apollo Program is not inconsistent with this model. Current missions LRO and GRAIL and potential future missions such as a lunar geophysical network and a sample return from the South Pole-Aitken basin will shed additional light on the bulk composition of the Moon. This will provide additional tests for the Giant impact concept.

Results of the Lunar Exploration Analysis Group GAP-SAT (Specific Action Team) I and II examination of Strategic Knowledge Gaps for the Moon First Scenario for Human Exploration of the Solar System. Members of the GAP-SAT Teams I and II. Reported by C.K. Shearer, Institute of Meteoritics, Department of Earth and Planetary Science, University of New Mexico, Albuquerque, NM 98122. (cshearer@unm.edu)

The Lunar Exploration Analysis Group (LEAG) was tasked by the Human Exploration Operations Mission Directorate (HEOMD) to establish a Specific Action Team (SAT) to evaluate and provide findings that define existing Strategic Knowledge Gaps (SKGs) in the context of implementing the "Moon first" option, which is one of the destinations being considered by NASA's Human Space Flight Architecture Team and the International Space Exploration Coordination Group's Global Exploration Roadmap (GER). The "GAP-SAT" analysis consisted of two teams (GAP-SAT I and II).

The LEAG "GAP-SAT" team I identified important SKG and placed them within the context of (1) enabling or enhancing components in the "Moon First" scenario, (2) the Planetary Science Decadal Survey, (3) the LEAG Lunar Exploration Roadmap, and (4) NASA's Human Space Flight Architecture Team's (HAT) mission scenario development. The SAT concluded that following the completion of Lunar Reconnaissance Orbiter mission (LRO) there are no SKGs that would inhibit the flight of an early Apollo-style mission (Apollo 11, 12, 14). However, in the context of a "Moon First Scenario" which develops assets and capabilities for human activity within the Earth-Moon system (EMS) and beyond EMS to Near Earth Asteroids and Mars, there are numerous SKGs that enable and enhance a more mature human exploration of the Moon. Specific SKGs are dependent upon the architecture of the "Moon First Scenario". We concluded that resource exploration and utilization (ISRU) is a "game changer" in how humans explore the Solar System by creating an infrastructure that enables a sustainable human presence. Prior to robotic missions, SKGs can be filled with on-going missions, ISS, Earth-based technology development, and lunar samples studies. SKGs that can be partially or totally retired in this manner include: solar resources, regolith resources, lunar ISRU production efficiency, predicting solar activity, geodetic grid & navigation, maintaining peak human health, effect of dust on human and instrument performance, modeling blast ejecta, and lunar mass concentrations and distribution that influence the accuracy of navigation predictions, the ability to do precision landing and the stability of spacecraft left in orbit for long periods. A systematic robotic precursor campaign can be used to fill additional SKGs to enable and enhance a "Moon First Scenario". Although these robotic missions emphasize SKGs tied to investigating unexplored lunar terrains, prospecting for potential resources, and resource utilization, they are apt for filling SKGs relevant to plasma environment and electrical charging, radiation on the lunar surface, effect of dust on technology and biology, surface trafficability, and propulsion-induced ejecta. In addition to filling SKGs, robotic and early human missions both enable and enhance important lunar and solar system science that has been identified in the NRC Planetary Science Decadal Survey, other NRC studies, and the LEAG Exploration Roadmap. There are numerous SKG tied to the "Moon First" Scenario that cross-cut other destinations.

The LEAG GAP-SAT I analysis was the first step in exploring SKG for lunar exploration. A second LEAG SAT (GAP-SAT II) is currently involved in providing a quantitative description of measurements that are required to fill knowledge gaps, identifying the fidelity of the measurements needed, and if relevant, providing examples of existing instruments capable of making the measurements. The results of this analysis will be completed prior to the LEAG annual meeting taking place at the Goddard Space Flight Center on October 22-24, 2012. We will report the conclusions of the analysis conducted by both LEAG GAP-SAT Teams I and II.

Questions about Lunar Origin S. Fred Singer <singer@sepp.org>

Introduction: In 1975 William K. Hartmann and Donald R. Davis suggested that, at the end of the planet formation period, several satellite-sized bodies had formed that could collide with the planets or be captured. They proposed that one of these objects may have collided with the Earth, ejecting refractory, volatile-poor dust that could coalesce to form the Moon. This collision could help explain the unique geological properties of the Moon.

The impact hypothesis was devised mainly to circumvent what was thought to be a low probability of lunar capture (Singer 1968, 1986). (Yet, strangely, capture appears to be the preferred hypothesis for the origin of the outer moons of Jupiter and some other planetary satellites.) But the impact hypothesis has similar probability problems that are hardly ever mentioned -- in addition to more fundamental problems, all of which can be overcome only with various *ad hoc* assumptions.

Another advantage of 'impact' over 'capture' was thought to be the chemical composition of the Moon, which resembles that of the Earth' mantle. But recent findings show substantial and unexplained differences.

12 Questions: The impact hypothesis (Hartmann; Benz, Cameron, Melosh; Canup, Asphaug) of lunar origin seems to have found general acceptance – in spite of the fact that its probability is low and the physics of the lunar formation is not readily transparent, being obscured by a complicated computer program. Nevertheless, one can raise certain questions that an impact process should answer:

1. For what range of impact parameters *a* is there an appreciable chance of forming the Moon? If *a* is close to the Earth radius *R*, then the impact is only glancing and the process becomes operationally indistinguishable from "capture"; if *a*<<R, then the probability of forming a Moon from Earth material appears low (as evident from arguments of angular momentum conservation).

2. Therefore how many Mars-like bodies must impact in order to have a reasonable chance to produce the present Moon? And why is impact origin more probable than capture? Also: If there are so many bodies available, why didn't it happen on Venus or Mars?

3. In the calculation, what is the assumed pre-impact spin of the Earth? The initial papers on impact formation of the Moon did not consider a pre-impact rotation of the Earth. What restraints are there on the pre-impact angular momentum? E.g., could a retrograde impact produce the Moon? Or: How to be sure that the total angular momentum matches the present value of the Earth-Moon system? How does the Earth spin angular momentum vector change during and following the impact? What fraction of the total angular momentum is taken up by the debris emanating from the impact? What fraction is carried away by the escaping debris?

4. What happens to the splashed-out material from the impact; how many particles escape and how many return on ballistic orbits? Whence comes the angular momentum for a bound lunar orbit? How and where does "captured" material assemble and what exactly is the initial lunar orbit?

Plus 8 more qestions

Conclusion: We will discuss how to decide on which lunar origin hypothesis is more probable. Capture or Impact.

References: Singer, S.F. *Geophys. J. Royal Astron. Soc*. 15, 205-226, 1968; "Origin of the Moon by Capture" in *The Moon* (W. Hartmann et al., ed.) LPI, Houston, 1986. pp, 471-485.
Canup, R.M. and E. Asphaug 2001. *Nature*, **412**, 708-712
Canup, R. M. 2004. *Icarus* **168** (2): 433
Borg, L. et al. 2011. *Nature* **477,** 70–72
Saal, A. E. 2008. *Nature* **454**, 192-195

PREDICCS: A SPACE RADIATION PREDICTION TOOL FOR LUNAR, PLANETARY, AND DEEP SPACE EXPLORATION. H. E. Spence[1], N. A. Schwadron[1], M. Gorby[1], C. Joyce[1], M. Quinn[1], M. LeVeille[1], S. Smith[1], J. Wilson[1], L. Townsend[2], and F. Cucinotta[3], [1]Space Science Center, EOS, University of New Hampshire (8 College Road, Durham, NH 03824, Harlan.spence@unh.edu), [2] University of Tennessee, Knoxville, TN, [3] NASA Johnson Space Center, Houston, TX.

Introduction: We describe the PREDICCs space radiation prediction and forecasting tool and provide early results from recent and historic lunar, planetary, and deep space applications. While robotic missions routinely explore beyond near-Earth space, where the dual cocoons of Earth's strong magnetic field and thick atmosphere protect us from galactic cosmic rays (GCR) and solar energetic particles (SEP), only a scant few manned Apollo missions ever ventured further outward and faced the risks to astronauts of space radiation omnipresent in deep space. At geostationary orbit distances and beyond (i.e., all locations greater than a tenth of the distance to the Moon), GCRs pose a relatively weak but incessant source of energetic ionizing radiation. The GCR component varies slowly with the solar cycle (in anti-phase) and presents a radiation dose risk for all long-duration missions, with higher risk at solar minimum when GCR intensity maximize. In deep space, SEPs ride on top of this slowly varying radiation dose, delivering episodic intervals of powerfully intense radiation from somewhat lower energy particles accelerated during solar explosive events. Though short in duration (typically hours to days), SEPs can deliver as much equivalent dose as GCR does in months to a year. Risks of GCR and SEPs exist for both robotic and manned missions. For instance, during the Apollo era, the March 1972 SEP event delivered a powerful dose of ionizing radiation at the Moon, but which fortunately occurred between two Apollo missions. A similar event during the Mars Odyssey mission crippled the MARIE instrument. .

PREDICCS: Motivated by this radiation risk, enabled by advanced scientific understanding of the underlying physics of SEPs and GCR variability, and supported by NASA's ESMD and SMD funds, we have developed the PREDDICs space radiation prediction and forecasting tool. We leverage the Earth-Moon-Mars Radiation Environment-Module (EMM-REM) developed under the NASA Living With a Star (LWS) program and extend it to predict the dose, dose rate, and equivalent dose owing to GCR and SEPs throughout the inner heliosphere. The PREDDICs model has been validated through incorporation of and comparison with radiation measurements near Earth and also at the Moon with the Cosmic Ray Telescope for the Effects of Radiation (CRaTER) instrument on NASA's Lunar Reconnaissance Orbiter (LRO) mission. In this presentation, we provide a summary of the PREDICCs model, and then show how the model can be and is being used to predict and forecast the radiation environment throughout the inner solar system. We will show comparisons between predictions and CRaTER observations not only at the Moon, but also predications for other exploration destinations, such as Mars, where with the successful landing of Mars Science Laboratory, we will be able to further validate the model through comparison with such radiation detection instruments as RAD and DAN.

TRAVERSE PLANNING USING LUNAR RECONNAISSANCE ORBITER NARROW ANGLE CAMERA DIGITAL ELEVATION MODELS. E. J. Speyerer[1], S. J. Lawrence[1], J. D. Stopar[1], K. N. Burns[1], and M. S. Robinson[1], [1]School of Earth and Space Exploration, Arizona State University, Tempe, AZ (espeyerer@ser.asu.edu).

Introduction: Recent lunar missions provide important new geologic and topographic datasets for the Moon. To supply precise measurements, execute preparatory investigations, and collect ground-truth samples for these remotely sensed datasets, future precursor landers and rovers are required. One of the primary goals of the Lunar Reconnaissance Orbiter (LRO) is to deliver datasets that can be used to plan future missions to the lunar surface including landers and rovers. Digital elevations models (DEMs) derived from select LRO Narrow Angle Camera (NAC) stereo image pairs provide surface topography, slopes, and roughness at down to the 2 m scale (depending on the resolution of the input images) [1,2]. By considering multiple datasets, including those derived from the NAC DEMs, we determine least energy traverse maps of key exploration sites that can aid planning future rover mission.

Traverse Planning Tool: To plan traverses investigating key exploration sites, the raster DEM is converted into a network of equally spaced nodes. The spacing between nodes can be as fine as the original raster DEM, or several times larger depending on the size of the region, required accuracy of the traverse, and computational constraints. Each node connects to its six neighboring nodes to form a graph structure. The energy required, or cost, to traverse from one node to a neighboring node is dependent on an array of variables derived from the NAC DEM, the model rover, and other data sources:

- Down track slope (NAC DEM)
- Cross track slope (NAC DEM)
- Terrain ruggedness (NAC DEM)
- Solar panel orientation (NAC DEM, model rover)
- Rolling resistance (a model rover)
- Turning capabilities (a model rover)

Using Dijkstra's algorithm [3], the lowest energy traverse paths from an initial node to all the nodes in the network are calculated. This framework is flexible over a broad scale of terrain types and scalable from localized regions to large exploration sites.

Energy and Traverse Maps: Maps derived from these calculations show the energy needed to traverse from the initial node to all the other nodes in the network (Figure 1). In addition to identifying relative energy to traverse from one site to another, these maps also identify areas that are not accessible to the model rover given a pre-defined set of constraints such as the maximum traversable slope.

When using Dijkstra's algorithm, the lowest cost path to travel to each node in the network is also stored. By selecting any traversable point on the map, the lowest cost path from the initial node is identified.

Tool for Future Exploration: A traverse planning tool such as the one employed here is key for any future lunar mission planning activities. These maps identify least energy traverse paths, as well as delimit traversable and inaccessible areas around each exploration site. We can also use this tool to identify the required capabilities and operational characteristics a future prospecting rover would need in order to reach key targets of scientific interest at a specific site. Future development will focus on adding other datasets and cost parameters such as boulder populations derived from Diviner measurements and LOLA-derived surface roughness.

References: [1] Robinson et al. (2010) Space. Sci. Rev. [2] Burns et al. (2012) ISPRS [3] Dijkstra (1959) Numerische Mathematik.

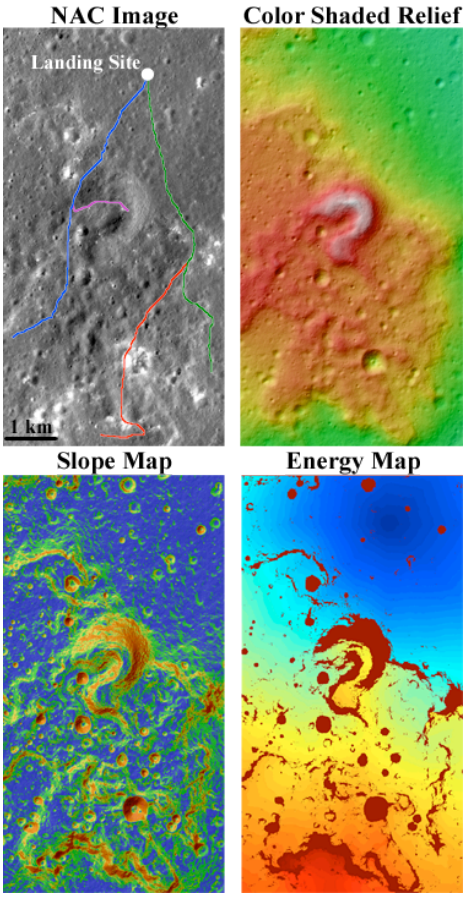

Figure 1- NAC image (M111965782L/R) with potential low energy rover traverses in the Marius Hills region with corresponding shaded relief, slope, and energy map derived from a NAC DEM.

INTERPLANETARY CONDITIONS DURING THE APOLLO MISSIONS: IMPLICATIONS FOR THE STATE OF THE LUNAR ENVIRONMENT. T. J. Stubbs[1,2,3], D. A. Glenar[4,3], A. P. Jordan[5,3], Y. Wang[1,2,3], R. R. Vondrak[2,3], M. R. Collier[2,3], W. M. Farrell[2,3], M. I. Zimmerman[6,2,3], N. A. Schwadron[5], and H. E. Spence[5,3], [1]University of Maryland, Baltimore County, [2]NASA Goddard Space Flight Center, [3]NASA Lunar Science Institute, [4]New Mexico State University, [5]University of New Hampshire, [6]ORAU/NPP. (Timothy.J.Stubbs@nasa.gov).

Introduction: The interplanetary conditions coinciding with the Apollo missions had important implications for the state of the lunar environment experienced by the astronauts, and measured by the many scientific investigations carried aboard the command modules and deployed on the Moon's surface. The first comprehensive overview is presented of the space plasma, solar ultraviolet, energetic particle, geomagnetic, and meteoroid stream conditions encountered by the Moon during Apollo. This includes an investigation of the location of the Moon with respect to the Earth's bow shock and magnetopause boundaries in order to assess whether it encountered either the magnetosheath or the hot tenuous plasmas of the magnetosphere, respectively, during these missions. The interplanetary conditions during the Apollo missions are placed into the context of the last four solar cycles, and subsequent lunar missions, as well as extreme events, such as occurred during August 1972.

Data Sources: We use the OMNIWeb dataset of interplanetary conditions at 1 AU. The parameters examined are: $F_{10.7}$ (solar UV proxy); interplanetary magnetic field $|B|$; the concentration n, proton temperature T_{proton}, and flow speed $|V|$ of the solar wind; the flux of energetic protons $F_{\mathrm{MeV\ protons}}$; and the K_P index (as a proxy for solar wind conditions). The $F_{\mathrm{MeV\ protons}}$ used here are good for characterizing the high fluxes during episodic solar energetic particle events, as opposed to the galactic cosmic ray background.

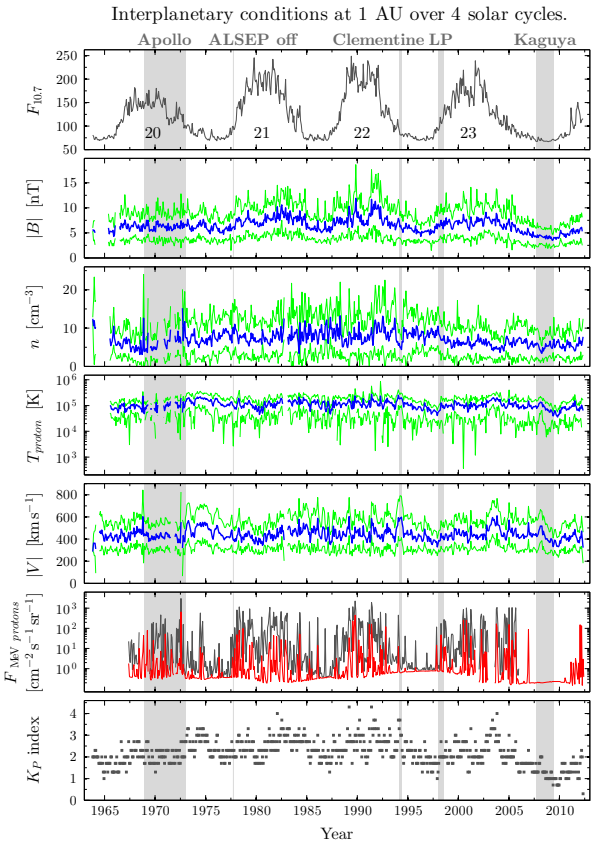

Space Age Overview: The figure shows parameters averaged over a 27-day solar rotation period. In the panels showing $|B|$, n, T_{proton}, and $|V|$, the blue lines indicate the average and the green lines the standard deviation. $F_{\mathrm{MeV\ protons}}$ for energies >1 MeV and >10 MeV are shown by gray and red lines, respectively. The solar cycle modulation is seen in all parameters to some extent, but especially $F_{10.7}$. Indicated at the top are important intervals for lunar science and exploration: the Apollo era (1968–1972), Apollo Lunar Surface Experiments Package (ALSEP) switch off, and the Clemetine, Lunar Prospector and Kaguya missions. The Apollo missions were the only ones to fly during a solar maximum (from the peak through the declining phase). However, Cycle 20 was typically less active than later solar cycles.

Radiation Hazards: The Apollo missions were fortunate to fly during relatively benign conditions, which is reflected in the average radiation measured by passive dosimeters flown on each mission. A maximum skin dose of 1.14 rads (rem) was measured during Apollo 14 – this is very low when compared to the maximum operational dose, which was set at 400 rads. If an Apollo mission had flown during the August 1972 solar flares and coronal mass ejections, then the crew could have experienced moderate acute radiation sickness without effective counter-measures.

Meteoroid Streams: All missions, except Apollo 13, coincided with established IAU meteoroid streams. In particular, Apollo 12 flew during the peak of the 1969 Leonids, which had an exceptionally high zenithal hourly rate of 400. Similarly, Apollo 15 and 17 flew during the Persieds and Geminids, respectively, both of which are strong annual streams. This may be related to observations of lunar horizon glow reported during those missions, whether related to resonant scattering by exospheric neutrals or sunlight scattered from exospheric dust.

MONTE CARLO SIMULATIONS IN SUPPORT OF ORBITAL NEUTRON DETECTIOND BY THE LEND INSTRUMENT ON BOARD OF LRO SPACECRAFT. Jao-Jang Su[1], Robert Khachatryan[2], Roald Sagdeev[1], Daniel Usikov[1], Gennady Milikh[1], Gordon Chin[3]

[1]Department of Physics, University of Maryland, College Park, MD 20742

[2]Department of Physics, University of California, Santa Cruz, 1156 High Street, Santa Cruz, CA 95060

[3]NASA Goddard Space Flight Center, Greenbelt, MD 20771

Introduction: The early detection of lunar neutrons produced by precipitation of galactic cosmic ray (GCR) particles in the upper layer of lunar soil goes back to Apollo Moon landing (Apollo 17) epoch. Since then it has been developed into its own type of remote sensing (Lunar Prospector/1998-1999; LRO/2009-till now), which is especially sensitive for singling out the information on presence of hydrogen (e.g. frozen water inside permanently shadowed craters) from neutron based cosmo-chemistry data. The final interpretation technique relies on comprehensive Monte Carlo simulation of neutron production by GCR and subsequent leakage from the Moon. Until now such extensive simulation was carried mostly with the use of MCNPX code [1], [2].

Model Description: Here we report on the use of alternative MC code GEANT4, developed at CERN and offered as the open source software [3]. We believe that cross-comparison and inter-calibration of both codes will add more weight to the importance, versatility and reliability of Monte Carlo approach for neutron detection based planetary remote sensing. As a first step we compare basic results for neutron leakage from lunar soil (for several modeled elemental compositions). Then GEANT4 code was used to study the modification of neutron leakage in presence of top layer of dry and wet regolith. These data were applied to analysis of physical nature of SNRs (Suppressed Neutron Regions) found by LEND in polar areas of the Moon [4].

References: [1] Lawrence D.J. et al., (2006) *JGR, 111*, doi:10.1029/2005JE002637. [2] Mitrofanov I.G. et al. (2008) *Astrobiology, 8*, doi:10.1089/ast.207.0158. [3] Agostinelli S. et al., (2003) *Nuclear Instr. Method in Phys. Res., 506*A, 250-303. [4] Mitrofanov I.G. et al. (2010) *Science, 330*, doi:10.1126/science.1185696.

Water, Water, Everywhere: But How to Find and Use It on the Moon!

Lawrence A. Taylor, lataylor@utk.edu, Planetary Geosciences Institute, Earth & Planetary Sciences, University of Tennessee, Knoxville, TN 37996

The last few years has seen the Moon go from "bone-dry" all the way to almost hosting the "Winter Olympics". The paradigm from 1973 for the production of nanophase metallic iron (np-Fe) in the lunar soil was the reduction of FeO in the micrometeorite melts by solar-wind hydrogen. This should produce water as a product from the combination of the hydrogen and the oxygen from the FeO. Yet, Larry Taylor in 1995 could find nil by FTIR examination of agglutinitic glass.

Fast forward to the persistent search for OH in apatite by electron microprobe analysis, led by Francis McCubbin that spurred on several other endeavors. In 2008, Alberta Saal's team determined minor, but real, hydrogen in pyroclastic beads. This was followed in 2010 by teams led by Jim Greenwood, Yang Liu (and later by Jeremy Boyce), and Francis McCubbin, aided by Eric Hauri, culminating in pubs by these teams in 2011-2012. The annual Lunar and Planetary Science Conference continues to be the exciting venue for such discoveries. Onward to Hauri's 'water' in lunar olivine melt inclusions. accompanied by Yang Liu's proof of the presence of OH by FTIR. Next, back to the agglutinates

More recently in 2012, Yang's team demonstrated a "hidden reservoir" of H, OH, and HOH in lunar soil agglutinitic glasses, up to >500 ppm. These impact-produced glasses consist of upwards of 80 % of the fine soil. Thus, the agglutinates are a very real reservoir for lunar water, from several sources. But the remote sensing community has been active with lunar orbiters.

Enter Carle Pieters's Moon Mineralogy Mapper team, who first observed OH in reflectance spectra of the Moon, to be subsequently verified by Roger Clark with re-examined Cassini data and Jessica Sunshine, with the EPOXY flyby data, which also hinted at a "dew" like quality for this OH. They all reported together in 9/2009. Then came the LCROSS impactor, with its trailing spectrometers sensing water, water-ice, and many volatile components indicative of cometary water. This was proof for the presence of water-ice in the permanently shadowed craters at the poles, following strong hints by various neutron-spectrometer signals on Pathfinder and LEND/LRO.

Let us take count of the possible sources of OH, HOH, water, and water-ice as seen In and On the Moon: 1) indigenous water from the lunar magmas; 2) water in agglutinates from Solar-wind hydrogen reduction; 3) meteorite and micro-meteorite contamination, accounting for up to 2 wt% (e.g., carbonaceous chondrites); 4) cometary water, particularly collected at the poles; 5) solar-wind proton-induced OH-HOH. All this water, BUT how much?

Paul Spudis and his Mini-SAR team came up with a modest estimate of only 600 million tonnes of water-ice, and only surveying the North Pole. The MMM team came up with something like a liter of water. LCROSS found lots more. But, the major unknown for lunar OH-HOH around the Moon is in the agglutinates, which in general comprise ~50 wt% of lunar regolith.

Any settlement to the Moon will require In-Situ Resource Utilization (ISRU) of lunar materials. And water for human and plant consumption is required, with the use of hydrogen and oxygen for rocket fuels as a major and substantial need. Where the landing is located will require different sources of water, even with the possible need for oxygen production from lunar soil directly as reviewed by Taylor and Carrier (1973) (e.g., hydrogen reduction of soil). The nature of lunar water, its quantities, its capture, and needs form the basis for this presentation.

LEND: GOING BEYOND NOMINAL ANGULAR RESOLUTION Daniel Usikov[1], Tim McClanahan[2], Roald Sagdeev[1], Robert Khachatryan[3], Gennady Milikh[1], Gordon Chin[3], Jao-Jang Su[1]

[1]Department of Physics, University of Maryland, College Park, MD 20742

[2]NASA Goddard Space Flight Center, Greenbelt, MD 20771

[3]Department of Physics, University of California, Santa Cruz, 1156 High Street, Santa Cruz, CA 95060

The omnidirectional channel of LEND for epithermal neutrons (SETN) since the start of operations in 2009 have accumulated more than 10^9 neutron events. This data was used to generate the neutron suppression maps of the Moon with nominal resolution (~60 km). The volume of statistical database (still storing at the pace of about 10 cps) now is sufficient to go beyond nominal resolution of SETN by introducing the set of multiply overlapping pixels.

We applied such approach in the framework of several alternative computational techniques of deconvolution such as Conjugate Gradient, Iterative Gaussian Smoothing, Weiner and Regularized Deconvolution [1] to construct "super-resolution " maps (up to 20 km) for a few selected areas with most pronounced presence of hydrogen (Shoemaker PSR, NSRs, and others).

References: [1] McClanahan T.P. et al. (2010), *Computers & Geosciences*, *36*, 1484-1493.

The Lunar Reconnaissance Orbiter: Plans for the Extended Science Mission and Next Steps for Lunar Science and Exploration, R. R. Vondrak[1], J. W. Keller[1], G. Chin[1], J. B. Garvin[1], N. E. Petro[1], [1]Goddard Space Flight Center, Greenbelt MD 20771.

Introduction: The Lunar Reconnaissance Orbiter spacecraft (LRO), launched on June 18, 2009, began with the goal of seeking safe landing sites for future robotic missions or the return of humans to the Moon as part of NASA's Exploration Systems Mission Directorate (ESMD). In addition, LRO's objectives included the search for surface resources and the measurement of the lunar radiation environment. After spacecraft commissioning, the ESMD phase of the mission began on September 15, 2009 and was completed on September 15, 2010 when operational responsibility for LRO was transferred to NASA's Science Mission Directorate (SMD). The SMD mission was scheduled for 2 years and completed in September of 2012. Under SMD, the Science Mission focused on a new set of goals related to understanding the geologic history of the Moon, its current state, and what it can tell us about the evolution of the Solar System.

Having recently marked the completion of the two-year Science Mission, we will review here the major results from the LRO for both exploration and science and discuss plans and objectives going forward including plans for an Extended Science Mission that will last until September, 2014. We will also discuss the LRO legacy data set and suggest future directions beyond LRO for science and exploration objectives. Some results from the LRO mission are: the developent of comprehensive high resolution maps and digital terrain models of the lunar surface; discoveries on the nature of hydrogen distribution, and by extension water, at the lunar poles; measurement of the daytime and nighttime temperature of the lunar surface including temperature below 30 K in permanently shadowed regions (PSRs); direct measurement of Hg, H_2, and CO deposits in the PSRs; evidence for recent tectonic activity on the Moon; and high resolution maps of the illumination conditions at the poles.

The objectives for the Extended Science Mission under SMD address four themes: 1) The nature of polar volatiles, 2) Lunar differentiation and early evolution, 3) The lunar impact record, 4) The Moon's interaction with its external environment.

The instruments, which were describe in detail previously[1], include ***Lunar Orbiter Laser Altimeter (LOLA)***, PI, David Smith, NASA Goddard Space Flight Center, Greenbelt, MD, ***Lunar Reconnaissance Orbiter Camera (LROC)***, PI, Mark Robinson, Arizona State University, Tempe, Arizona, ***Lunar Exploration Neutron Detector (LEND)***, PI, Igor Mitrofanov, Institute for Space Research, and Federal Space Agency, Moscow, ***Diviner Lunar Radiometer Experiment (DLRE),*** PI, David Paige, University of California, Los Angeles, ***Lyman-Alpha Mapping Project (LAMP)***, PI, Alan Stern, Southwest Research Institute, Boulder, Colorado, ***Cosmic Ray Telescope for the Effects of Radiation (CRaTER)***, PI, Harlan Spence, University of New Hampshire, New Hampshire, and ***Mini Radio-Frequency Technology Demonstration (Mini-RF)***, P.I. Ben Bussey, Applied Physics Laboratory, Maryland.

Figure 1 The fully assembled and thermal blanketed spacecraft.

Data Access: All of the LRO data are added to the Planetary Data System on three month intervals, with a latency of no more than 6 months. As of June 15, 2012 more than 325 TBytes of data have been made available for science and exploration.

References: [1] Vondrak, R.R., Keller, J.W., and Russell, C.T., (Ed.s), 2010, Lunar Reconnaissance Orbiter Mission, New York, Springer.

COSMIC RAY ALBEDO PROTON YIELD CORRELATED WITH LUNAR ELEMENTAL ABUNDANCES. J. K. Wilson[1], H. E. Spence[1], A. W. Case[2], J. B. Blake[3], M. J. Golightly[1], J. Kasper[2], M. D. Looper[3], J. E. Mazur[3], N. Schwadron[1], L. W. Townsend[4], C. Zeitlin[5], [1]Space Science Center, University of New Hampshire, Durham, NH, (jody.wilson@unh.edu), [2]High Energy Astrophysics Division, Harvard CFA, Cambridge, MA, [3]The Aerospace Corporation, Los Angeles, CA, [4]Department of Nuclear Engineering, University of Tennessee, Knoxville, TN, [5]Southwest Research Institute, Boulder, CO.

Introduction: High energy cosmic rays constantly bombard the lunar regolith, producing secondary "albedo" or "splash" particles like protons and neutrons, some of which escape back to space. Two lunar missions, Lunar Prospector and the Lunar Reconnaissance Orbiter (LRO), have shown that the energy distribution of albedo neutrons is modulated by the elemental composition of the lunar regolith[1-4], with reduced neutron fluxes near the lunar poles being the result of collisions with hydrogen nuclei in ice deposits[5] in permanently shadowed craters. Here we investigate an analogous phenomenon with high energy (~100 MeV) lunar albedo *protons*.

CRaTER Instrument: LRO has been observing the surface and environment of the Moon since June of 2009. The CRaTER instrument (Cosmic Ray Telescope for the Effects of Radiation) on LRO is designed to characterize the lunar radiation environment and its effects on simulated human tissue. CRaTER's multiple solid-state detectors can discriminate the different elements in the galactic cosmic ray (GCR) population above ~10 MeV/nucleon, and can also distinguish between primary GCR protons arriving from deep space and albedo particles propagating up from the lunar surface.

Summary of Results: We use albedo protons with energies greater than 60 MeV to construct a cosmic ray albedo proton map of the Moon. The yield of albedo protons is proportional to the rate of lunar proton detections divided by the rate of incoming GCR detections. The map accounts for time variation in the albedo particles driven by time variations in the primary GCR population, thus revealing any true spatial variation of the albedo proton yield.

Our current map is a significant improvement over the proof-of-concept map of Wilson et al.[6]. In addition to including twelve more months of CRaTER data here, we use more numerous minimum ionizing GCR protons for normalization, and we make use of all six of CRaTER's detectors to reduce contamination from spurious non-proton events in the data stream.

We find find that the flux of lunar albedo protons is indeed correlated with elemental abundances at the lunar surface. In general the yield of albedo protons from the maria is 1.1% ± 0.4% higher than the yield from the highlands. In addition there appear to be localized peaks in the albedo proton yield that are co-located with peaks in trace elemental abundances as measured by the Lunar Prospector Gamma Ray Spectrometer.

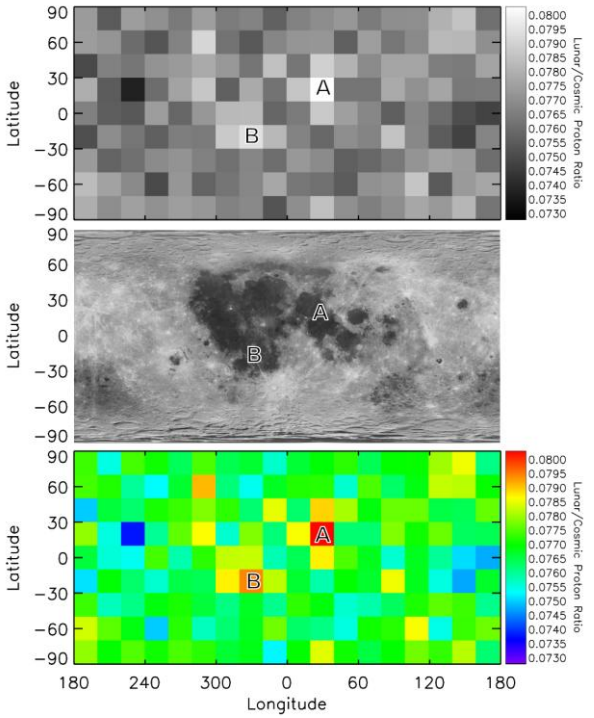

Figure 1. Grayscale (*Top*) and color-coded (*Bottom*) lunar albedo proton maps. *Middle*: Clementine white-light mosaic of lunar surface.

References: [1] Feldman W. C. et al. (1998) *Science, 281*, 1496-1500. [2] Gasnault, O. et al. (2001) GRL, 28, 3797-3800. [3] Maurice, S. et al. (2004) *JGR, 109*, E07S04. [4] Mitrofanov I. G. et al. (2010) *Science, 330*, 483-486. [5] Feldman W. C. et al. (1997) *JGR, 102*, 25565-25574. [6] Wilson, J. K. et al. (2012) *JGR, 117*, E00H23.

Toward understanding the lunar electrostatic environment in the vicinity of complex polar topography. M. I. Zimmerman[1,2] (michael.i.zimmerman@nasa.gov), W. M. Farrell[1,2], T. L. Jackson[1,2], and T. J. Stubbs[1,2,3] Goddard Space Flight Center, Greenbelt, MD, [2]NASA Lunar Science Institute, Ames Research Center, Moffett Field, CA, [3]Center for Research and Exploration in Science and Technology, University of MD, Baltimore County.

Introduction: Permanently shadowed regions (PSRs) are rich in complexity, due to the solar wind's interaction with the surface [1-3 and references therein]. For instance, mini plasma wakes are thought to form downstream of topographic obstructions, giving rise to electric fields that divert solar wind protons toward the surface [1-3]; diverted keV protons may sputter volatiles from the surface or implant to drive surface chemistry. In addition, the charge state of an astronaut suit or other exploration infrastructure is governed by the interplay between incident plasma currents (as modulated by wake formation) and tribocharging from frictional contact with the surface [1]. Results from ongoing computational plasma physics research at Goddard Space Flight Center are presented investigating the effects of complex topography on downstream wake formation, which feeds forward into quantifying exploration charging hazards and efforts related to prospecting for natural lunar resources.

Simulations: A combination of codes – one is open-source [4] and another has been developed solely at Goddard Space Flight Center – is used to simulate the solar wind flowing past various representative lunar topographic geometries. The solar wind is represented as a flowing collection of bunches of electrons and protons continuously resupplied upstream, and any particles incident on the surface contribute to the local surface charge as well as emitting secondary particles in some cases. The system evolves self-consistently according to the local electrostatic fields over many simulation timesteps, allowing detailed wake formation and quasisteady structure to be simulated in two spatial dimensions.

Results: Fig. 1 shows simulated proton fluxes downstream of step-like and inclined crater walls. In the former case, the primary contribution to the electric field is the ambipolar field at the wake flank (not shown). However, the inclined surface collects a significant number of electrons due to its proximity to the bulk solar wind, and a strong surface electric field develops which draw ions more swiftly toward the surface. Other geometries have been simulated, including arcing surfaces across a variety of spatial scales, as well as multi-step craters. First steps toward understanding and predicting the electrostatic environment within PSRs will be demonstrated through a comparison with simulation and theory, and implications for exploration hazards as well as volatile sequestration will be presented.

References: [1] Zimmerman, M. I. et al. (2012), *JGR*, in press, [2] Zimmerman, M. I. et al. (2011), *GRL, 38*, L19202, [3] Farrell et al. (2010), *JGR, 115*, E03004, [4] Verboncoeur et al. (1995), *Comp. Phys. Comm., 87*, 199.

Acknowledgements: This research was supported by an appointment to the NASA Postdoctoral Program at the Goddard Space Flight Center, administered by Oak Ridge Associated Universities through a contract with NASA. The support of LPROPS grant NNX08AN76G and the NASA Lunar Science Institute and DREAM virtual institute through grant NNX09AG78A are gratefully acknowledged, as well as the generous allocation of computing resources by Dr. Timothy McClanahan at Goddard Space Flight Center.

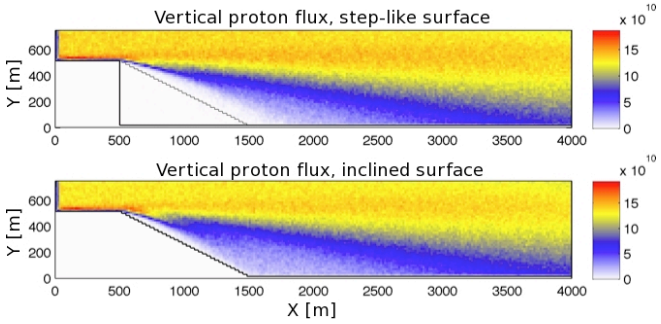

Fig. 1: Simulated proton flux downstream of (top) a step-like and (bottom) an inclined polar crater wall. The light gray inclined line in the top panel is the location of the surface from the bottom panel, provided for comparison.

NOTES

NOTES